JAN 1972
RECEIVED

BB

Vol IV

(NASA-CR-145602) APOLLO NOTES, VOLUME 4 N75-77159
(Bissett-Berman Corp.) 190 p

Unclas
00/98 39883

Complete
Vol IV
VSm 4-29-65

APOLLO NOTES
TABLE OF CONTENTS

No.	Title	Author
151.	Prediction of Re-Entry Dive Angle and Miss Distance for the Return to Earth Phase	C. Siska
152.	Optimum Time for a Single-Boost Correction To the Lunar Ascent Trajectory to Minimize the Rendezvous Miss	C. H. Dale
153.	MSFN Tracking of a Truck Vehicle During Lunar Descent to Perilune	C. H. Dale
154.	Further Estimates of Earth-Moon Injection Errors, II	H. Engel
155.	Effect of Uncertainty in Parameters Which Are Not Estimated	L. Lustick
156.	Rotation of Covariance Matrix Into Other Coordinate Systems	L. Lustick
157.	Clock Time and Clock Rate	H. Engel
158.	Effect of Unknown Rotations of Apollo Vehicle	H. Engel
159.	Effect of Range Bias Information on Re-Entry Prediction in Return-to-Earth Phase	C. Siska
160.	Introduction to LEM Truck G and N	H. Engel
161.	Comparison of Schmidt Common Method with Maximum Likelihood Method for the Case of a Straight Line	L. Lustick
162.	Bissett-Berman Presentation at Houston, 9 January 1964	G. F. Floyd

Dear Hugo.

163. Pitfalls of Best Linear Estimates

164. Application of the MSFN to LEM Aborts

165. A Method for Calculating the Explicit Form of the Rotation Matrix which Carries Two Initial Vectors Into Two Terminal Vectors of the Same Length

166. Determination of Attitude of Spacecraft Via Application of Two Non-Collinear Boosts

167. Accuracy of Attitude Determination Based On MSFN Measurement of the Motion of the Transponder with Respect to the C.G.

168. Ground Station Determination of LEM Attitude

169. Checkout of Revised Error Program

170. An Approximate Technique to Estimate the Range Errors Due to the Troposphere

171. Bissett-Berman Presentation at Houston, 11 February 1964

APOLLO NOTE NO. 151

C. Siska
10 December 1963

PREDICTION OF RE-ENTRY DIVE ANGLE AND MISS DISTANCE FOR THE RETURN TO EARTH PHASE

Introduction

This paper examines a particular Return-to-Earth trajectory (starting from the lunar sphere of influence, LSOI), with the viewpoint of determining prediction accuracies for the re-entry dive angle and associated re-entry miss distance.

A safe landing using a zero-lift (emergency) atmosphere trajectory requires that the dive angle be predictable with a $\sigma = 0.1^{\circ}$ (see Apollo Note No. 53). This indicates the degree of accuracy with which the Return-to-Earth orbit should be determined before a midcourse correction can be efficiently executed. To minimize the velocity impulse, such correction should take place early in the return orbit and therefore, it is preferable to determine the orbit with the necessary degree of accuracy as soon as possible.

Although the optimum position for midcourse corrections is yet to be investigated in detail, a representative example of a two impulse correction mode is examined in Apollo Note No. 9. The example cited indicates that the first correction is made roughly at a radial position about 65% to 70% of the radius where tracking data is initiated. Since, in our case, tracking is assumed to start at the LSOI (342,000 km), this implies a first correction at about a 250,000 km. radius from the Earth, or about 35 hours to re-entry (see Figure 3).

A rough criterion of adequacy in return orbit prediction is therefore to be able to predict the dive angle with a σ of 0.1° by the time the vehicle is about 35 hours flight time from re-entry.

Prediction accuracies for the dive angle are examined for various combinations of the following parameters:

1. Either two or three tracking stations
2. Tracking duration from the LSOI

3. Range and/or range rate as the measurable
4. Range data with or without bias
5. A priori information on initial position

Item 5 above is included so as to anticipate the effect of tracking within the LSOI. The results from such tracking would appear as a priori data for the Earth-centered part of the return trajectory. At this writing, however, instrumentation of hyperbolic trajectories has not yet been completed, so that the selected values of a priori position at the LSOI are completely arbitrary.

Discussion of Assumptions

Several simplifications have been made in the situation geometry in order to simplify computations. First, the Earth is considered stationary during tracking observation so as to avoid station-to-station transfer, and therefore the latitudes of the tracking stations* involved were averaged so as to provide an average "look" at the returning vehicle. The resultant station locations appear as in Figure 1.

Additionally, the return orbit is considered to lie in the equatorial plane. Although the inclination angle of the orbit does not affect the dive angle prediction, it does influence the miss distance prediction (since this is computed assuming a rotating Earth). However, if the inclination angle is not too large, the root mean square miss distance (consisting of components within and normal to the reference orbit plane) should adequately describe the deviation for angles other than zero inclination.

It is assumed that only one station at a time collects observation data, so that a time sharing collection plan exists. This implies that each station can transmit as well as receive. Insofar as the number of

---

* The complex of tracking stations' assumed consisted of Goldstone, Madrid, Guam, Antigua, Ascension, Canberra, and Carnarvon.

observation points developed is less than what can be achieved using simultaneous data reception and processing by all stations, the time sharing plan appears to be conservative in estimation of prediction accuracy. In particular, each of three stations is assumed to obtain six one minute observations every twenty minute interval, while in the case of two stations, each station obtains nine one minute observations every twenty minute interval. Measurements errors for range and range rate are assumed to have standard deviations of 15 meters and 3 cm/sec., respectively.

The reference trajectory for the return-to-Earth has the characteristics outlined in Figure 2. Also included is a graph of radius versus time as presented in Figure 3 so that one can interpret time intervals in terms of radial position.

Results For Three Stations

The results using range plus range rate data differed so little from those using range data alone, that in the following, range plus range rate results are not presented.

Figure 4 shows the standard deviation in dive angle estimate as a function of time to re-entry for the case of three observing stations. The requirement for a dive angle $\sigma = 0.1^{\circ}$ is not adequately fulfilled by range rate data alone, since this accuracy is achieved at 13 hours to re-entry (or approximately 44 hours of tracking from the LSOI). If the a priori estimates of the position components x_o, y_o, z_o at the LSOI have a σ of 9 km., then the required accuracy is obtained at 27 hours to re-entry. This is not very satisfactory so that adequate prediction using range rate data above, requires a priori position estimates with a σ less than 9 km.

In the case of range data alone with an unknown constant bias, a dive angle σ of 0.1° is obtained at 37 hours to re-entry. According to the rough criterion stated in the introduction, this would appear to be marginally adequate. However, the primary source of bias

in range data stems from uncertainty in the value of the speed of light. Since this value is known to within an error of one part in a million, the range bias should have a maximum standard deviation of 342 meters (at the initial radius of 342,000 km.). This is considerably less than the predicted value of the unknown bias as will be shown later. Consequently, a priori information of the range bias will improve the case under discussion toward the values indicated in Figure 4 for the curve labeled range data with zero bias. Computations showing the effect of a priori information on range bias will be deferred to a later report.

Finally, it is seen that having a priori position data considerably improves the data obtained using range observations with an unknown constant bias.

Figure 5 shows the root mean square miss distance at re-entry (on the 400,000 ft. spherical re-entry surface). The RMS miss associated with dive angle predictions of 0.1° accuracy is of the order 20 to 50 km.

Two Station Results

Figure 6 shows the dive angle prediction accuracy for two stations (located as (1) and (2) in Figure 1). Note that range rate data alone is not adequate for prediction purposes unless there is a priori position information with accuracy on the order of 1.5 km. in each position co-ordinate. Note also that a priori information on range bias for the case of two stations is useless, since, even with range bias equal to zero (i.e., perfect information of the bias), the prediction accuracy for dive angle is inadequate. Here, a priori position information must be on the order of a σ equal to 2 km. in each position component to meet the accuracy criterion on dive angle.

It is noted that each set of two station data which has no a priori position information develops an ill-conditioned information matrix with a resulting poor inverse.

Figure 7 shows the corresponding results for the RMS miss distance. When the dive angle σ is 0.1°, the RMS miss again lies in the region between 20 and 50 km.

Prediction of Orbital Elements

Figure 8 indicates the accuracy with which the orbital elements of the Earth-centered part of the return trajectory can be estimated. The last column, labeled max.bias, depicts the largest deviation in predicting an unknown range bias amongst the set of observing stations. Generally, the magnitude of the deviation was quite similar for each observing station.

As mentioned before, a priori information of the range bias indicates a maximum deviation of 342 meters. Whenever the predicted estimate of the unknown bias is greater than this value, the a priori bias information should improve the tabulated results. Consequently, in all pertinent cases, improved prediction estimates are expected except in the case for 3 station range data with a priori position information.

It is noted that several of the cases computed yield unrealistic results for dive angle prediction. For example, an error $\Delta\dot{y}_o$ which increases the value of $\dot{y}_o$ by more than 1 meter/sec., would result in a trajectory which completely misses the re-entry sphere, unless there are other compensating errors (such as negative errors to $\dot{x}_o$). Such condition exists in the instance of 2 stations using range data with zero bias as shown by the deviations in $\dot{y}_o$ in Figure 8. Predicted orbits which miss the re-entry sphere should be excluded from consideration in computing dive angle (and miss distance) estimates. Then the estimates which follow are qualified with a conditional probability of occurrence.

Generally, whenever the dive angle estimates meet the criterion of $\sigma = 0.1^{\circ}$, the above considerations can be neglected.

The influence of a priori position data can be easily seen by examining the y_o and z_o estimates in the pertinent cases. In most

instances, the result of observations does not significantly improve the a priori estimates illustrating the difficulty in predicting initial position components y_o, z_o normal to the initial radius x_o.

Concluding Remarks

To summarize results, it appears that with tracking initiated at the LSOI, re-entry dive angle can be adequately predicted under the following minimum conditions:

1. Three station range data with unknown constant bias.
2. Three station range rate data with a priori information on each position component better than 9 km.
3. Two station range data with unknown constant bias and a priori information on each position component better than 2 km.
4. Two station range rate data with a priori information on each position component better than 1.5 km.

Additionally, when the dive angle is predicted with a $\sigma = 0.1^o$ the RMS re-entry miss distance is of the order 20 to 50 kms.

A continuation of the investigation of the return-to- Earth phase will involve the examination of:

1. Tracking within the LSOI.
2. Employment of midcourse corrections.
3. Timewise visibility of representative return trajectories to an observing station complex.

Station	Latitude	Longitude
1	-20°	+50°
2	+20°	-50°
3	-20°	-50°

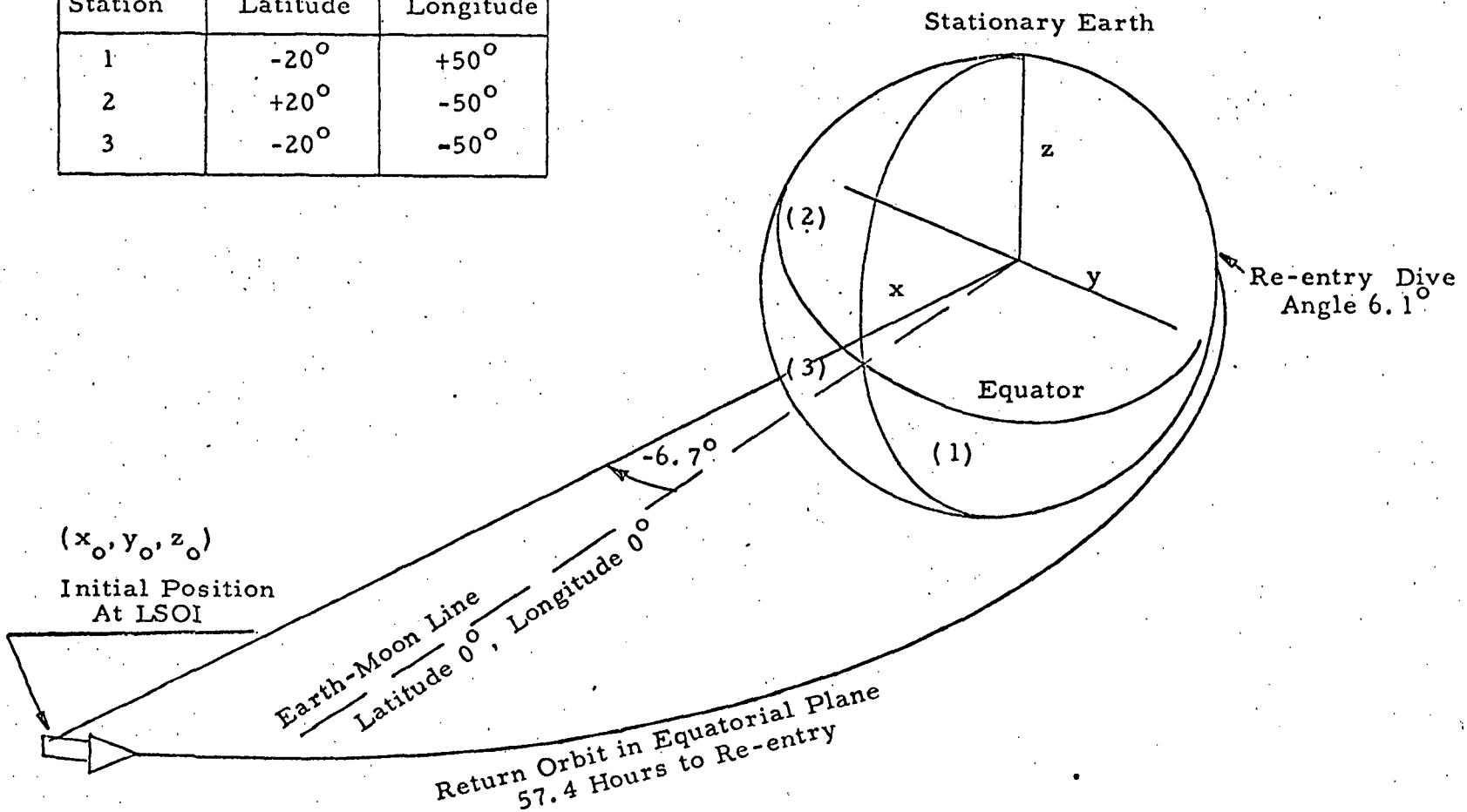

Figure 1.

Return-to-Earth Phase Tracking Geometry

ELEMENTS

$x_o = .3424310 \times 10^9$ m.

$y_o = 0$

$z_o = 0$

$\dot{x}_o = -.8541829 \times 10^3$ m/sec.

$\dot{y}_o = .2079809 \times 10^3$ m/sec.

$\dot{z}_o = 0$

OTHER PARAMETERS

$E = -.7807680$ km.^{2}/sec.^{2} (energy)

$H = .7121911 \times 10^5$ km.^{2}/sec. (momentum)

$e = .9748952$ (eccentricity)

$R_p = .6425795 \times 10^4$ km. (perigee radius)

$T = .2534944 \times 10^6$ sec. (time to perigee from x_o)

$R_F = .6492920 \times 10^4$ km. (re-entry radius; 400,000 ft. altitude)

$t_F = .2067903 \times 10^6$ sec. (time to R_F from x_o)

$\sigma_F = 6.094276$ degrees (dive angle at R_F)

Figure 2.

Return-to-Earth Reference Orbit Characteristics

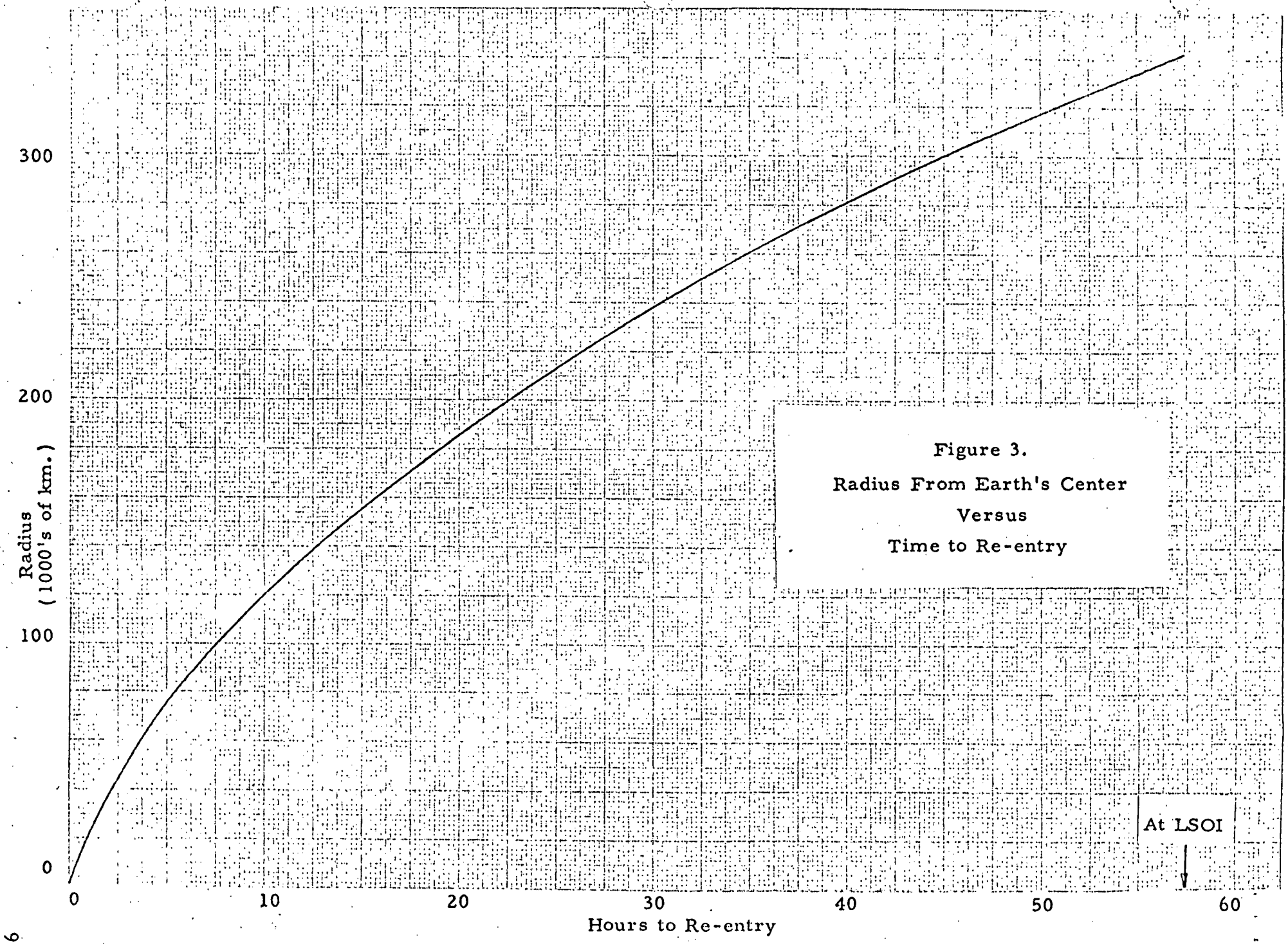

Figure 3.
Radius From Earth's Center
Versus
Time to Re-entry

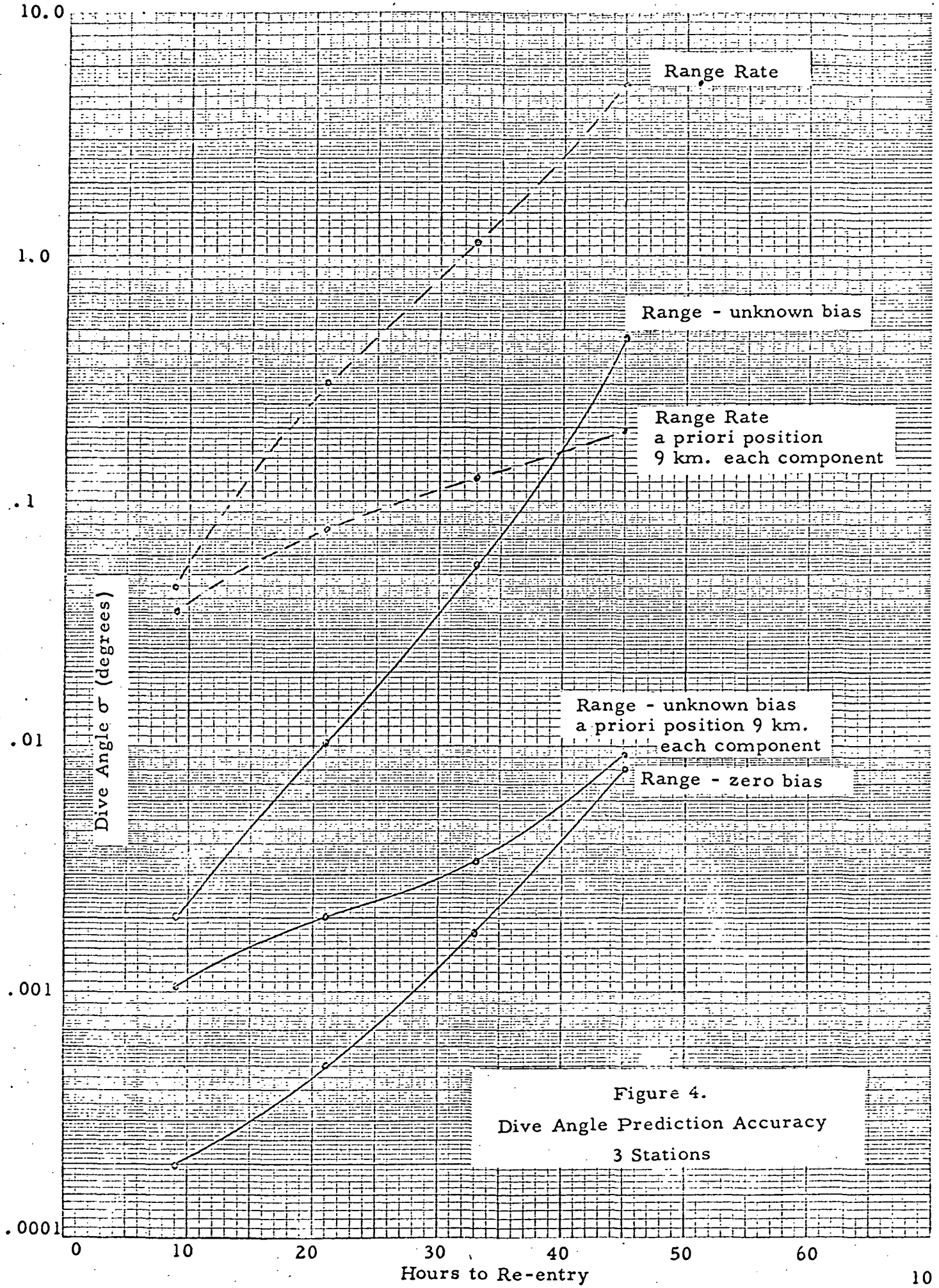

Figure 4.

Dive Angle Prediction Accuracy

3 Stations

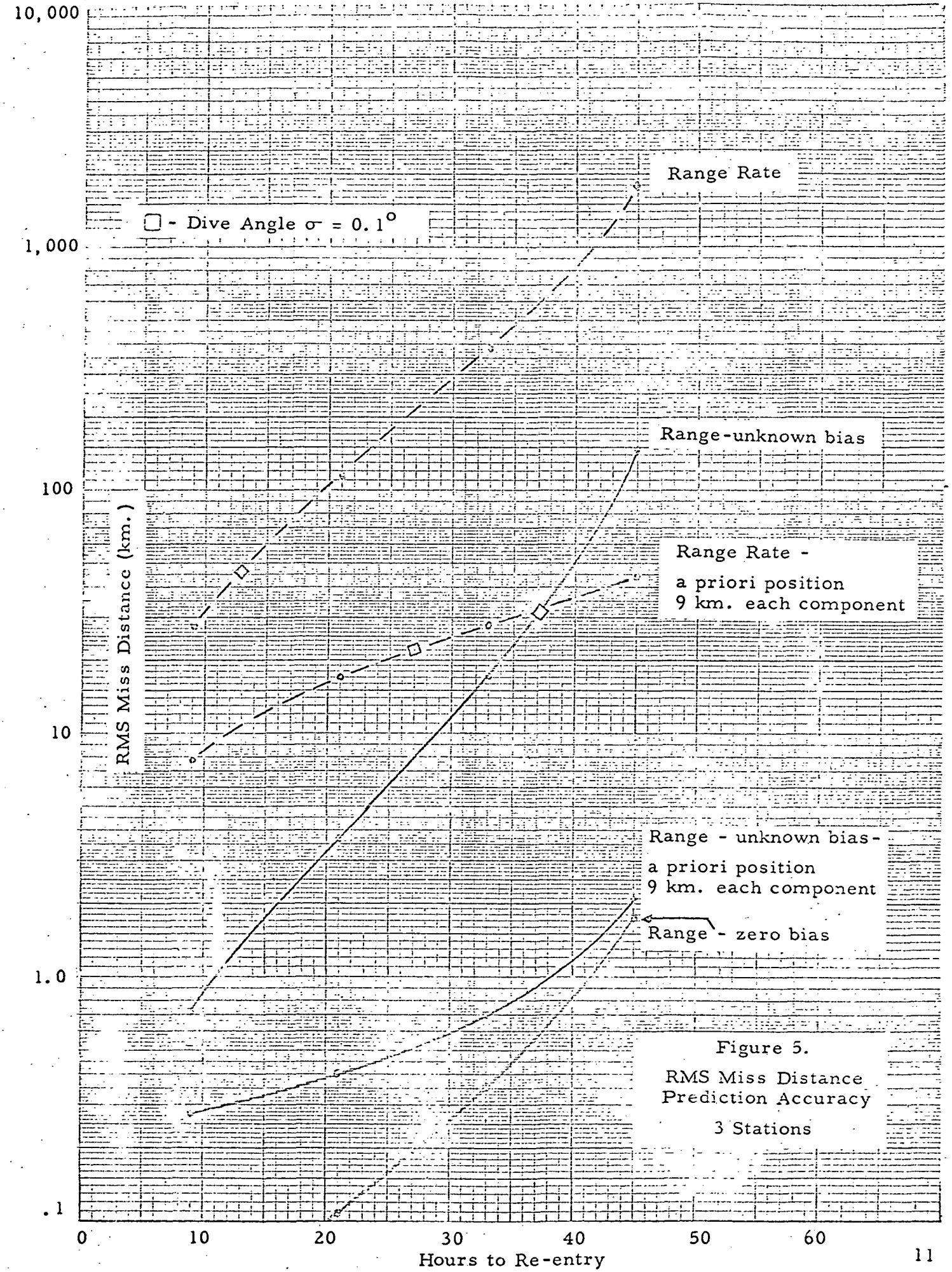

Figure 5.

RMS Miss Distance
Prediction Accuracy

3 Stations

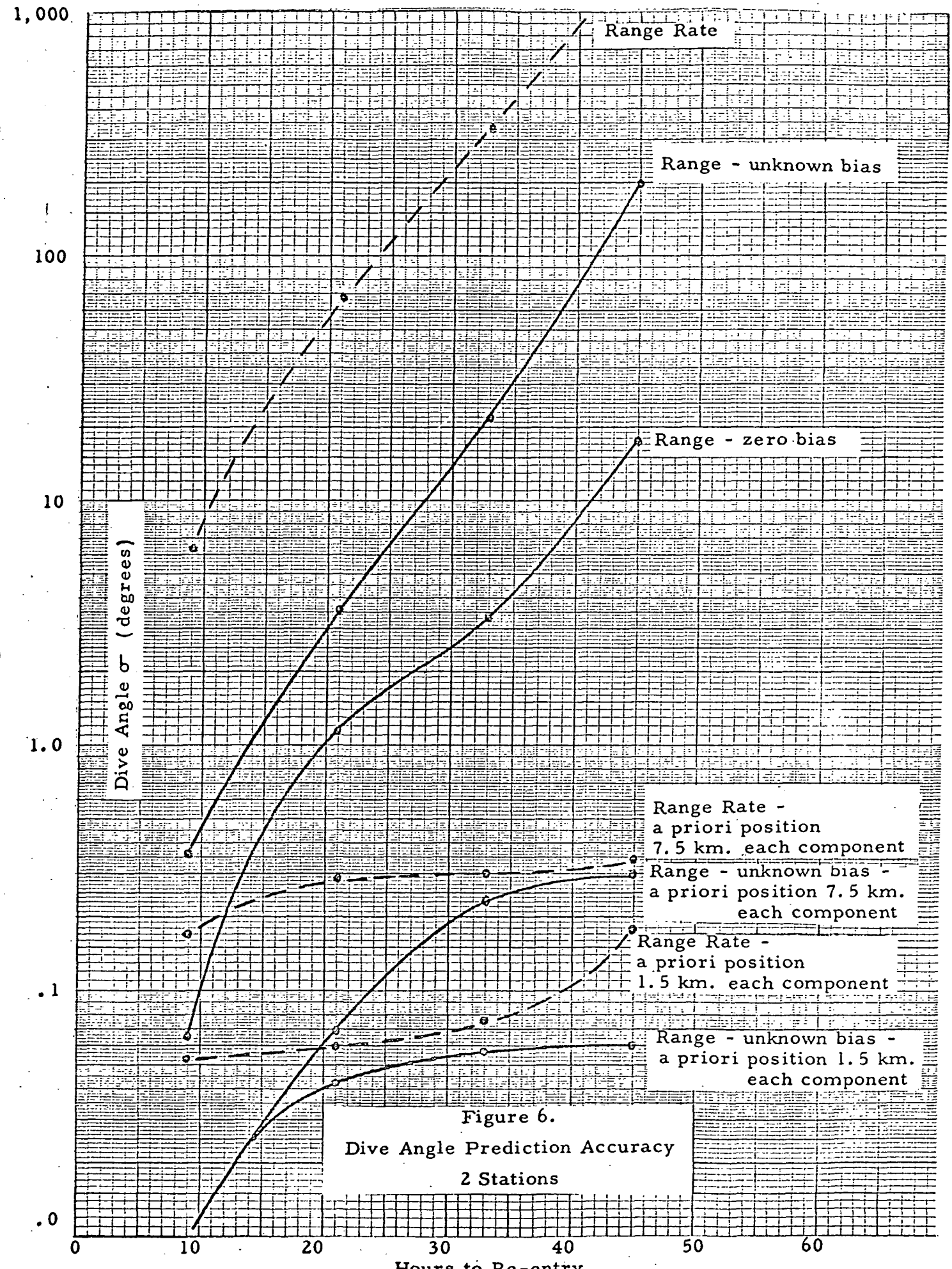

Figure 6.

Dive Angle Prediction Accuracy

2 Stations

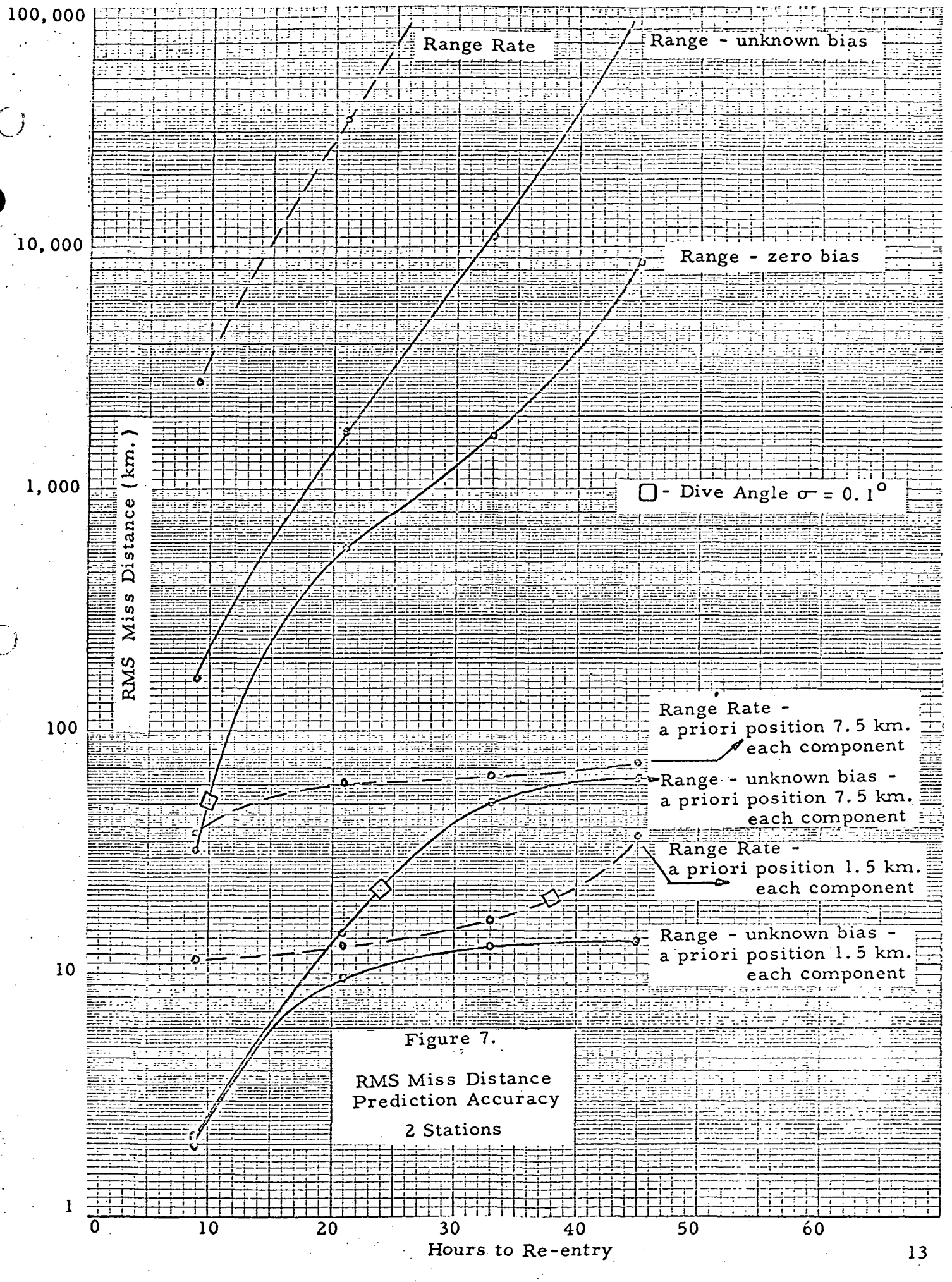

Figure 7.

RMS Miss Distance Prediction Accuracy

2 Stations

	Standard Deviation of Orbit Elements						
	x_o (m)	y_o (m)	z_o (m)	$\dot{x}_o$ $\left(\frac{m}{s}\right)$	$\dot{y}_o$ $\left(\frac{m}{s}\right)$	$\dot{z}_o$ $\left(\frac{m}{s}\right)$	max. bias (m)
Range -	.82 + 04*	.20 + 07	.42 + 07	.12 + 01	.53 + 01	.11 + 02	.49 + 05
	.91 + 03	.25 + 06	.53 + 06	.16 + 00	.65 + 00	.13 + 00	.64 + 04
Unknown Bias	.17 + 03	.60 + 05	.12 + 06	.36 - 01	.15 + 00	.29 + 00	.13 + 04
	.24 + 02	.13 + 05	.24 + 05	.80 - 02	.33 - 02	.58 - 01	.27 + 03
Range	.42 + 03	.90 + 04	.90 + 04	.55 - 02	.24 - 01	.24 - 01	.46 + 03
a priori position 9/9/9**	.93 + 02	.90 + 04	.90 + 04	.55 - 02	.24 - 01	.24 - 01	.18 + 03
	.44 + 02	.89 + 04	.90 + 04	.55 - 02	.24 - 01	.22 - 01	.15 + 03
Unknown bias	.18 + 02	.73 + 04	.86 + 04	.46 - 02	.18 - 01	.20 - 01	.12 + 03
Range	.17 + 01	.93 + 02	.22 + 03	.91 - 04	.33 - 02	.78 - 02	
	.13 + 01	.51 + 02	.14 + 03	.40 - 04	.75 - 03	.24 - 02	
Zero bias	.10 + 01	.35 + 02	.10 + 03	.25 - 04	.25 - 03	.11 - 02	
	.84 + 00	.27 + 02	.82 + 02	.18 - 04	.11 - 03	.58 - 03	
Range Rate	.89 + 05	.22 + 08	.47 + 08	.14 + 02	.58 + 02	.12 + 03	
	.18 + 05	.56 + 07	.11 + 08	.35 + 01	.15 + 02	.29 + 02	
	.47 + 04	.18 + 07	.36 + 07	.11 + 01	.47 + 01	.91 + 01	
	.12 + 04	.49 + 06	.85 + 06	.31 + 00	.12 + 01	.20 + 01	
Range Rate -	.55 + 04	.90 + 04	.90 + 04	.60 - 02	.82 - 01	.18 - 00	
a priori position 9/9/9	.33 + 04	.90 + 04	.90 + 04	.58 - 02	.55 - 01	.12 - 00	
	.20 + 04	.90 + 04	.90 + 04	.56 - 02	.38 - 01	.75 - 01	
	.10 + 04	.90 + 04	.90 + 04	.56 - 02	.27 - 01	.42 - 01	

* The set of 4 numbers corresponds to 45, 33, 21, and 9 hours to re-entry and is to be read as $.82 \times 10^{+4}$ etc.

** The numerical values associated with a priori position are the deviations in the x_o, y_o, z_o co-ordinates expressed in kilometers.

Figure 8 a.

Prediction Accuracies for Orbital Elements - Return-to-Earth - 3 Stations

	Standard Deviation of Orbit Elements						
	x_o (m)	y_o (m)	z_o (m)	$\dot{x}_o$ $\left(\frac{m}{s}\right)$	$\dot{y}_o$ $\left(\frac{m}{s}\right)$	$\dot{z}_o$ $\left(\frac{m}{s}\right)$	max. bias (m)
Range -	.19 + 07	.16 + 10	.34 + 10	.98 + 03	.40 + 04	.85 + 04	.52 + 06
Unknown Bias	.22 + 06	.18 + 09	.37 + 09	.11 + 03	.45 + 03	.91 + 03	.30 + 05
	.40 + 05	.27 + 08	.58 + 08	.16 + 02	.70 + 02	.14 + 03	.77 + 04
	.46 + 04	.24 + 07	.52 + 07	.15 + 01	.61 + 01	.13 + 01	.18 + 04
Range	.75 + 04	.75 + 04	.75 + 04	.46 - 02	.12 - 00	.25 - 00	.75 + 04
a priori position 7.5/ 7.5/7.5	.60 + 04	.75 + 04	.75 + 04	.46 - 02	.95 - 01	.21 - 00	.60 + 04
	.16 + 04	.75 + 04	.75 + 04	.46 - 02	.31 - 01	.63 - 01	.16 + 04
Unknown bias	.25 + 03	.66 + 04	.73 + 04	.40 - 02	.16 - 01	.21 - 01	.30 + 03
Range	.18 + 06	.14 + 09	.28 + 09	.85 + 02	.34 + 03	.70 + 03	
	.34 + 05	.25 + 08	.54 + 08	.15 + 02	.67 + 02	.13 + 03	
Zero bias	.12 + 05	.91 + 07	.19 + 08	.55 + 01	.22 + 02	.46 + 02	
	.67 + 03	.52 + 06	.11 + 07	.31 + 00	.13 + 01	.27 + 01	
Range Rate	.24 + 08	.19 + 11	.42 + 11	.12 + 05	.49 + 05	.10 + 06	
	.34 + 07	.25 + 10	.54 + 10	.15 + 04	.66 + 04	.13 + 05	
	.79 + 06	.52 + 09	.11 + 10	.21 + 03	.13 + 04	.27 + 04	
	.85 + 05	.42 + 08	.88 + 08	.17 + 02	.11 + 03	.22 + 03	
Range Rate -	.75 + 04	.75 + 04	.75 + 04	.52 - 01	.14 - 00	.33 - 00	
a priori position 7.5/ 7.5/7.5	.75 + 04	.75 + 04	.75 + 04	.48 - 01	.12 - 00	.28 - 00	
	.73 + 04	.75 + 04	.75 + 04	.48 - 01	.11 - 00	.27 - 00	
	.46 + 04	.75 + 04	.75 + 04	.48 - 02	.72 - 01	.16 - 00	

Figure 8 b.

Prediction Accuracies for Orbital Elements - Return-to-Earth - 2 Stations

APOLLO NOTE NO. 152

C. H. Dale
27 November 1963

OPTIMUM TIME FOR A SINGLE-BOOST CORRECTION TO THE LUNAR ASCENT TRAJECTORY TO MINIMIZE THE RENDEZVOUS MISS

After the ascent engine cut-off, the LEM will coast for some time during which the MSFN can track and predict orbit errors. Under the assumptions of this note, a single boost will then be made by the LEM to reduce the CSM/LEM miss at rendezvous. As the time allowed for tracking increases, the knowledge regarding the required correction increases. Thus with perfect boost capability, that is boost without errors, the longer one waits before making the correction the smaller will be the rendezvous miss. Note that this is accentuated because for greater pre-boost tracking times, less time remains for any remaining velocity errors to propagate. With perfect boost capability the actual trajectory errors after boost will nominally equal the covariance matrix of tracking errors at the time of boosting. These errors will propagate causing some rendezvous miss.

This situation is complicated in reality by the fact that boost corrections can not be made perfectly. From Apollo Note No. 14, a reasonable assumption is that the magnitude of an error in a boost correction is directly proportional to the magnitude of the boost correction. It is also likely that the direction of that error is spherically distributed. These assumptions may be analytically expressed by:

$$\sigma\dot{x}^2 = \sigma\dot{y}^2 = \sigma\dot{z}^2 = \left(0.0nV_1\right)^2 \qquad (1)$$

where n is probably about 1 or 2 and V_1 is the magnitude of the MSFN estimated boost correction. At the termination of ascent thrust, V_1 is equal to the boost cut-off error, V_o. However, as the time required for

tracking elapses, the required correction to reduce the rendezvous miss to zero propagates and grows. As will be shown later, $V_1/V_o = 3.28$ after twenty-five minutes of tracking. Thus the errors introduced to the trajectory, $\sigma_{\dot{x}}$, $\sigma_{\dot{y}}$, and $\sigma_{\dot{z}}$, due to boosting increase with tracking time.

The object of this note is to determine the optimum time to correct the LEM trajectory, with increased time decreasing the miss due to tracking errors but increasing the miss due to boosting errors. The analysis is of course limited to tracking the LEM during the Earth-visible portion of its trajectory.

The Propagation of Cut-Off Errors $\left[V_1 = f(V_0, t)\right]$:

The following is an analytic explanation of how an initial error in the ascent cut-off velocity, V_o, will propagate with time into a larger required boost correction, V_1.

Note, first of all, that only "in-plane" errors in the cut-off velocity need be considered. This rather fortuitous fact rests simply on the assumption of a 180^o Hohmann ascent. Thus an initial small out-of-plane error simply rotates the plane of the ascent trajectory. The nominal rendezvous with the CSM would still occur at the same point in time and space.

In Apollo Note No. 10, the perturbation equations are used to express the perturbed position and velocity of the LEM at some time, t, after boost cut-off as a function of the initial velocity errors. No initial position errors are assumed. Defining $\dot{x}_o$ as the initial error in horizontal velocity and $\dot{y}_o$ as the initial error in the local vertical velocity, then the future errors in position are:

for an error, $\dot{x}_o$	for an error, $\dot{y}_o$	
$\frac{x_1}{\dot{x}_o} = \frac{2}{\omega}\left(2\sin\omega t - \frac{3\omega t}{2}\right)$	$\frac{x_1}{\dot{y}_o} = \frac{2}{\omega}(\cos\omega t - 1)$	(2)
$\frac{y_1}{\dot{x}_o} = \frac{2}{\omega}(1 - \cos\omega t)$	$\frac{y_1}{\dot{y}_o} = \frac{2}{\omega}\left(\frac{\sin\omega t}{2}\right)$	(3)

where ω is the approximate central angular rate of the nominal ascent trajectory. Then by differentiation:

$$\frac{\dot{x}_1}{\dot{x}_o} = 4\cos\omega t - 3 \qquad \frac{\dot{x}_1}{\dot{y}_o} = -2\sin\omega t \tag{4}$$

$$\frac{\dot{y}_1}{\dot{x}_o} = 2\sin\omega t \qquad \frac{\dot{y}_1}{\dot{y}_o} = \cos\omega t \tag{5}$$

Now the correct velocity at x_1, y_1, t is defined to return the LEM to $x = 0$, $y = 0$ in the time remaining, t_{go}. If T is the total time for the Hohmann maneuver and $\omega T = 180^o$, then ωt may be defined as θ and $\omega (T-t) = \pi - \theta$. From Apollo Note No. 7, Equations (11) and (12), we can write:

$$x(t_{go}=0) \equiv 0 = \frac{\dot{x}_2}{\omega}\left[4\sin(\pi-\theta) - 3(\pi-\theta)\right] + \frac{\dot{y}_2}{\omega}\left[2\cos(\pi-\theta) - 2\right] + x_1 + y_1\left[6\sin(\pi-\theta) - 6(\pi-\theta)\right] \tag{6}$$

$$y(t_{go}=0) \equiv 0 = \frac{\dot{x}_2}{\omega}\left[2 - 2\cos(\pi-\theta)\right] + \frac{\dot{y}_2}{\omega}\left[\sin(\pi-\theta)\right] + y_1\left[4-\cos(\pi-\theta)\right] \tag{7}$$

where $\dot{x}_2$ and $\dot{y}_2$ are the correct LEM perturbation velocities after boost to return the LEM to a zero miss rendezvous. Using the auxillary Equations (2) and (3), these Equations, (4) and (5), may be solved for $\frac{\dot{x}_2}{\dot{x}_o}$ and $\frac{\dot{y}_2}{\dot{x}_o}$ assuming an error in the initial horizontal velocity, and for $\frac{\dot{x}_2}{\dot{y}_o}$ and $\frac{\dot{y}_2}{\dot{y}_o}$ assuming an error in the initial vertical velocity.

Now if the perturbations before and after the boost are expressed for an initial error, $\dot{x}_o$, and $\dot{y}_o$ separately:

for an error, $\dot{x}_o$	for an error, $\dot{y}_o$	
$\frac{\Delta\dot{x}}{\dot{x}_o} = \frac{\dot{x}_2}{\dot{x}_o} - \frac{\dot{x}_1}{\dot{x}_o}$	$\frac{\Delta\dot{x}}{\dot{y}_o} = \frac{\dot{x}_2}{\dot{y}_o} - \frac{\dot{x}_1}{\dot{y}_o}$	(8)
$\frac{\Delta\dot{y}}{\dot{x}_o} = \frac{\dot{y}_2}{\dot{x}_o} - \frac{\dot{y}_1}{\dot{x}_o}$	$\frac{\Delta\dot{y}}{\dot{y}_o} = \frac{\dot{y}_2}{\dot{y}_o} - \frac{\dot{y}_1}{\dot{y}_o}$	(9)

An initial basic assumption is that $\dot{x}_o$ and $\dot{y}_o$ are random variables of equal size and probability. Thus the expected correction, $\Delta\dot{x}$, due to some initial error, v_o, should be the root mean square of the two components of Equation (8).

$$\frac{\Delta\dot{x}}{v_o} = \sqrt{\frac{1}{2}\left[\left(\frac{\Delta\dot{x}}{\dot{x}_o}\right)^2 + \left(\frac{\Delta\dot{x}}{\dot{y}_o}\right)^2\right]} \tag{10}$$

$$\frac{\Delta\dot{y}}{v_o} = \sqrt{\frac{1}{2}\left[\left(\frac{\Delta\dot{y}}{\dot{x}_o}\right)^2 + \left(\frac{\Delta\dot{y}}{\dot{y}_o}\right)^2\right]} \tag{11}$$

Now since $\Delta\dot{x}$ and $\Delta\dot{y}$ are orthogonal components of the boost correction, Δv, then

(12)

$$\frac{\Delta v}{v_o} = \sqrt{\left(\frac{\Delta\dot{x}}{v_o}\right)^2 + \left(\frac{\Delta\dot{y}}{v_o}\right)^2} = \sqrt{\frac{1}{2}\left[\left(\frac{\Delta\dot{x}}{\dot{x}_o}\right)^2 + \left(\frac{\Delta\dot{x}}{\dot{y}_o}\right)^2 + \left(\frac{\Delta\dot{y}}{\dot{x}_o}\right)^2 + \left(\frac{\Delta\dot{y}}{\dot{y}_o}\right)^2\right]}$$

This equation is plotted in Figure 1 and expresses the magnitude, Δv, of the expected boost correction for a given magnitude, v_o, of error in the initial ascent velocity, all as a function of elapsed time (or angle)

after ascent engine cut-off.

Statistics and the Use of the Computer Program

The computer program, outlined in Apollo Note No. 82, can be used to calculate the covariance matrix of the orbit parameter estimators at any time as a function of the type of MSFN stations and the duration of tracking. Defining:

A_o = a priori information matrix at T_o, the initiation of tracking at the end of ascent boosting.

C_o^{-1} = the information matrix due to tracking for T_1, the time just prior to the correction boost

Then the total information matrix just prior to boosting is C_1^{-1} which is

$$C_1^{-1} = A_o + C_o^{-1} \tag{13}$$

The covariance matrix just prior to boosting, C_1, is the inverse of the information matrix

$$C_1 = \left[A_o + C_o^{-1}\right]^{-1} \tag{14}$$

The actual expected position and velocity errors after boosting take the form of a covariance matrix. The errors are made up of two parts: first, there is the error due to tracking uncertainty, which is simply C_1; and second, there is an expected error in making the boost. If from Equation (12) a boost of magnitude Δv is required, then V_1 may be defined as the MSFN estimate of Δv. Thus the magnitude of V_1 is equal to the vector sum of Δv and the three velocity error components of C_1. Defining these three components (the fourth, fifth, and sixth diagonal components of C_1) as V_2 then from Equation (1)

$$\sigma\dot{x}^2 = \sigma\dot{y}^2 = \sigma\dot{z}^2 = 0.0n\,V_1 = 0.0n\left(\Delta v + \left|V_2\right|\right) \tag{15}$$

The covariance matrix immediately after boosting may be defined as C_2

$$C_2 = C_1 + \begin{bmatrix} 0 & 0 & 0 & 0 & 0 & 0 \\ 0 & 0 & 0 & 0 & 0 & 0 \\ 0 & 0 & 0 & 0 & 0 & 0 \\ 0 & 0 & 0 & \sigma\dot{x}^2 & 0 & 0 \\ 0 & 0 & 0 & 0 & \sigma\dot{y}^2 & 0 \\ 0 & 0 & 0 & 0 & 0 & \sigma\dot{z}^2 \end{bmatrix} \tag{16}$$

Due to a computational difficulty a slight approximation was made to Equation(15). This approximation consists of neglecting $0.0n V_2$ in the boost. Thus where the three diagonal components should be exactly

$$(C_2)_{44} = (C_1)_{44} + 0.0n\left(\Delta v + \sqrt{(C_1)_{44}^2 + (C_1)_{55}^2 + (C_1)_{66}^2}\right)$$

$$(C_2)_{55} = (C_1)_{55} + 0.0n\left(\Delta v + \sqrt{(C_1)_{44}^2 + (C_1)_{55}^2 + (C_1)_{66}^2}\right)$$

$$(C_2)_{66} = (C_1)_{66} + 0.0n\left(\Delta v + \sqrt{(C_1)_{44}^2 + (C_1)_{55}^2 + (C_1)_{66}^2}\right)$$

in actual practice the square root term has been neglected. It is easy to see that this causes a maximum error in the estimate of the velocity error after boost when Δv is zero. Even in this case the error in the estimate is only n% (about 1 or 2 %). This is surely a second order effect which will shift the optimum time of boost only a small amount.

The covariance matrix at rendezvous, C_r, at rendezvous time = T_r, can be computed by the transformation

$$C_r = Q(T_r)\, C_2 Q^T(T_r) \tag{17}$$

as given in Apollo Note No. 95.

Computations and Results (data sets 61 through 79)

The optimum time for a single-boost correction will naturally depend on the quality of MSFN tracking. At this time it appears that our best estimate of reality is outlined in Apollo Note No. 148. Thus in the included computations two stations are assumed, Madrid and Johannesburg. Each Doppler station measures change in range, which can be viewed as measurement of range with a fixed, unknown bias. In this case σ R has been assumed to be 0.6 meters for one minute uncorrelated samples. The "standard" lunar ascent trajectory used herein is described in Apollo Note No. 135 (with the a priori information matrix designated as A_1).

Figure 2 shows the 1 σ minimum miss near rendezvous (defined as the closest approach) as a function of the time of boost correction. This function is shown with $0.0nV_o$ as a parameter. To reiterate, n is the per cent error that can be expected in the velocity of the boost correction and V_o is the expected error in the perilune or ascent-cut-off velocity. Following is an example calculation based upon the use of this data:

> Assume that the expected value of the LEM ascent engine cut-off error is 12 meters per second (equally likely in any direction). Assume further that the corrective boost may be made with an expected error of 1.5% of the necessary magnitude of correction (again the error is assumed to be spherically distributed). Thus n = 1.5 and $0.0n\ V_o = .18$. In Figure 2 the minima of all curves of various values of $0.0n\ V_o$ have been connected. From this cross-plot the point, $0.0n\ V_o = .18$, may be entered giving a minimum miss of about 1.2×10^3 meters with an optimum boost time near 19 minutes after ascent engine cut-off. It may also be noted that for this example case, the minimum miss doubles for a variation of about 6 minutes either way from optimum.

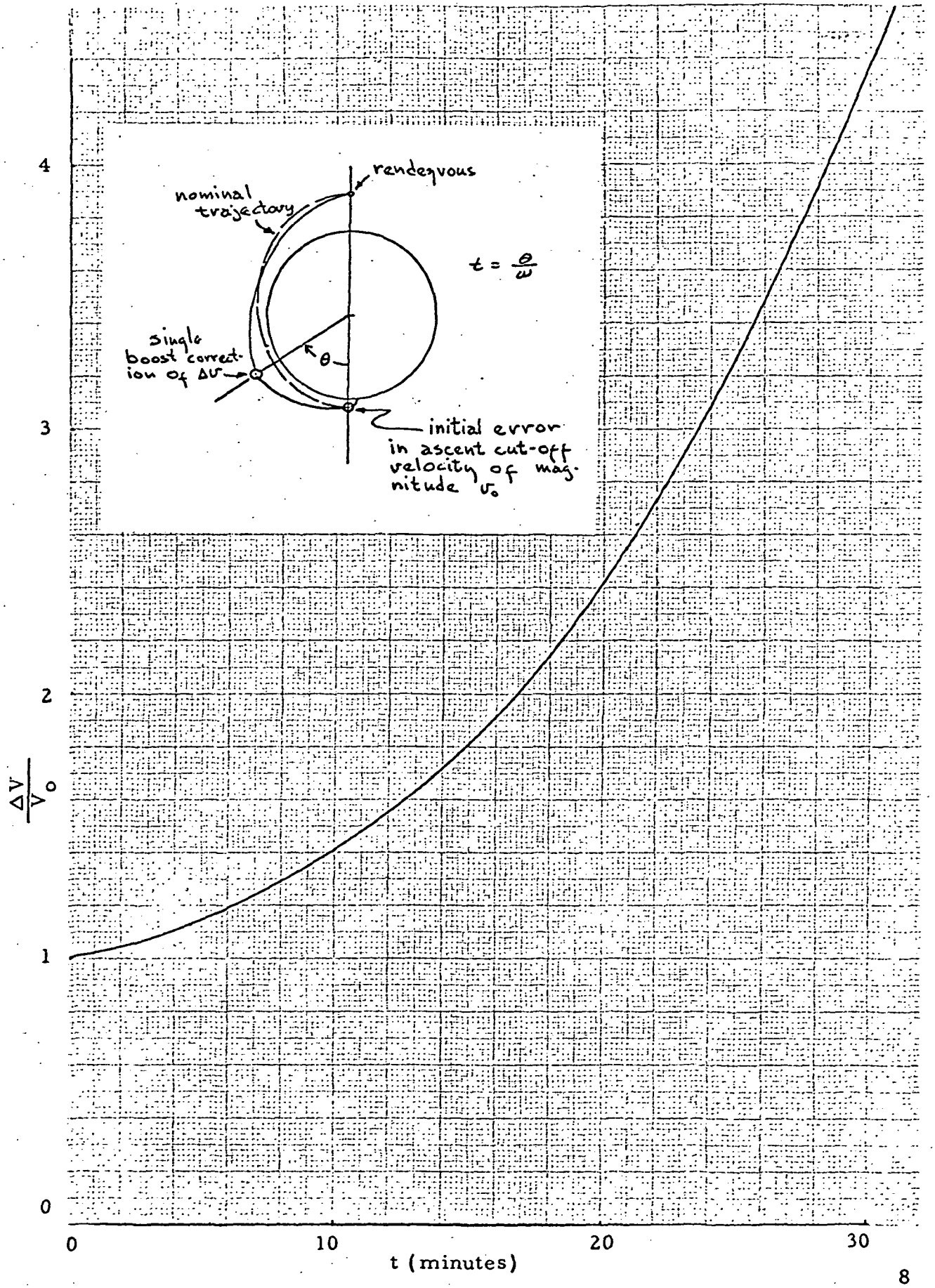

Figure 1.

Growth in Magnitude of the Single-Boost Correction as a Function of Time after Ascent Engine Cut-Off

Two Stations (Madrid and Johannesburg) with A Priori Information. Measurable was Range with a Bias. σ R = 0.6 Meters for One Minute Observations

n ≡ % error of corrective boost
V_o ≡ magnitude of error in perilune velocity

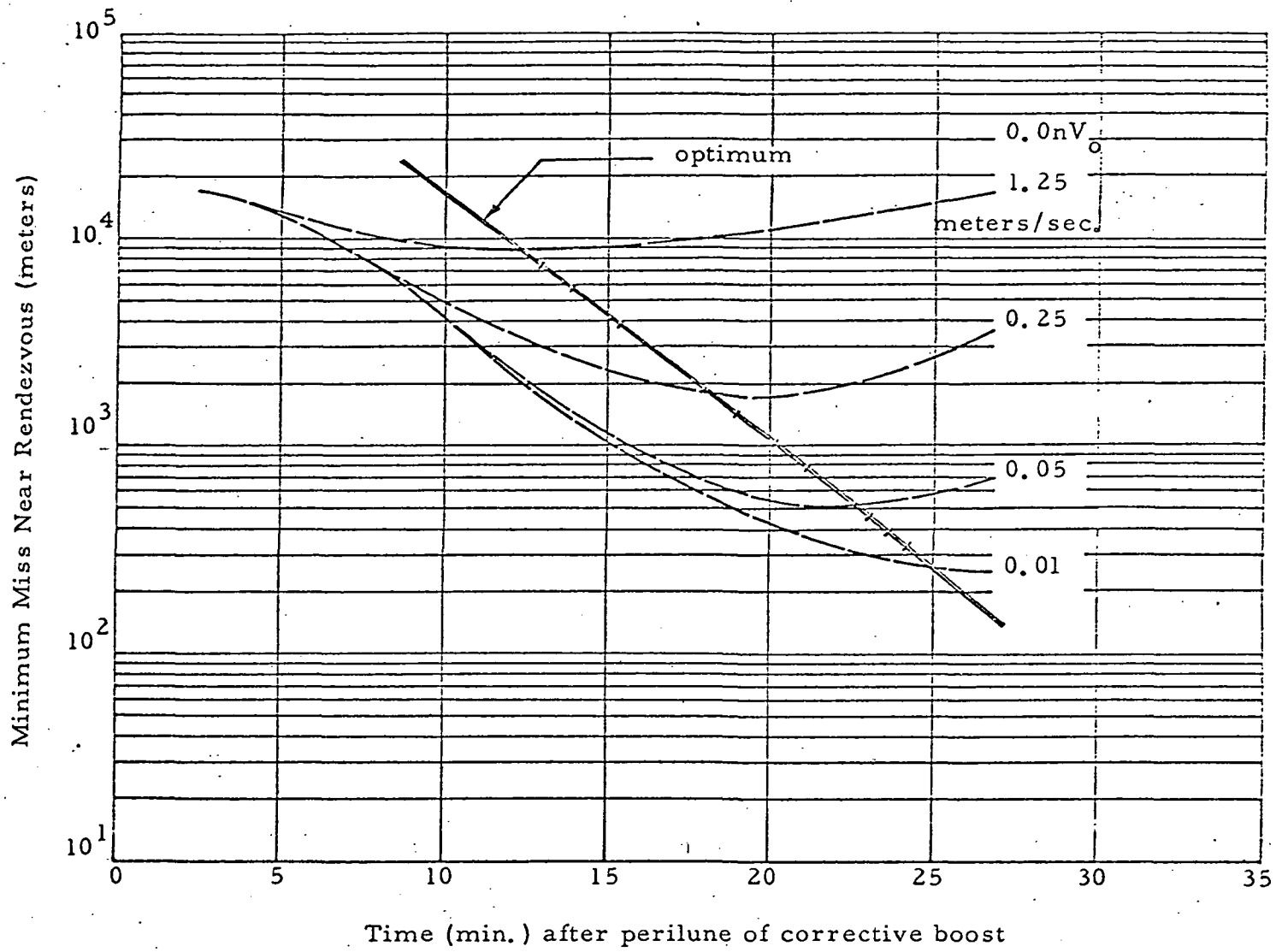

Figure 2.

Expected Minimum Miss Near Rendezvous for a Single Corrective Boost as a Function of MSFN Tracking Time Before Boosting

APOLLO NOTE NO. 153 C. H. Dale

MSFN TRACKING OF A TRUCK VEHICLE DURING LUNAR DESCENT TO PERILUNE

This note discusses the ability of the MSFN to aid in the lunar descent of a truck or supply vehicle. In the case studied the vehicle is initially in an 80 nautical mile circular lunar orbit. When the vehicle is directly opposite the Earth a Hohmann maneuver is initiated which will bring the truck to a point about 8 miles above the lunar surface and in the apparent center of the lunar disk at perilune. The time between the initiation of the descent (apolune) and perilune is 58.05 minutes, and from Apollo Note No. 109, it can be seen that for the first 25 minutes of the descent the vehicle will not be usable from the Earth. Thus, roughly 33 minutes of tracking are available to the MSFN. Figure 1 shows the geometry of the tracking problem.

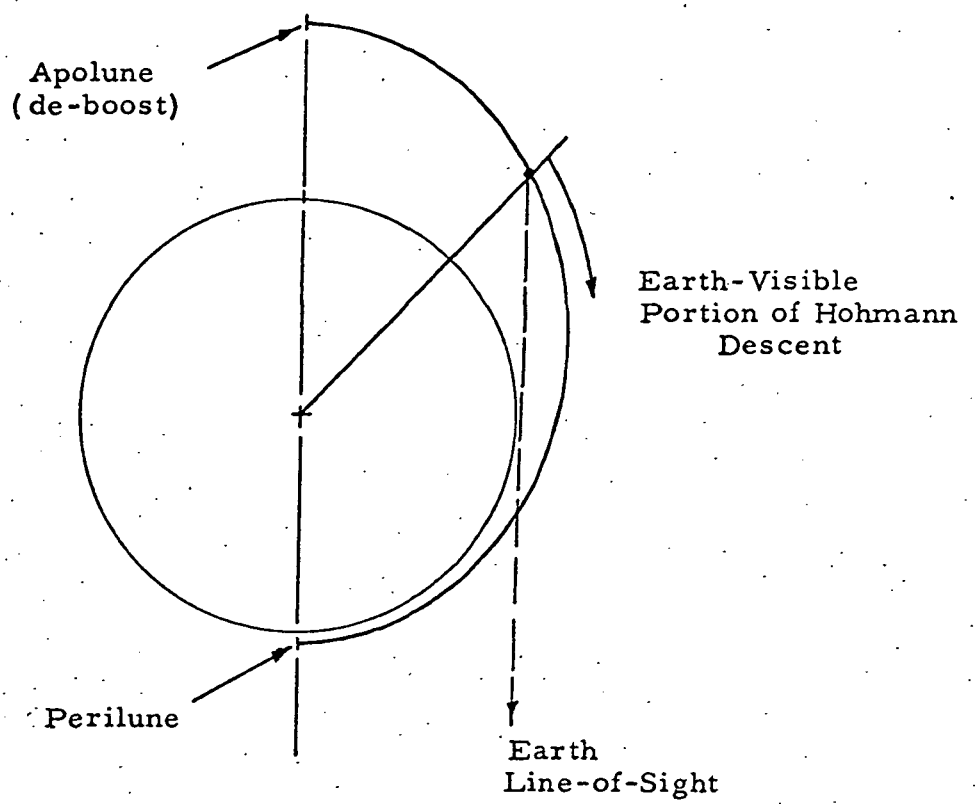

Figure 1.
A Sketch of the Geometry

Following the notation of previous Apollo Notes, the inputs to this problem are as follows:

A_1	=	.188546 + 7 m	
A_4	=	.0	
A_5	=	.158171 + 4 m/sec.	
GAM ID	=	.1 + 1	
BETA	=	.18308 + 2 deg.	
XI	=	.0 deg.	
ETA	=	.180 + 3 deg.	
ZETA	=	.0 deg.	
LAMBDA	=	.410 + 2 deg.	for Madrid; -.260 + 2 deg. for Johannesburg
ALPHA	=	-.400 + 1 deg.	for Madrid; .280 + 2 deg. for Johannesburg
OMEGA E	=	.729116 - 4 rad/sec.	
OMEGA M	=	.4236 - 6 rad/sec.	
RHO E	=	.63781 + 7 m	
RHO M	=	.385 + 9 m	
MU	=	.4896 + 12 $m^3/sec.^2$	
BIG L	=	.150 + 2 deg.	
SMA L	=	.900 + 2 deg.	Program 1 Data Sets 82, 83
SD IND	=	1	
S IND	=	1	
TJ	=	30, 35, 45, 58 min.	
Q IND	=	.0	
QF	=	.5805 + 2 min.	
TI (initial)	=	.250 + 2 min.	
TI (interval)	=	.1 + 1 min.	

Immediately after boosting at apolune the truck vehicle has a reasonable idea of where it is. Using techniques similar to Apollo Note No. 42, an a priori information matrix may be generated.

Prior to boost the 1 σ position and velocity errors are a function of how often sightings have been made. An appropriate model might be:

a. landmarks known to 1/4 mile

b. 1 mn. sighting accuracy

c. 5 sightings

d. 5 minutes per sighting

e. sighting 4 min. prior to the separation and/or de-orbit

Now according to the "Abstract of Meeting of Guidance Analysis Panel on LEM Guidance of January 11, 1963, at MIT/IL," the expected initial errors before de-boost are:

$x, \dot{x}$ = 245 ft. and 0.6 ft/sec. away from the Moon

$y, \dot{y}$ = 820 ft. and 0.2 ft/sec. along the track

$z, \dot{z}$ = 930 ft. and 0.9 ft/sec. out of plane

The de-boost is 44 ft/second, correct to 0.5 ft/sec., and will occur in about 3.5 seconds. The accelerometers are accurate to about 0.0085 ft/sec.^{2} and the initial platform alignment may be assured to be within 0.5 mils. Thus the errors in velocity components after boosting can be assumed to be:

$$\sigma\dot{x} = \sqrt{(.6)^2 + (.0085 \times 3.5)^2 + (44 \times .005)^2} = .64 \text{ ft/sec.} = .20 \text{ m/sec.}$$

$$\sigma\dot{y} = \sqrt{(.2)^2 + (.0085 \times 3.5)^2 + (.5)^2} = .54 \text{ ft/sec.} = .16 \text{ m/sec.}$$

$$\sigma\dot{z} = \sqrt{(.9)^2 + (.0085 \times 3.5)^2 + (44 \times .005)^2} = .93 \text{ ft/sec.} = .28 \text{ m/sec.}$$

The initial satellite velocity is 5,233 ft/sec. and about a 0.1 second timing error is reasonable. Thus the positional errors after de-boosting are about

$$\sigma x = \sigma x_o = 245 \text{ ft.} = 75 \text{ m.}$$

$$\sigma y = \sqrt{(820)^2 + (523)^2} = 973 \text{ ft.} = 300 \text{ m.}$$

$$\sigma z = \sigma z_o = 930 \text{ ft.} = 280 \text{ m.}$$

Now the above six terms are the square root of the variances, that is the diagonal components of the covariance matrix of a priori information. The a priori information matrix is the inverse of the a priori covariance matrix and is thus

$$A = \begin{bmatrix} .177 \times 10^{3} & 0 & 0 & 0 & 0 & 0 \\ 0 & .111 \times 10^{-4} & 0 & 0 & 0 & 0 \\ 0 & 0 & .127 \times 10^{-4} & 0 & 0 & 0 \\ 0 & 0 & 0 & .25 \times 10^{2} & 0 & 0 \\ 0 & 0 & 0 & 0 & .39 \times 10^{2} & 0 \\ 0 & 0 & 0 & 0 & 0 & .13 \times 10^{2} \end{bmatrix}$$

In practice the actual a priori information may well vary from that shown above, and so cases were computed assuming no a priori information.

At perilune a radar altimeter can be used to measure altitude (x within a constant) and altitude rate. What cannot be easily measured directly with an unmanned truck are y, $\dot{y}$, z and $\dot{z}$. These are shown in Figures 2 and 3. From these results it would appear that the MSFN can do a quite reasonable job of AGC updating at least fifteen minutes prior to perilune (the initiation of thrusting descent). Further studies of the IMU and AGC during the thrusting descent to touchdown would be required to estimate the footprint and general velocity accuracies at touchdown, however the perilune conditions shown in Figures 2 and 3 appear to be a good start.

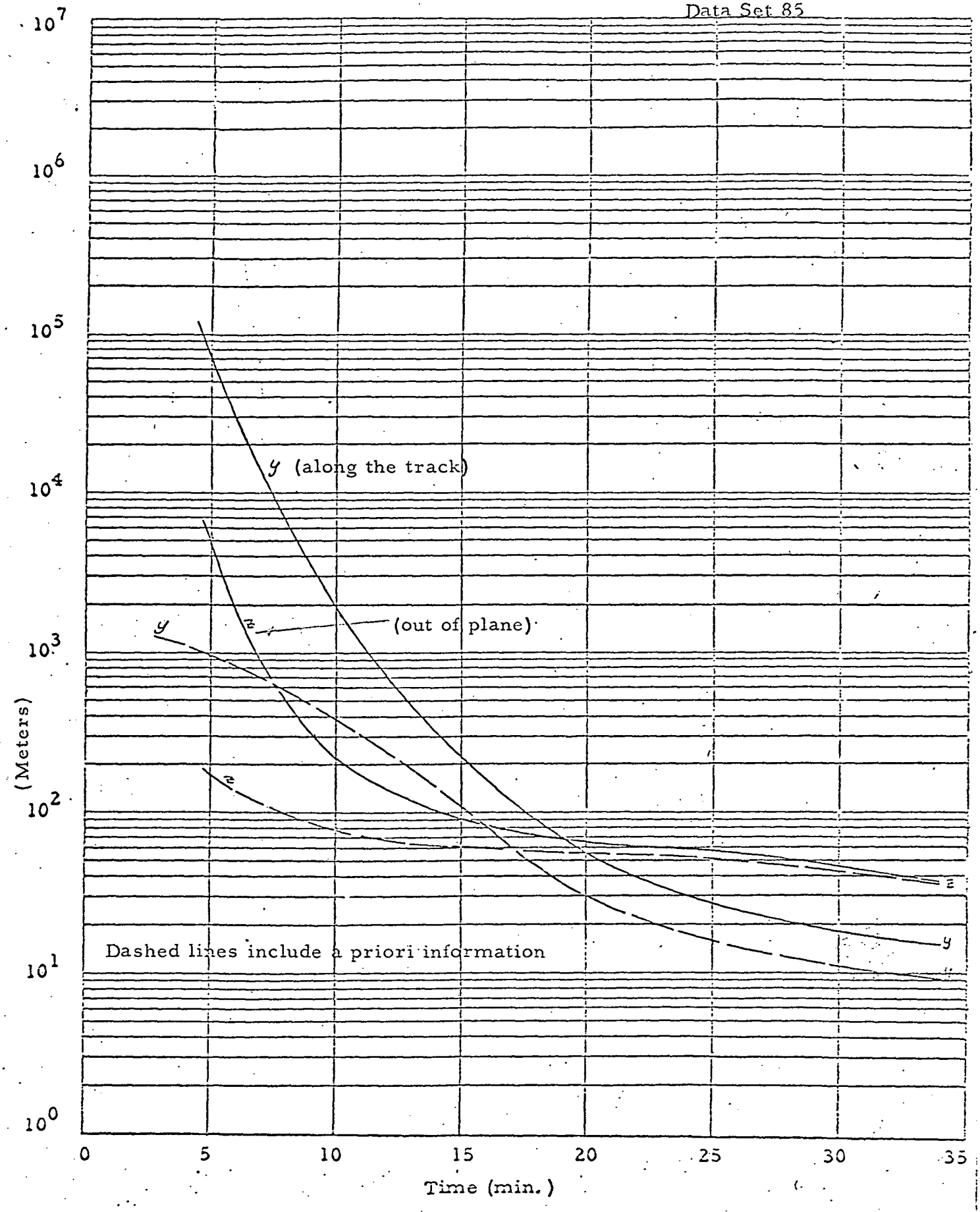

Figure 2.

Horizontal Positional Errors at Perilune for the Lunar Truck Descent as a Function of Tracking Time

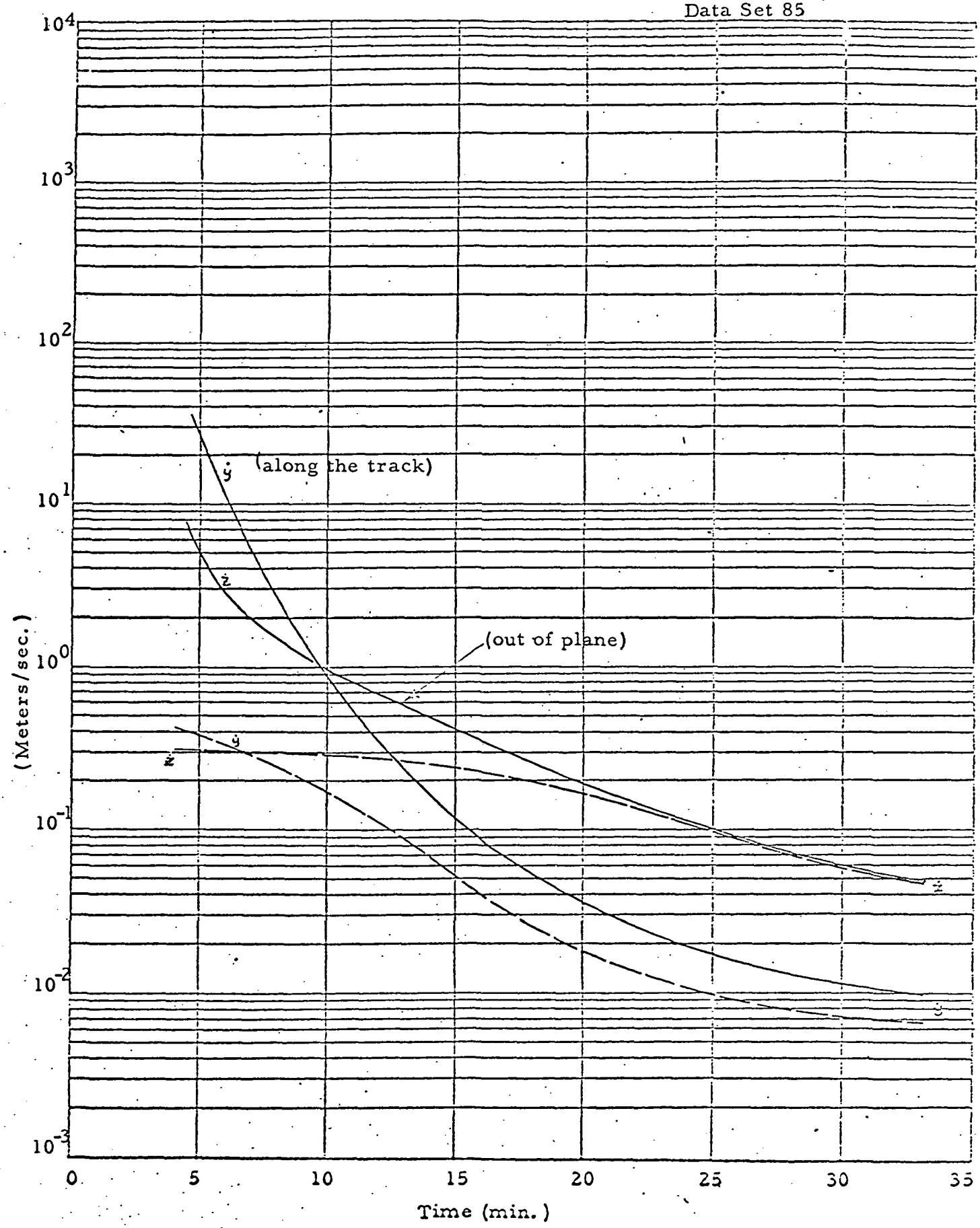

Figure 3.

Horizontal Velocity Component Errors at Perilune for the Lunar Truck Descent as a Function of Tracking Time

APOLLO NOTE NO. 154

H. Engel
16 December 1963

FURTHER ESTIMATES OF EARTH-MOON INJECTION ERRORS, II

This note adds one more case to those displayed in Apollo Note No. 142.

The cases exhibited now are:

1. UFS from Carnarvon and Canberra. Range data only, σ_R = 15 m. for 1 sec. samples. Unknown fixed range biases.

2. UFS from Carnarvon. Range and two angles, σ_R = 15 m., $\sigma_{\phi_1} = \sigma_{\phi_2} = 8 \times 10^{-4}$ rad. for 1 sec. samples.

3. FPS-16 from Carnarvon. Range and two angles, σ_R = 6 m., $\sigma_{\phi_1} = \sigma_{\phi_2} = 2 \times 10^{-4}$ rad. for 1 sec. samples.

4. 1 and 3 combined.

A single radar, either UFS or FPS-16, yields velocity to better than 1 ft/sec., with ten minutes of tracking, so the Go-NoGo decision can be made.

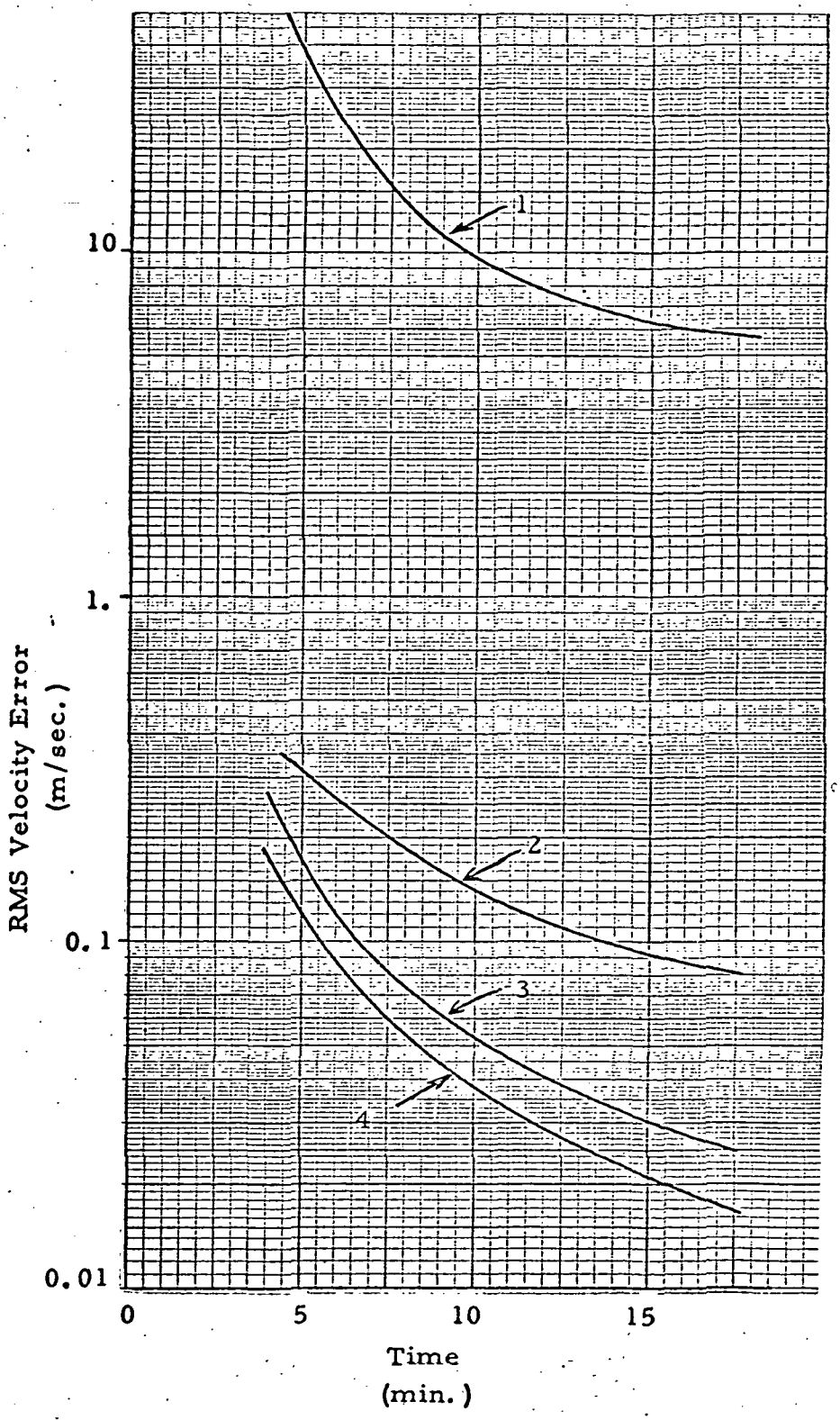
10
1.
0.1
0.01
RMS Velocity Error
(m/sec.)
0
5
10
15
Time
(min.)
1
2
3
4

APOLLO NOTE NO. 155

L. Lustick
19 December 1963

EFFECT OF UNCERTAINTY IN PARAMETERS WHICH ARE NOT ESTIMATED

Introduction

In the orbit determination problem, the measurable can be a function of parameters which are not known exactly. The purpose of this note is to determine the effect of the uncertainty in these parameters on the estimated orbit parameters. For example, the measurable is, in general, a function of the observing station location. If these parameters are not estimated, what effect do the uncertainties in these parameters have on the errors of the estimated orbit parameters.

Discussion

Let

M_k = measured quantity at time t_k

M_{c_k} = computed correct value of measurable at t_k

$A_{j=1-6}$ = orbit parameters to be estimated

$b_{j=1-n}$ = parameters not to be estimated

Then from the likelihood expressions the Δa_j are defined from equation (1)

$$\left[C_{i=1-6,\ j=1-6}\right]\left[\Delta a_{i=1-6,\ j=1}\right] = \left[W_{i=1-6,\ j=1}\right]$$

$$C_{ij} = \sum_k^N \frac{\partial M_{c_k}}{\partial a_i} \frac{\partial M_{c_k}}{\partial a_j}$$

$$W_{ij} = \sum_k^N \frac{\partial M_{c_k}}{\partial a_i} \left(M_k - M_{c_k}\right)$$

Now $M_k - M_{c_k} = n(t_i)$ if the unestimated orbit parameters are correct

However, since these unestimated parameters may be in error,

then

$$M_k - M_{c_k} = n(t_i) + \sum \frac{\partial M_{c_k}}{\partial b_j} \Delta b_j$$

let $n(t_i) = 0$ so that we can see the effect of errors in the b components. The equation for the Δa resulting from errors in b is presented below.

$$\left[C_{i=1\text{-}6,\ j=1\text{-}n}\right]\left[\Delta a_{i=1\text{-}6,\ j=1}\right] = \left[F_{i=1\text{-}6,\ j=1\text{-}n}\right]\left[\Delta b_{i=1\text{-}n,\ j=1}\right]$$

where: $F_{ij} = \sum \frac{\partial M_{c_k}}{\partial a_i} \frac{\partial M_{c_k}}{\partial b_j}$

$$\Delta a = C^{-1} F \Delta b$$

$$\Delta a \Delta a^T = C^{-1} F \Delta b \left[C^{-1} F \Delta b\right]^T = C^{-1} F \Delta b \Delta b^T F^T C^{-1}$$

$$\therefore \quad \boxed{\overline{\Delta a \Delta a^T} = C^{-1} F \ \overline{\Delta b \Delta b^T}\ F^T C^{-1}}$$

The total error due to noise and uncertainty in the b components is presented below.

$$\boxed{\overline{\Delta a \Delta a^T}_{\text{Total}} = C^{-1} + C^{-1} F \overline{\Delta b \Delta b^T} F^T C^{-1}}$$

In general $\overline{\Delta b \Delta b^T}$ is an n x n covariance matrix defining the uncertainty in the b components (unestimated parameters). In most cases, the $\overline{\Delta b \Delta b^T}$ matrix will be an n x n matrix with non-zero elements only on the principle diagonal.

The above analyses can be extended to the case of more than one measurable and/or observing stations in the following manner.

$$C_1 \Delta a = F_1 \Delta b_1$$

$$C_2 \Delta a = F_2 \Delta b_2$$

$$C_3 \Delta a = F_3 \Delta b_3$$

then

$$(C_1 + C_2 + C_3)\ \Delta a = F_1 \Delta b_1 + F_2 \Delta b_2 + F_3 \Delta b_3$$

let Δb = column vector of all unestimated parameters

$$C = C_1 + C_2 + C_3$$

$$F = F_1 + F_2 + F_3$$

where F_1, F_2 and F_3 each have same number of columns as Δb has rows (ZERO's have been added in the appropriate columns).

then

$$C \Delta a = F \Delta b$$

and

$$\overline{\Delta a \Delta a^T} = C^{-1} F \overline{\Delta b \Delta b^T} F^T C^{-1}$$

If studies are to be performed to determine the effect of uncertainty in unestimated parameters, it might be desirable to program this separately as it only requires obtaining an inverse of a 6 x 6 matrix, and the required elements of the F matrix are contained in the information matrix.

BISSETT BERMAN

APOLLO NOTE NO. 156

L. Lustick
20 December 1963

ROTATION OF COVARIANCE MATRIX INTO OTHER COORDINATE SYSTEMS

Purpose

The purpose of this note is to describe the transformation in the covariance matrix if the coordinate system undergoes a general rotation.

Introduction

If the problem of orbit determination is to be applied to problems where the vehicle goes from the sphere of influence of planet (1) to the sphere of influence of planet (2), it will be desirable to determine the covariance matrix in the planet (2) coordinate system at the time when its vehicle crosses from planet (1) to planet (2) influence. This note defines the transformation required.

Discussion

Let (Δy) = errors in y coordinate system

(Δx) = errors in rotated coordinate system

$$t_{ij} = \begin{pmatrix} t_{11} & t_{12} & t_{13} \\ t_{21} & t_{22} & t_{23} \\ t_{31} & t_{32} & t_{33} \end{pmatrix} = \text{transformation that rotates vector in y coordinate system to vector in x coordinate system}$$

The covariance matrix in the y coordinate system is presented below. Elements 1 - 6 are dependent on the coordinate system, and the other elements are independent of the coordinate system.

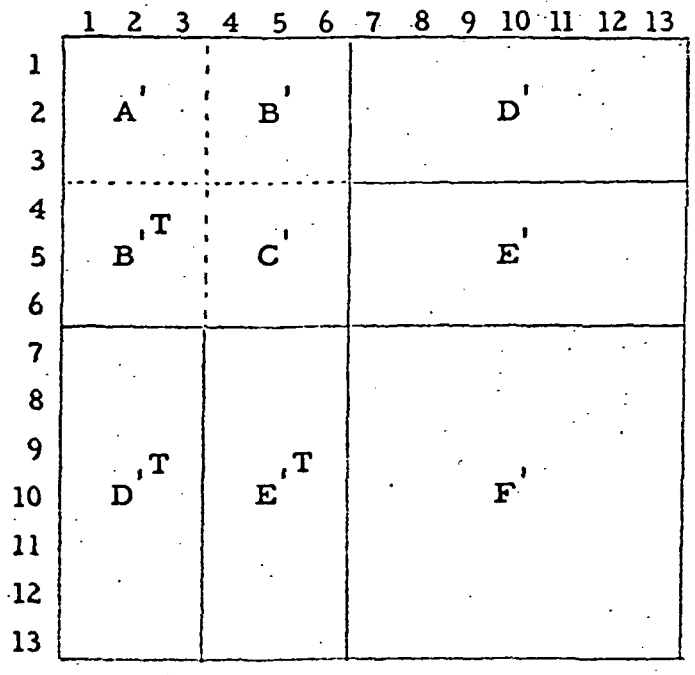

The corresponding covariance matrix in the rotated x coordinate system is presented below.

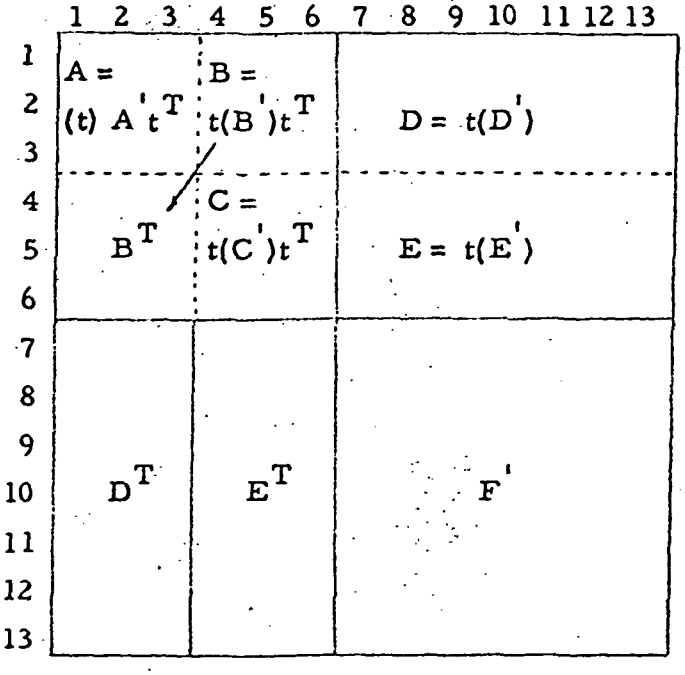

BISSETT BERMAN

APOLLO NOTE NO. 157

H. Engel
23 December 1963

CLOCK TIME AND CLOCK RATE

It has been proposed that three-way ranging or three-way Doppler be used in determining Apollo vehicle orbit from ground stations in order to gain the advantages of plural ground stations, without requiring more than one transponder in the vehicle.

In these three-way modes one ground station, hereinafter called the "master," sends radar transmissions to the vehicle, which repeats these transmissions back to all the stations. The stations other than the master are called "slave" stations.

It is important that the clocks, i.e., frequency standards, at the slave stations have an accurately known relationship to that at the master. We shall illustrate this point by two examples. In both examples we assume noise-free clocks. That is, we take that time kept by the master clock as a reference time t_M, and assume that the time indicated by the slave clock is

$$t = t_M + k\,t_M + b$$

in which k and b are constants. For the problem we are considering here, short term random variations in the clock rates may be ignored.

By means of one-way low frequency Loran the clock at the slave station can be kept within $\pm$ 1 μ sec. of the clock at the master, provided the locations of both stations are known exactly. This, however, is not good enough to be used without further compensation.

Let us consider a ranging mode wherein the master transmits a range code to the vehicle at a scheduled time, and which in turn the vehicle retransmits to the slave station. If the clock at the slave is in error by 1 μsec., the apparent distance the signal has traveled differs by 300 m from the actual distance it has traveled, corresponding to an error of at least 150 m in the apparent vehicle position.

Alternatively, let us consider a Doppler mode. By counting the Doppler cycles from some initial time we can determine the change in range from that initial time. In this case we do not have to know the constant b, but for long total times of observation we must know the slave clock error rate k. The error in the change in range in the time t_M, as observed by Doppler counting at the slave station, is greater than $3 \times 10^8 k t_M/2$ m. for t_M in seconds. If we assume that the clock rate at the slave station is in error by one part in 10^{10}, then after one hour of observation the error in the observed change in range will exceed 54 m. ($54 = 3 \times 10^8 \times 10^{-10} \times 3600/2$).

The lower bound on the error in the change in range as observed by Doppler counting at the slave station is shown as a function of total time of observation and clock rate error in Figure 1. Also shown in this figure is a curve indicating the time in which the clock error changes by 1 μ sec.

One solution to the problem is to build more accurate clocks; this is expensive.

Another solution is to provide a better means for correcting the slave clocks. An Earth satellite equipped with a transponder could be used for this purpose provided its orbit was known to sufficient accuracy.

A third solution is to place additional transponders on the vehicle so that the three-way mode is unnecessary. This is highly undesirable.

A fourth means is to time-share the vehicle transponder, thereby avoiding the three-way mode, but this means that the change in range from time 0 cannot be measured by any station using Doppler counting.

A fifth solution is to derive the clock rate error from the observed data. The accuracy with which this can be done is not immediately evident, being bound up with the kinematics of the orbit. It can however be determined in desired instances through a modification of the error analysis program of Apollo Note No. 82. In this case,

wherein the clock rate error is to be determined on the basis of range-rate measurements, we consider the clock rate error $\underline{k}$ as an additional orbit parameter in obtaining the information matrix corresponding to observations from the slave station.

In the error analysis program we treat the range change measurement by Doppler counting as though we were measuring the range at each sampling time, but with a fixed, unknown range bias*.

The computed value of range from the master is compared with the measured change in range and the computed initial value.

$$R_{Mc} - B_{Mc} - \Delta R_{Mm} = \hat{n}_M$$

The apparent error $\hat{n}_M$ in the range from the master is the computed range from the master R_{Mc}, less the computed initial range from the master B_{Mc}, less the measured change in range from the master ΔR_{Mm}.

The computed value of range from the master to the vehicle to the slave is compared with measured change in this quantity and the computed initial value

$$S_c - B_c - \Delta S_m = \hat{n}$$

The apparent error $\hat{n}$ in this total range measurement is the computed value S_c, less the computed initial value B_c, less the measured change in range S_m. Now,

$$S = R_M + R_S$$

---

* Recall that we are neglecting the clock "noise" so the errors are uncorrelated except for the clock rate error which we are treating separately.

so we can write

$$(S_c - R_{Mc}) - (B_c - B_{Mc}) - (\Delta S_m - \Delta R_{Mm}) = \hat{n} - \hat{n}_M$$

or

$$R_{Sc} - B_{Sc} - \Delta R_{Sm} = \hat{n} - \hat{n}_M$$

Further, the computed range from the slave station is not merely the change due to vehicle and station motion, but also includes a term $k\, t_M c/2$ to account for the error in slave clock rate.

In the absence of other factors, such as station location errors, then, a 7 by 7 information matrix is obtained for measurements from the master station --6 orbit parameters and range bias--and an 8 x 8 information matrix for measurements from the slave station. The eighth row and column correspond to the clock rate error.

We have $\partial R_{Sc} / \partial (1/2\ kc) = t_M$

and

$$C_{8j} = \sum_{p=1}^{M} \frac{\partial R_{Sc}(t_M)}{\partial a_j}\ t_M$$

We also have an increased Q matrix with $Q_{i8} = \delta_{i8} = Q_{8i}$.

Combining the information matrices from the master station and a slave station results in a 9 by 9 matrix.

The a priori information matrix should also be 9 by 9, reflecting a priori knowledge of the range biases and the clock rate error.

A question still remains concerning the noise to be associated with the slave station measurements since the estimated noise is $\hat{n} - \hat{n}_M$. We do not know what portion of the noise is correlated with the noise observed by the master station. Inasmuch as we are

not yet prepared to treat the case of correlated noise, the easy but unjustified way out is to treat the noise as uncorrelated, but with a variance twice that of the measurement noise associated with the master station.

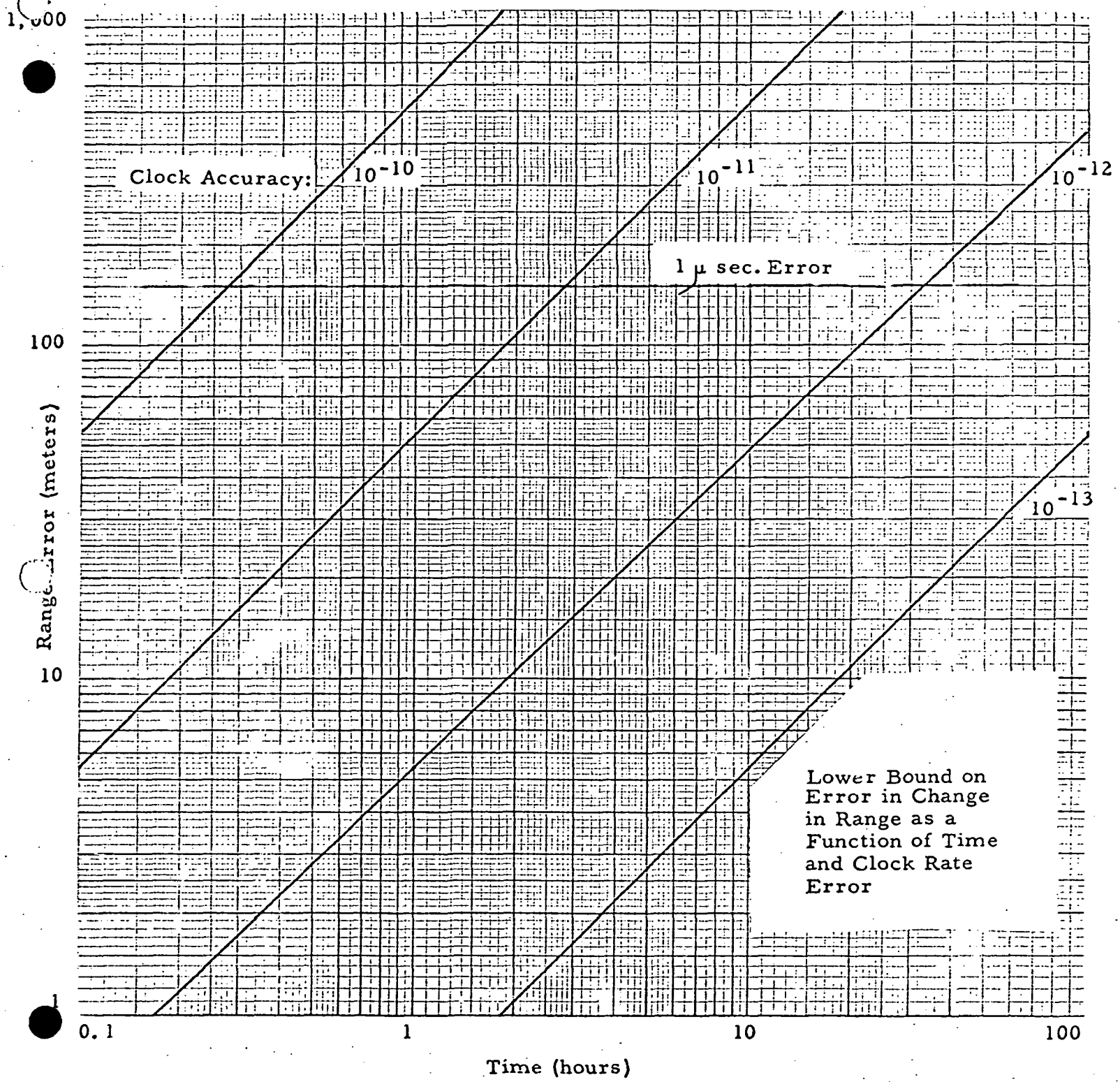
1,000
100
10
1
Range Error (meters)
Clock Accuracy:
10^{-10}
10^{-11}
10^{-12}
10^{-13}
1 μ sec. Error
Lower Bound on Error in Change in Range as a Function of Time and Clock Rate Error
0.1
1
10
100
Time (hours)

DISCARD

APOLLO NOTE NO. 158

H. Engel
23 December 1963

EFFECT OF UNKNOWN ROTATIONS OF APOLLO VEHICLE

Introduction

The UFS radar can measure changes in range to an accuracy better than the dimensions of the Apollo vehicles. The range measured is the range to the transponder antenna on the vehicle. Thus, if the ground is not informed of the vehicle attitude, changes in vehicle attitude may cause greater changes in range than the noise on the change in range measurements.

In this note we point out how the effect of unknown changes in range on the estimated orbit parameters can be determined, and suggest a means by which these errors can be reduced.

Error Estimation

Letting Q_i be the covariance matrix of the i-th set of measurements, letting y_i^* be the (column vector) i-th set of measurements, and letting y_i be the computed value of these measurements, we know that the most likely set of orbit parameters is that which maximize the quantity $\mathcal{L}$,

$$\mathcal{L} = -\frac{1}{2} \sum_{i=0}^{n} (y_i^* - y_i)^T \, Q_i^{-1} \, (y_i^* - y_i)$$

In order to maximize $\mathcal{L}$, we set its first partial derivatives with respect to the orbit parameters a_k equal to zero.

$$0 = \sum_{i=0}^{n} \left(\frac{\partial y_i}{\partial a_k}\right)^T Q_i^{-1} \, (y_i^* - y_i) + \sum_{i=0}^{n} (y_i^* - y_i)^T \, Q_i^{-1} \left(\frac{\partial y_i}{\partial a_k}\right)$$

Since Q_i is a symmetric matrix this reduces to

$$0 = \sum_{i=0}^{n} \left(\frac{\partial y_i}{\partial a_k}\right)^T Q_i^{-1} (y_i^* - y_i).$$

Now, an error e_i (column vector) in the measurables, due to displacement of the vehicle transponder antenna will result in a change Δa_j in parameter a_j. Using a linear approximation, we have

$$0 = \sum_{i=0}^{n} \left(\frac{\partial y_i}{\partial a_k}\right)^T Q_i^{-1} \left(y_i^* + e_i - y_i - \sum_{j=1}^{m} \frac{\partial y_i}{\partial a_j} \Delta a_j\right)$$

or

$$0 = \sum_{i=0}^{n} \left(\frac{\partial y_i}{\partial a_k}\right)^T Q_i^{-1} \left(e_i - \sum_{j=1}^{m} \frac{\partial y_i}{\partial a_j} \Delta a_j\right)$$

Solving this set of m simultaneous linear equations for Δa (column vector) we find

$$\Delta a = C^{-1} \sum_{i=0}^{n} \left(\frac{\partial y_i}{\partial a}\right)^T Q_i^{-1} e_i$$

where

$$C = \sum_{i=0}^{n} \left(\frac{\partial y_i}{\partial a}\right)^T Q_i^{-1} \left(\frac{\partial y_i}{\partial a}\right)$$

In the particular case in which the measurements at time t_i are not correlated, the first of these two equations reduces to

$$\Delta a = C^{-1} \sum_{j=1}^{\ell} \sum_{i=0}^{n} \frac{\partial y_{ij}}{\partial a} \frac{e_{ij}}{\sigma_{ij}^2}$$

in which y_{ij} and e_{ij} are the j-th elements of y_i and e_i, and σ_{ij}^2 is the variance associated with y_{ij}.

In the more special case in which the measurement noise is stationary, we have

$$\Delta a = C^{-1} \sum_{j=1}^{\ell} \frac{1}{\sigma_j^2} \sum_{i=0}^{n} \frac{\partial y_{ij}}{\partial a} e_{ij}$$

Now, C^{-1} is obtained as part of the present computer error analysis program. Further, if the errors e_{ij}, due to vehicle orientation, are expressed as functions of time, then it is possible to evaluate

$$\sum_{i=0}^{n} \frac{\partial y_{ij}}{\partial a} \frac{e_{ij}}{\sigma_{ij}^2} \quad \text{or} \quad \frac{1}{\sigma_j^2} \sum_{i=0}^{n} \frac{\partial y_{ij}}{\partial a} e_{ij}$$

by means of small changes to the computer error analysis program. Then only matrix multiplications are necessary to find Δa.

Error Reduction

The measurement errors introduced by the vehicle attitude or changes in attitude are characterized by low frequency components, while the radar noise has a correlation time of less than a second. In fact, during unpowered flight it is only necessary to initiate a change in attitude at widely separated intervals, and the vehicle will normally have only a small rate of rotation. The possibility exists, then, of plotting the estimated measurement errors as a function of time and manually introducing corrections to reduce or eliminate these errors. The same results could be obtained automatically by fitting the residuals with a low order polynomial.

This procedure is indicated schematically in Figure 1. In Figure 1, we show the residual errors, for one kind of measurement, these errors being due to noise in the measurements and changes in vehicle attitude. In this figure we also show the extreme error that

could result from a difference of vehicle attitude. In this same figure we have indicated an estimate of the portion of the error due to vehicle rotation.

If this estimate of vehicle attitude is fed back as an input to the computer the residuals will be smaller. It is still a moot point as to the improvement in orbit parameters obtainable as a result of this process. Let us illustrate this by means of an example.

In Figure 2 we show an attempt to estimate a single constant by means of a sequence of measurements that are corrupted by random uncorrelated noise and a slowly varying error of limited magnitude. A least-squares estimate of the constant will make the average estimated measurement error zero. If we attempt to remove the slowly varying error, we will still be left with the zero frequency component of this error.

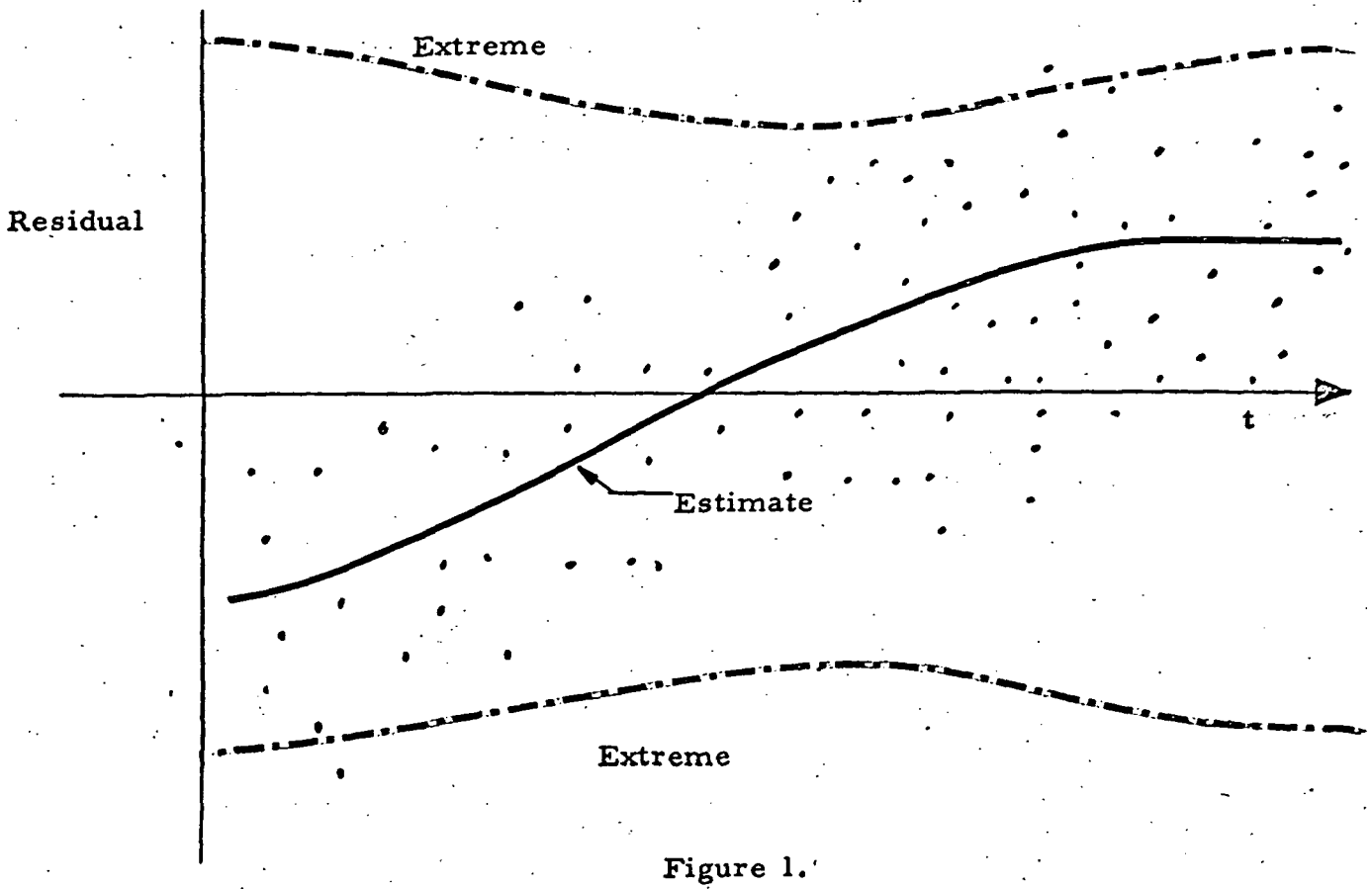

Figure 1.

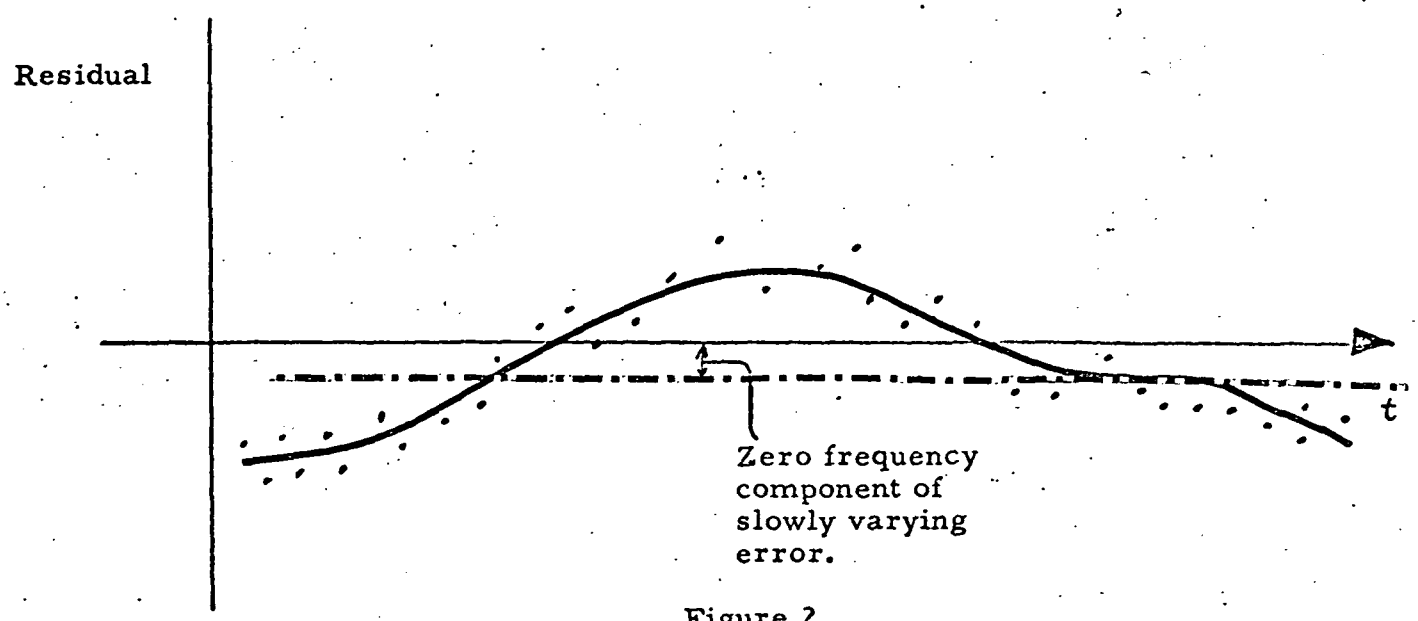

Figure 2.

BISSETT
BERMAN

APOLLO NOTE NO. 159

C. Siska
27 December 1963

EFFECT OF RANGE BIAS INFORMATION ON RE-ENTRY PREDICTION IN RETURN-TO-EARTH PHASE

1. Introduction

This report represents a continuation of the analysis of re-entry conditions for the Earth-centered part of the Return-to-Earth trajectory (see Apollo Note No. 151). In this instance, the effect of a priori information of the unknown range bias upon prediction accuracy is investigated.

A primary source of range bias results from the uncertainty (approximately 1 part in 10^6) in evaluating the speed of light. This yields a standard error of about 340 meters for distances up to the lunar sphere of influence (LSOI) and therefore represents the order of magnitude of the maximum error in predicting range bias.

As in the previous note, the results presented are geared to the assumption of a time-sharing data collection operation amongst the stations involved. Thus, the sampling rate for each of three stations is taken to be 6 observations per 20 minute interval and for each of two stations, 9 observations per 20 minute interval. Errors in the measurement values are assumed to be 3 cm./sec. for range-rate and 15 meters for range. Later in this report, it will be shown how to manipulate the presented results to conform to different assumptions relative to the sampling rate and measurement errors.

2. Results For Three Stations

The solid curves in Figure 1 represent new results while the dashed curves (which appear in Apollo Note No. 151) are presented for comparison purposes. In this case the value of the a priori range bias σ_- has been taken to be 620 meters.

It is evident that if the assumed constant range bias for each station can be determined with a deviation on the order of 620 meters, there is no problem in predicting re-entry dive angle, even without a priori position data. This presumes that the desired upper limit for the dive angle σ is 0.1°. Note that a priori range bias information does not aid in prediction when a priori position data is available.

Figure 2 presents the corresponding prediction accuracy of the RMS miss distance on the re-entry sphere. The dashed curves again are from Apollo Note No. 151, except that the upper two curves, labeled range-rate and range-unknown bias, have been corrected (resulting in each curve being displaced slightly downward).

3. Results For Two Stations

In this case the a priori range bias σ has been taken to be 510 meters. The solid curves in Figure 3 show the new data. Note that a priori bias estimates coupled with a priori position estimates enable the dive angle to be predicted well below the desired value of $\sigma = 0.1^{\circ}$.

Figure 4 presents the RMS miss distance accuracy. Here the upper three dashed curves have again been corrected from those appearing in Note 151 by a slight downward displacement.

4. Prediction of Orbital Elements

The accuracy with which the orbital elements can be predicted using a priori estimates of range bias is shown in Figure 5. In the last column, labeled $b_{max.}$, is shown the maximum deviation of the range bias estimator amongst the number of stations involved (the differences between the stations being small).

5. Manipulation of Results

It has been customary, for given sampling rates, to present results using the best available measurement errors, such as 3 cm./sec.

for range-rate and 15 meters for range. However, if one wished to change these assumptions, then the presented results can be manipulated to conform to the changed assumptions under certain conditions.

To illustrate these conditions, consider the form of the i, jth element in the information matrix C (see, for example, Equation 11 in Apollo Note No. 77),

$$C_{ij} = \sum_{k=1}^{N_1} \frac{1}{\sigma_1^2} \frac{\partial f(t_k)}{\partial a_i} \frac{\partial f(t_k)}{\partial a_j} + \sum_{\ell=1} \frac{1}{\sigma_2^2} \frac{\partial g(t_\ell)}{\partial a_i} \frac{\partial g(t_\ell)}{\partial a_j} \qquad (1)$$

where a_i, a_j $(i, j = 1, 2 \ldots M)$ are the orbital elements which can include items like constant biases for each station.

Here, each sum represents a set of observations. In general, the sets may be associated with different station locations, measurables, measurement errors, and sampling rates. However, it is usually assumed that the sample points are uniformly distributed over the data collection interval, so that, for example, $t_{k+1} - t_k = \Delta t_k$ = a constant time interval between sample points over the collection interval $N_1 \Delta t_k$.

Equation (1) can therefore be written essentially as

$$C_{ij} = \frac{N_1}{\sigma_1^2} \overline{f}_{ij} + \frac{N_2}{\sigma_2^2} \overline{g}_{ij} \qquad (2)$$

where $\overline{f}_{ij}$ is the average value of $\frac{\partial f(t_k)}{\partial a_i} \frac{\partial f(t_k)}{\partial a_j}$ over the time interval $N \Delta t_k$.

Rearranging Equation (2), we have

$$C_{ij} = \frac{N_1}{\sigma_1^2} \left[\overline{f}_{ij} + \frac{N_2}{N_1} \frac{\sigma_1^2}{\sigma_2^2} \overline{g}_{ij} \right] \qquad (3)$$

The i, jth element in the covariance matrix, C^{-1}, will have the form

$$\overline{\Delta a_i \, \Delta a_j} = (C^{-1})_{ij} \, \frac{\sigma_1^2}{N_1} \; F\left(\frac{N_2}{N_1} \; ; \; \frac{\sigma_1^2}{\sigma_2^2} \; ; \; \overline{f}_{mn}, \; \overline{g}_{pq} \right) \qquad (4)$$

where the function F will contain products of $\overline{f}$ and $\overline{g}$ involving all the orbital elements.

Suppose one now changes the sampling rate so as to collect sets of N_1' and N_2' points with errors σ_1' and σ_2', and does this over the identical time periods as previously. Then, if the new points are uniformly distributed we have $N_1 \Delta t_k = N_1' \Delta t_k'$ and expect that $\overline{f}_{ij}' = \overline{f}_{ij}$, etc. Thus, we need only to insist that $N_2'/N_1' = N_2/N_1$ and $\sigma_1'/\sigma_2' = \sigma_1/\sigma_2$ in order for F = F' in Equation (4).

The new value for covariance matrix element will then satisfy the ratio,

$$\frac{(\overline{\Delta a_i \, \Delta a_j})'}{(\overline{\Delta a_i \, \Delta a_j})} = \left(\frac{\sigma_1'}{\sigma_1} \right)^2 \left(\frac{N_1}{N_1'} \right) \qquad (5)$$

Here we have the liberty of choosing independent values of σ_1' and N_1', but require that $\sigma_2' = \left(\frac{\sigma_2}{\sigma_1} \right) \sigma_1'$ and $N_2' = \left(\frac{N_2}{N_1} \right) N_1'$.

As an example, suppose we changed the present assumption of a time-sharing operation amongst 3 stations, each station obtaining 6 sample points every 20 minutes, to a simultaneous operation where each station obtained 20 points in a 20 minute interval. Letting $\sigma_1' = \sigma_1$, the new covariance element is, from Equation (5),

$$(\overline{\Delta a_i \, \Delta a_j})'_{new} = \frac{(6/20)}{(20/20)} \; (\overline{\Delta a_i \, \Delta a_j})_{old}$$

so that in this case, we can write,

New dive angle σ = $\sqrt{6/20}$ (old dive angle σ)

New range bias σ = $\sqrt{6/20}$ (old range bias σ)

and so forth.

6. Conclusions

Re-entry dive angle prediction for tracking (range) initiated at the LSOI is well within the requirement of $\sigma = 0.1^{\circ}$ for the cases,

1. three station tracking with a priori range bias estimates having a deviation of 620 meters and no a priori position estimates.

2. two station tracking with a priori range bias estimates having a deviation of 510 meters and a priori position estimates with a deviation of 7.5 km. in each position component.

The above is for a time-sharing data collection scheme amongst the stations with range measurement errors of 15 meters.

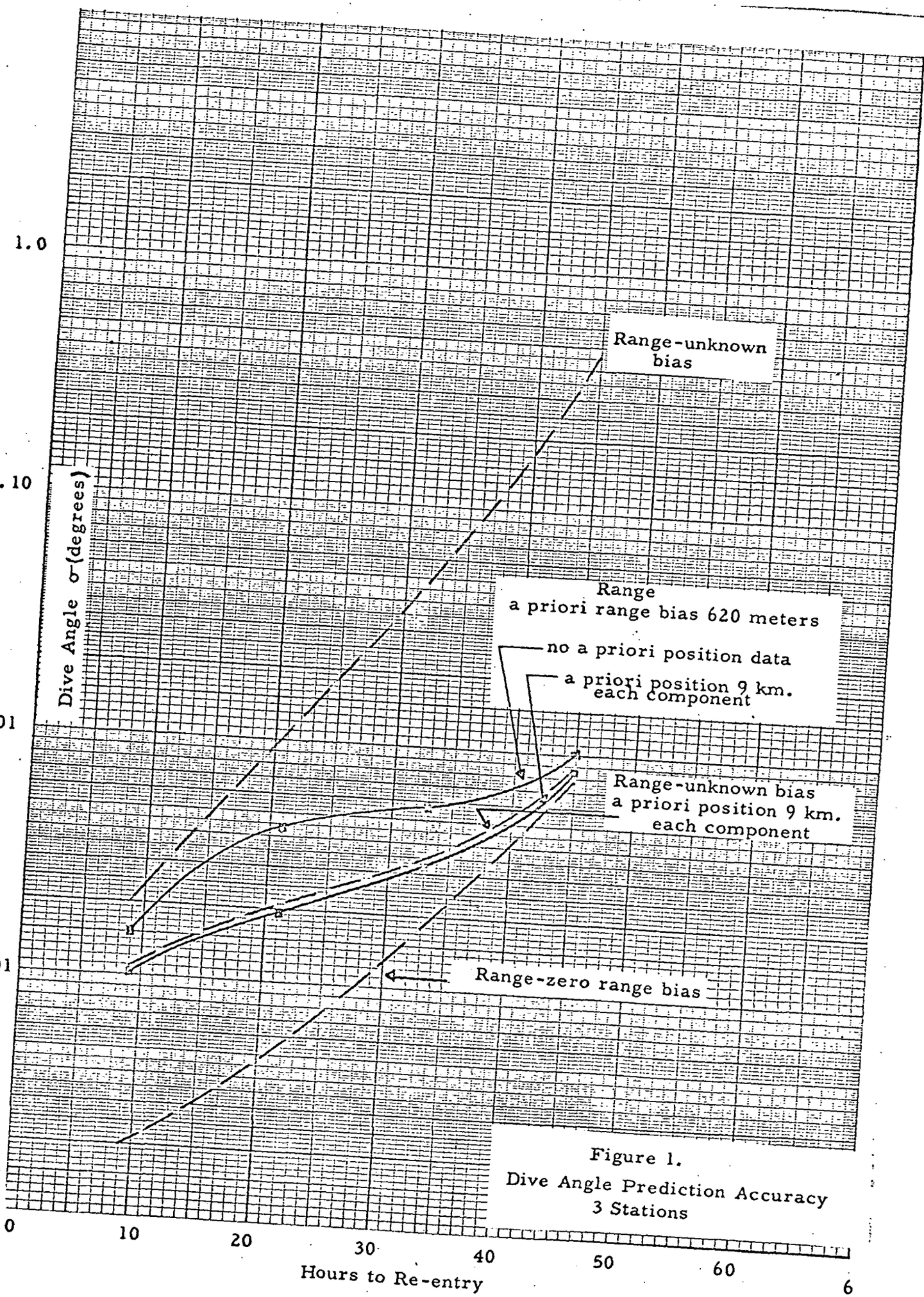

Figure 1.
Dive Angle Prediction Accuracy
3 Stations

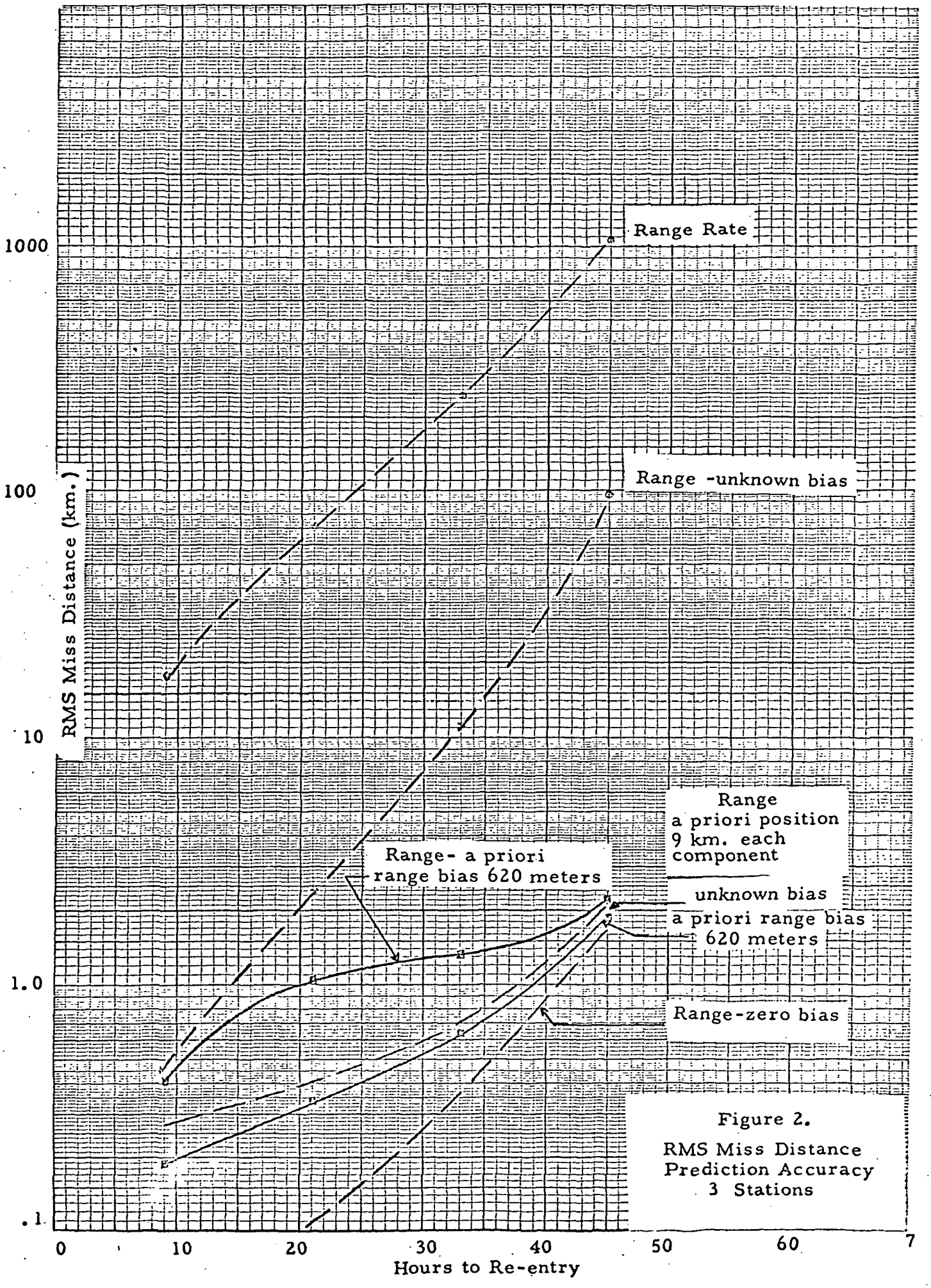

Figure 2.

RMS Miss Distance
Prediction Accuracy
3 Stations

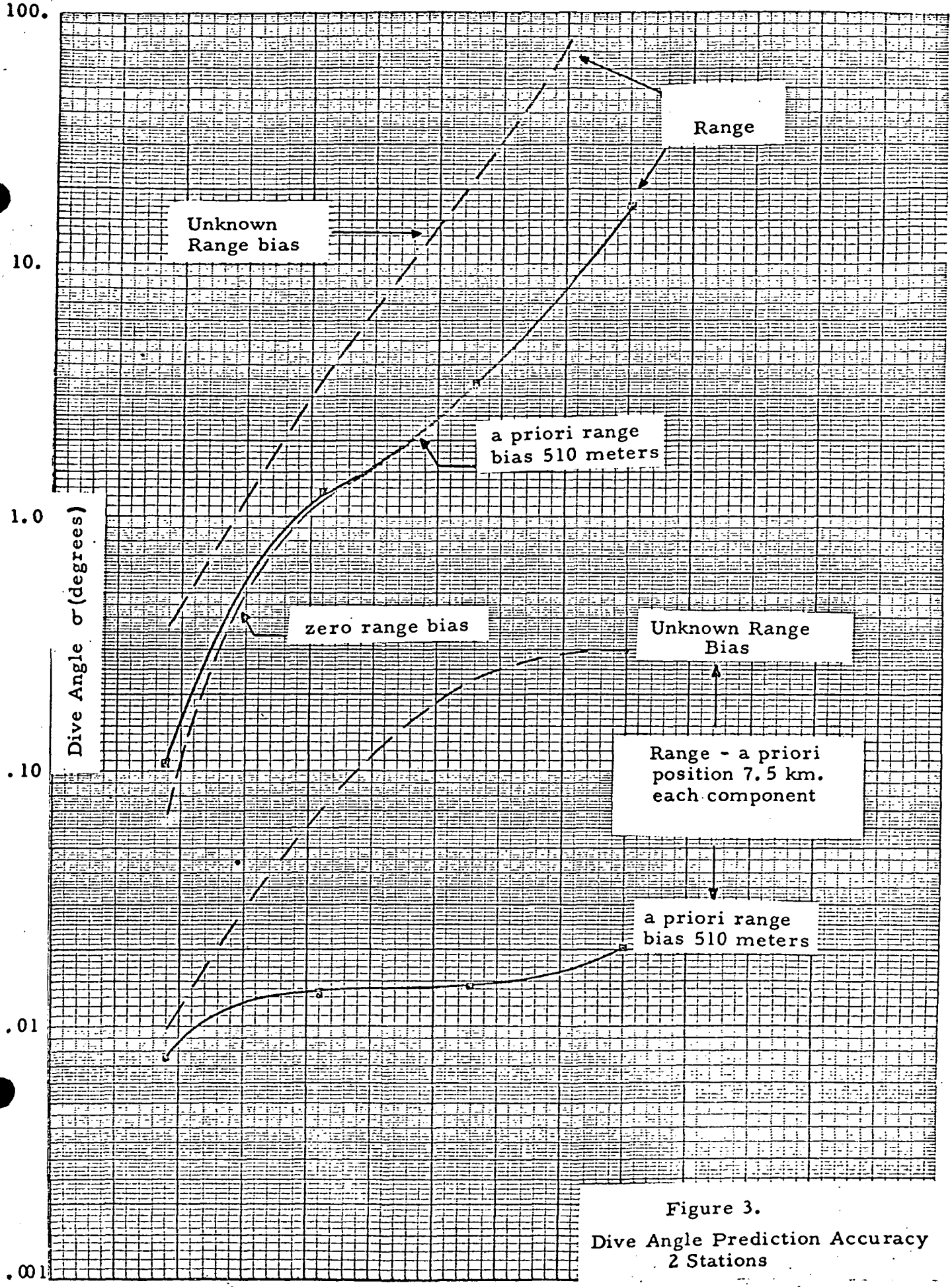

Figure 3.

Dive Angle Prediction Accuracy
2 Stations

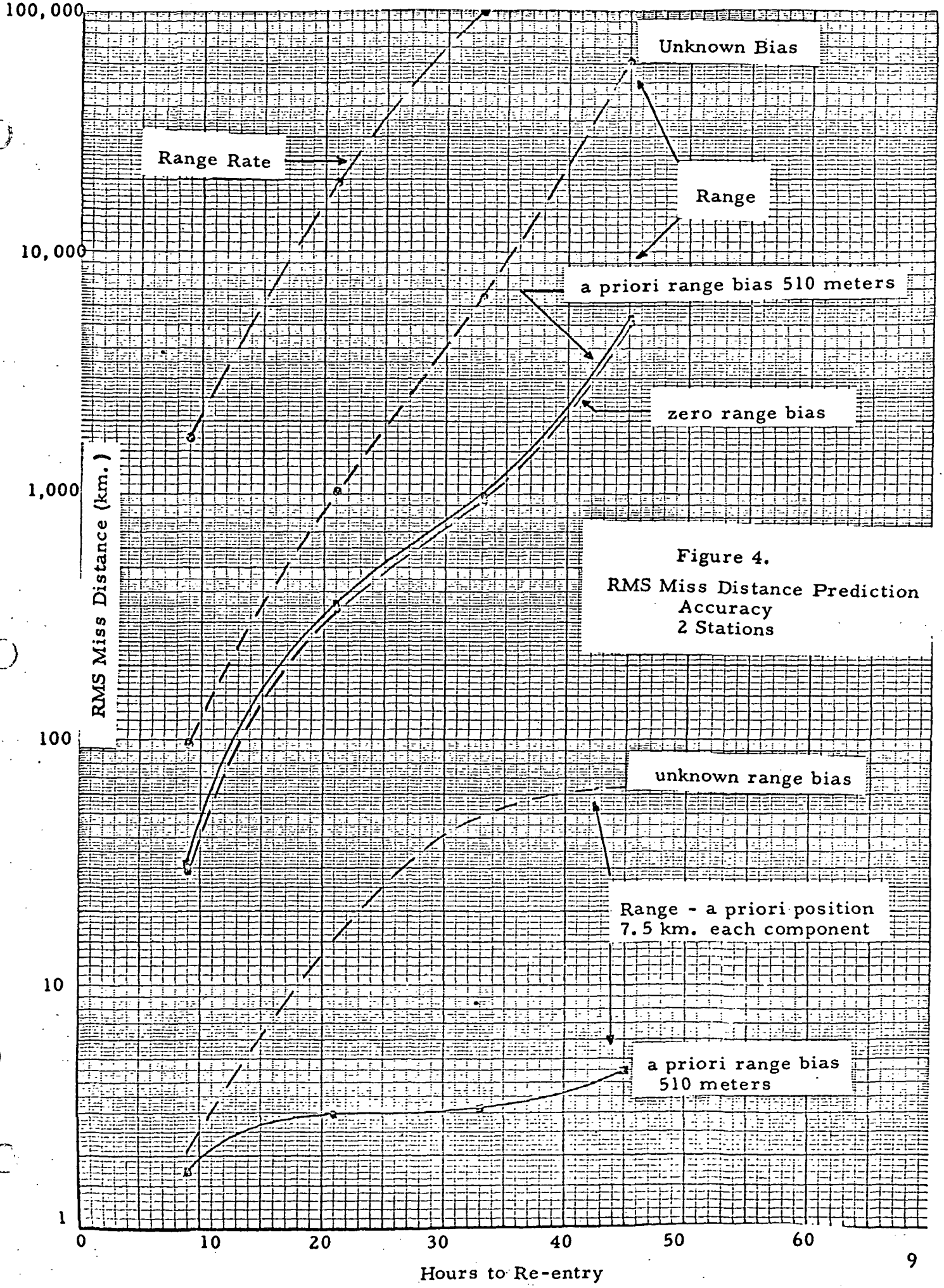

Figure 4.

RMS Miss Distance Prediction
Accuracy
2 Stations

Type of Data	Standard Deviation in a priori Data	Standard Deviation of Orbital Elements						
		x_o(m)	y_o(m)	z_o(m)	$\dot{x}_o$(m/s)	$\dot{y}_o$(m/s)	$\dot{z}_o$(m/s)	$b_{max.}$(m)
3 Stations Range	Range Bias 620 Meters	.29 + 03*	.29 + 05	.63 + 05	.18 - 01	.74 - 01	.16 - 02	.62 + 03
		.12 + 03	.26 + 05	.59 + 05	.16 - 01	.67 - 01	.15 - 02	.62 + 03
		.75 + 02	.24 + 05	.53 + 05	.15 - 01	.63 - 01	.13 - 02	.57 + 03
		.23 + 02	.12 + 05	.22 + 05	.73 - 02	.30 - 01	.55 - 01	.24 + 03
3 Stations Range	Range Bias 620 meters position 9 km. each component	.27 + 03	.86 + 04	.90 + 04	.53 - 02	.22 - 01	.24 - 01	.31 + 03
		.89 + 02	.86 + 04	.90 + 04	.53 - 02	.22 - 01	.23 - 01	.17 + 03
		.42 + 02	.85 + 04	.90 + 04	.52 - 02	.22 - 01	.22 - 01	.14 + 03
		.19 + 02	.71 + 04	.84 + 04	.44 - 02	.18 - 01	.21 - 01	.11 + 03
2 Stations Range	Range Bias 510 Meters	.40 + 06	.14 + 09	.28 + 09	.84 + 02	.35 + 03	.71 + 03	.51 + 03
		.35 + 05	.26 + 08	.55 + 08	.16 + 02	.67 + 02	.13 + 03	.51 + 03
		.13 + 05	.96 + 07	.20 + 08	.59 + 01	.24 + 02	.50 + 02	.51 + 03
		.13 + 04	.77 + 06	.16 + 08	.47 + 00	.20 + 01	.34 + 02	.44 + 03
2 Stations Range	Range Bias 510 meters position 7.5 km. each component	.36 + 03	.72 + 04	.74 + 04	.44 - 02	.20 - 01	.26 - 01	.38 + 03
		.36 + 03	.72 + 04	.74 + 04	.44 - 02	.19 - 01	.23 - 01	.38 + 03
		.35 + 03	.71 + 04	.74 + 04	.44 - 02	.19 - 01	.22 - 01	.37 + 03
		.21 + 02	.64 + 06	.72 + 04	.39 - 02	.16 - 01	.20 - 01	.24 + 03

* The set of 4 numbers corresponds to 45, 33, 21, and 9 hours to re-entry and is to be read as $.29 \times 10^{+03}$ etc.

Figure 5. Prediction Accuracies for Orbital Elements

Type of Data	Standard Deviation in a priori Data	Standard Deviation of Orbital Elements						
		x_o(m)	y_o(m)	z_o(m)	$\dot{x}_o$(m/s)	$\dot{y}_o$(m/s)	$\dot{z}_o$(m/s)	$b_{max.}$(m)
3 Stations Range	Range Bias 620 Meters	.29 + 03*	.29 + 05	.63 + 05	.18 - 01	.74 - 01	.16 - 02	.62 + 03
		.12 + 03	.26 + 05	.59 + 05	.16 - 01	.67 - 01	.15 - 02	.62 + 03
		.75 + 02	.24 + 05	.53 + 05	.15 - 01	.63 - 01	.13 - 02	.57 + 03
		.23 + 02	.12 + 05	.22 + 05	.73 - 02	.30 - 01	.55 - 01	.24 + 03
3 Stations Range	Range Bias 620 meters position 9 km. each component	.27 + 03	.86 + 04	.90 + 04	.53 - 02	.22 - 01	.24 - 01	.31 + 03
		.89 + 02	.86 + 04	.90 + 04	.53 - 02	.22 - 01	.23 - 01	.17 + 03
		.42 + 02	.85 + 04	.90 + 04	.52 - 02	.22 - 01	.22 - 01	.14 + 03
		.19 + 02	.71 + 04	.84 + 04	.44 - 02	.18 - 01	.21 - 01	.11 + 03
2 Stations Range	Range Bias 510 Meters	.40 + 06	.14 + 09	.28 + 09	.84 + 02	.35 + 03	.71 + 03	.51 + 03
		.35 + 05	.26 + 08	.55 + 08	.16 + 02	.67 + 02	.13 + 03	.51 + 03
		.13 + 05	.96 + 07	.20 + 08	.59 + 01	.24 + 02	.50 + 02	.51 + 03
		.13 + 04	.77 + 06	.16 + 08	.47 + 00	.20 + 01	.34 + 02	.44 + 03
2 Stations Range	Range Bias 510 meters position 7.5 km. each component	.36 + 03	.72 + 04	.74 + 04	.44 - 02	.20 - 01	.26 - 01	.38 + 03
		.36 + 03	.72 + 04	.74 + 04	.44 - 02	.19 - 01	.23 - 01	.38 + 03
		.35 + 03	.71 + 04	.74 + 04	.44 - 02	.19 - 01	.22 - 01	.37 + 03
		.21 + 02	.64 + 06	.72 + 04	.39 - 02	.16 - 01	.20 - 01	.24 + 03

* The set of 4 numbers corresponds to 45, 33, 21, and 9 hours to re-entry and is to be read as $.29 \times 10^{+03}$ etc.

Figure 5. Prediction Accuracies for Orbital Elements

DISSETT
BERMAN

APOLLO NOTE NO. 160

H. Engel
30 December 1963

INTRODUCTION TO LEM TRUCK G AND N

The LEM truck is an unmanned freight vehicle to land equipment on the Moon after separation from a CSM in orbit about the Moon. The CSM may be either manned or unmanned.

It is desirable to maximize the amount of useful equipment the LEM truck can land on the Moon. This amount can be increased by decreasing the weight of guidance and navigation equipment on the LEM, and properly choosing the LEM and CSM orbits. In both cases it is possible to cut some corners if necessary, because failure of the mission will not result in loss of life.

A number of guidance and navigation problems must be considered. Some of these are discussed below. We have cheated in a few places in this analysis, however, using unstated and unjustified assumptions, and treating errors in variables sometimes as statistical quantities and sometimes as biases. Nevertheless, the results indicate that there is a real possibility that a simple on-board guidance system would suffice for LEM landing.

Measuring Systems

A question to be answered relates to the amount of navigation equipment on board the LEM.

Using three MSFN radars and a single transponder on the LEM, the RMS errors in position and velocity of the LEM based on range change measurements are of the order of 90 meters and 0.075 meters/sec. using a standard deviation of 0.6 m. in range change measurements and with one set of measurements every minute. This, of course, requires that the Earth is aware of the vehicle attitude, since the transponder antenna is several meters from the LEM center of gravity. This also assumes that station location errors are negligible.

Continuing to make measurements of change in range with a standard deviation of 0.6 m., but at more frequent intervals--which is allowable since we are continuously counting Doppler cycles--we can always determine position in the direction of the Earth-Moon line with an accuracy of the order of 1 meter, and position in the two orthogonal to the order of 100 meters.

In determining LEM velocity from these range change measurements there is a trade-off between increasing accuracy of observation and increasing uncertainty due to LEM acceleration. If we arbitrarily choose an interval of five seconds, the velocity error along the Earth-Moon line resulting from radar errors is of the order of 0.17 m/sec. ($= 0.6 \text{ m } \sqrt{2} \text{ observation}^{1/2}/5 \text{ sec.}$) and 17. m/sec. in the orthogonal directions. If we assume that the LEM has a thrust acceleration of the order of 3.5 m/sec.^2 (1/3 Earth g), then five seconds thrust would lead to a velocity uncertainty of 17.5 m/sec.

An error of the order of 17.5 m/sec. in velocity is intolerable, so it is apparent that some on-board measuring equipment must be provided. We have already assumed some attitude measuring equipment in order to obtain the orbit measurement accuracy stated. We must also assume that there is at least one on-board accelerometer. If the thrust axis is kept sufficiently close to the center of gravity, a single longitudinal accelerometer might be sufficient. For the time being, let us assume that this is the case. Let us also assume an accuracy of 0.01 m/sec.^2 for this accelerometer, and that the accelerometer readings are transmitted to Earth as often as needed.

We assume that the radar measurements cannot be at less than one second intervals to be uncorrelated, and that the accelerometer readings are transmitted at one second intervals. Consider the one-dimensional problem in which the mean velocity in a <u>one second</u> interval can be computed as the change in measured position in the interval, and also as the computed velocity at the beginning of the interval plus one-half the acceleration measured in the middle of the interval. In the worst case the standard deviation of the measured change in range is σ_R,

$$\sigma_R = 0.6 \times 100 \text{ m}$$

$$= 60 \text{ m}$$

leading to a standard deviation of σ_1

$$\sigma_1 = 60 \text{ m } \sqrt{2} \text{ / } 1 \text{ sec.}$$

$$= 85 \text{ m/sec.}$$

in the estimate of velocity. The acceleration error of 0.01 m/sec.^{2} over a one second interval leads to a standard deviation of σ_2,

$$\sigma_2 = \sqrt{\sigma^2 + 0.01^2}$$

in the estimate of velocity. Combining these, and assuming the process has continued long enough to reach a limiting value of standard deviation, we have

$$\frac{1}{\sigma^2} = \frac{1}{85^2} + \frac{1}{\sigma^2 + 0.01^2}$$

or

$$\sigma = 0.85 \text{ m/sec.}$$

which is good enough.

An estimate of the lateral acceleration due to thrust can be obtained from the accelerometer and the attitude gyros. Refer to Figure 1.

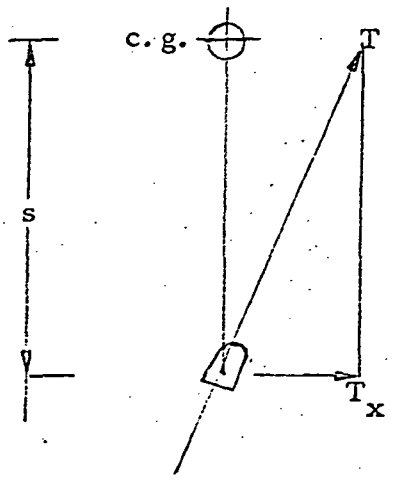

Figure 1.

The component of thrust normal to the line through the center of gravity is T_x. It has a moment arm s and results in an angular acceleration $\ddot{\theta}$.

$$T_x s = I \ddot{\theta}$$

in which I is the moment of inertia about the center of gravity. The lateral acceleration due to thrust is $\ddot{x}$

$$m\ddot{x} = T_x$$

Combining these two equations we find

$$\ddot{x} = \frac{I}{sm} \ddot{\theta}$$

or

$$\dot{x} = \frac{I}{sm} \dot{\theta} + c$$

Assuming that I, s and m each are known to 1 percent, and c is 0, we have that the error in lateral velocity is

$$\delta \dot{x} = \dot{x} \left(\frac{\delta I}{I} - \frac{\delta s}{s} - \frac{\delta m}{m} \right) + \frac{I}{sm} \delta \dot{\theta}$$

with the RMS value

$$\delta \dot{x}_{RMS} = \sqrt{3 \times 10^{-4} \dot{x}^2 + \left(\frac{I}{sm}\right)^2 (\delta \dot{\theta})^2}$$

Now, if $\dot{x}$ is limited to 50 m/sec., and the radius of gyration, $\sqrt{I/m}$, is of the order of s, and s is of the order of 5 meters, then

$$\delta \dot{x}_{RMS} < \sqrt{1.5^2 + (5 \delta \dot{\theta})^2}$$

Certainly $\delta \dot{\theta}$ will be known to better than 0.01 rad/sec., so $\delta \dot{x}_{RMS}$ is less than 1.5 m/sec.

Thus we see that each component of velocity apparently can be determined to better than 2 m/sec. during deboost to hover and landing.

Alternatively, in place of the mass flow meter required to find m, two lateral accelerometers could be used. In that case all components of velocity would be known to 0.85 m/sec. or better.

Up to this point we have ignored errors in knowledge of vehicle attitude. These are important because an error $\delta\theta$ in attitude results in an acceleration error $a_T \delta\theta$ normal to the intended thrust acceleration. Considering an attitude error about one axis only, with attitude fixed, combining radar and accelerometer data at one second intervals, and looking at the result after a long time, we have

$$\frac{1}{\sigma^2} = \frac{1}{85^2} + \frac{1}{\sigma^2 + (a_T \sigma_\theta)^2}$$

or

$$\left|a_T \sigma_\theta\right| = \frac{\sigma^2}{\sqrt{85^2 - \sigma^2}}$$

If σ is to be less than 1 m/sec., then $\left|a_T \sigma_\theta\right|$ must be less than 0.109 m/sec.^{2}, and if a_T can be as large as 3.5 m/sec.^{2}, σ_θ must be less than 0.031 radians. The Hohmann transfer from circular orbit and the deboost to touchdown require about an hour, so the angular rate error of the gyros must be less than 0.086 mils/sec., which is easily achieved.

We can then picture an on-board measurement system consisting of three strapped-down rate gyros with a drift offset of less than 0.086 mils/sec., and three accelerometers accurate to 0.01 m/sec.^{2}

The use of more than one Earth-based radar during deboost to hover and touchdown, however, has some communications disadvantages to be touched on later. It is worthwhile then to consider use of a single Earth-based radar during deboost to hover and touch down. At the start of deboost, position and velocity are known to

90 meters and 0.075 meters/sec. Using the on-board system already described would result in a velocity error of greater than 51 m/sec. at touchdown (= 1700 m/sec. boost x 0.03 rad. misalignment), resulting from gyro errors, and a velocity error of 2.5 m/sec. (=0.01 m/sec.^{2} x 250 sec.) resulting from accelerometer errors. It is apparent that significantly better gyros must be employed in this system. Introducing a gyro with a drift of 0.0002 mils/sec. reduces the error from this source to 1.1 m/sec.

Alternatively, 0.003 mils/sec. drift gyros can be used if a means for alignment accurate to 0.6 mils or better just prior to deboost is provided.

Computing and Guidance

The navigation and guidance computations may be performed either on board the LEM or on Earth. It is by far preferable to do the computations on Earth in order to avoid the mass of a computer in the LEM, but not all the computations can be done on the Earth, because the more than 2 second round trip time for communications is not consistent with the control dynamics of the LEM. Therefore, at least a portion of the guidance and navigation computations must be performed on board.

It is obvious that the radar data prior to the start of deboost should be processed on Earth. Offhand, it seems that all data except that closely associated with control of rocket thrust magnitude and attitude control could be Earth-based. The on-board system might appear as in Figure 2, in which the upper case letters represent commanded values. The x-attitude control loop is closed in the vehicle to keep the roll rate zero. The longitudinal thrust acceleration commands and the pitch and yaw rate commands are received intermittently and remembered. If the commanded thrust acceleration is zero, the attitude rate commands are directed to attitude control rockets. If the commanded thrust acceleration is not zero, the attitude rate commands control the thrust rocket direction. The

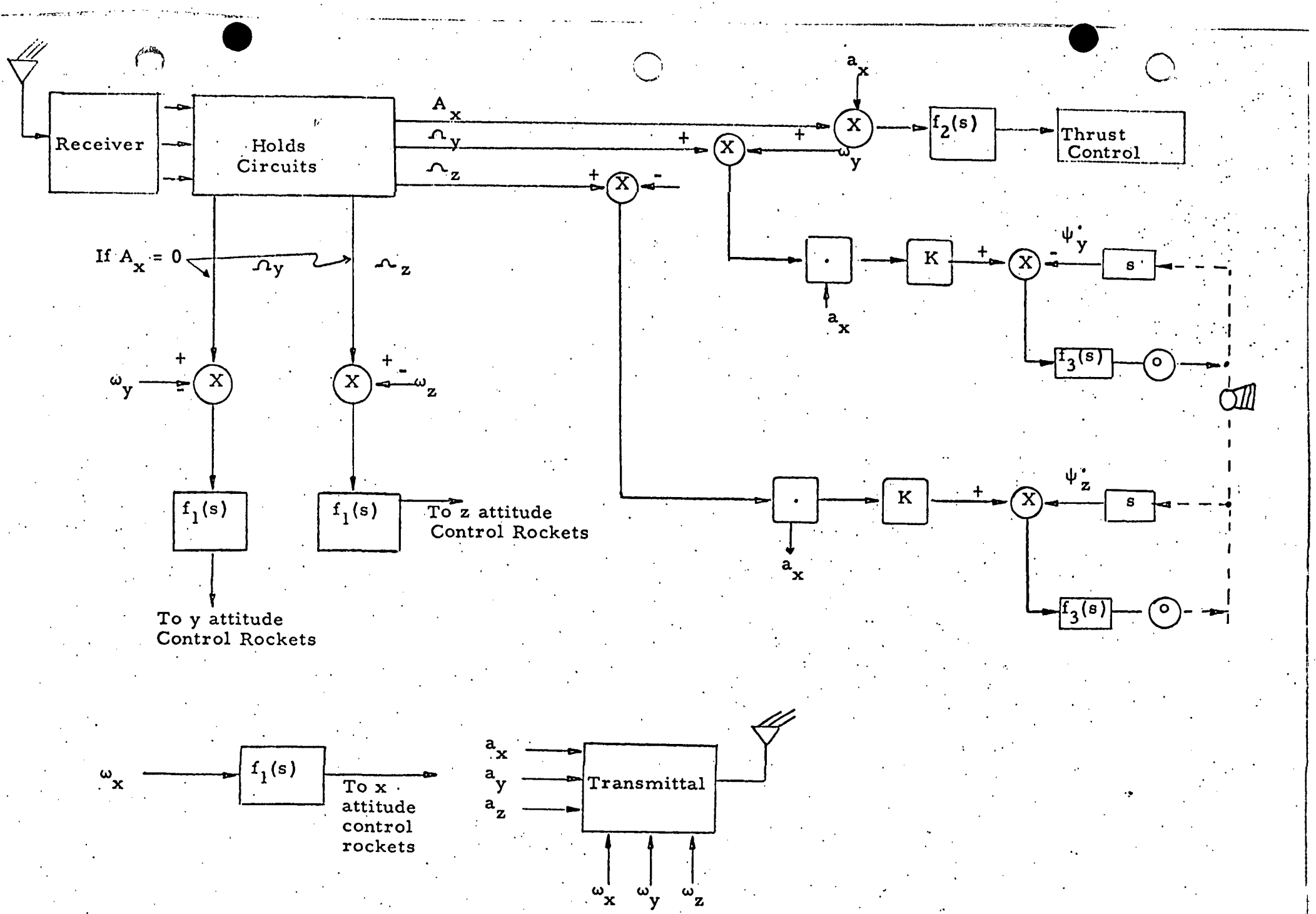
Receiver
Holds Circuits
A_x
Ω_y
Ω_z
If $A_x = 0$
ω_y
ω_z
$f_1(s)$
$f_1(s)$
To z attitude Control Rockets
To y attitude Control Rockets
a_x
$f_2(s)$
Thrust Control
ω_y
K
$\dot{\psi}_y$
s
$f_3(s)$
K
$\dot{\psi}_z$
s
$f_3(s)$
ω_x
$f_1(s)$
To x attitude control rockets
a_x
a_y
a_z
Transmittal
ω_x
ω_y
ω_z

measured accelerations and angular rates are transmitted continuously or at a high rate to Earth. In this fashion all the high speed control loops are contained within the LEM and require only "simple" servos. The lower bandwidth, more complex computations are performed on Earth on the basis of thrust acceleration and angular rate information transmitted continuously or at a high rate.

The most critical portion of the Earth-LEM loop will probably be that of attitude control if attitude is to be determined from strapped-down rate gyros. Let us consider an x' y' z' co-ordinate system with directions fixed in space, and with the vehicle axes related to this by means of the Euler angles shown in Figure 3. Then

$$\dot{\psi}_3 = \omega_x$$

$$\dot{\psi}_2 = \omega_y \cos\psi_3 - \omega_z \sin\psi_3$$

$$\dot{\psi}_1 = \omega_y \sin\psi_3 + \omega_z \cos\psi_3$$

If values of ω_x, ω_y and ω_z are received intermittently on Earth, either at fixed intervals or whenever a fixed increment occurs in ω_x, ω_y or ω_z, the above differential equations cannot be solved, but instead a set of difference equations must be solved. The difference between the solution of the difference equations and the differential equations must be examined to make sure it is negligible. This is a tough problem and will be left for another note.

The next step in increasing the on-board equipment is to transfer the attitude calculations to a computer on board the vehicle or to abandon the strapped-down gyros and put a stablepplatform in the LEM. Both can be expensive in terms of weight. In either case, there must be an on-board system for alignment just prior to deboost, or 0.0002 mil/sec. drift gyros must be used, or else three Earth-radars must be used to correct the on-board system.

Still another phase of operations that must be considered is the initial boost into the Hohmann transfer orbit. Here the LEM is

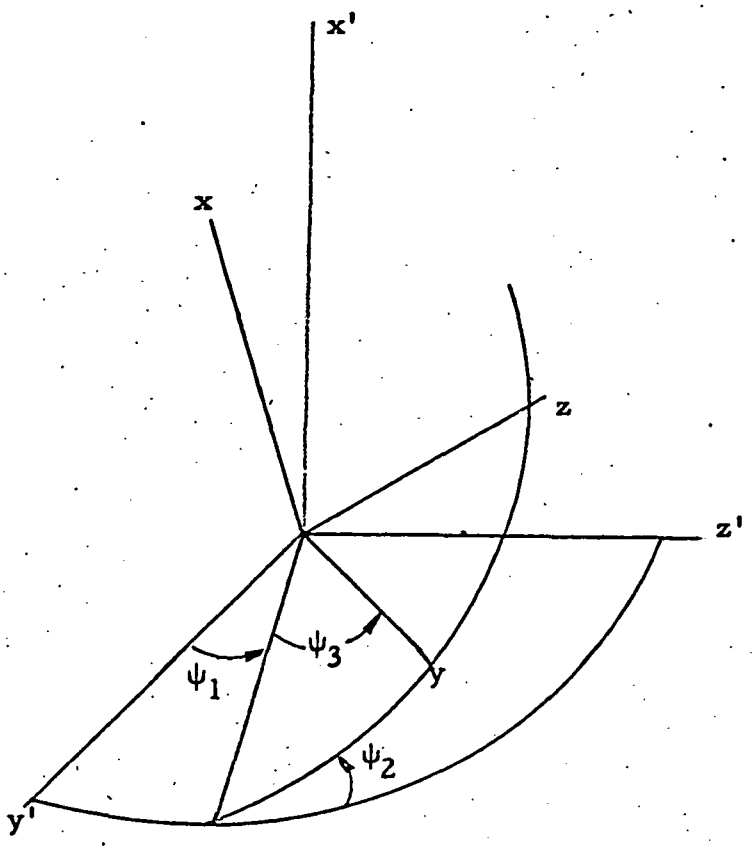

Figure 3.

not visible to the Earth, so either the maneuver must be commanded from the CSM or by a programmer on board the LEM. A simple programmer on board the LEM, consisting only of an integrator to control the total change in velocity would appear to be satisfactory.

Attitude Control Alignment

There are two separate sets of problems to be considered in LEM attitude control alignment. One of these is alignment prior to injection into the Hohmann transfer orbit. The other is alignment just prior to deboost.

Considering alignment prior to the Hohmann transfer first, the alignment tolerances are quite loose. Since the orbit is a Hohmann transfer, boost errors out of the plane of the orbit will have a negligible effect on perilune position. Likewise, boost errors in the vertical direction will not affect perilune altitude, and only slightly affect its position. In addition, tangential boost errors will not greatly affect perilune altitude, a boost error of 1 m/sec. resulting in a perilune altitude change of only about 1340 meters. Since the total boost required for injection into a Hohmann transfer orbit from 80 n. mi. altitude to 8 n. mi. altitude is just about 30 m/sec. several degrees misalignment can be tolerated.

The situation at the start of deboost to hover and touchdown is quite different. Here, as already indicated, the attitude must be known to 0.03 radians if three Earth radars are used during the descent, or to about 0.0007 radians if only one radar is used.

Let us consider the 0.03 radian case first. This can be easily obtained either by using star, Earth or Sun trackers, or by alignment prior to separation from the CSM simply by rotating the CSM-LEM pair to the proper orientation using the guidance and navigation equipment in the LEM.

The 0.0007 radian case is far more difficult. It must be accomplished either just prior to deboost using star trackers, or by means of a very elaborate alignment system involving both the

CSM and the LEM prior to separation. Neither of these is especially inviting, although the star tracker measurements do not have to be as accurate.

Communications

The principal problems in communications in LEM truck landing are the more than two second round-trip propagation, and the delays in communications between the MSFN radars and the computing facility.

The on-board navigation and guidance equipment, the MSFN radars, the computing facility and all the communication links constitute a servo system for LEM truck landing. This servo system has lags corresponding to the communications propagation times, and hence presents some possible difficulties in obtaining satisfactory, stable operation.

The problem is most severe during the hover-to-touchdown phase of operations; during the prior phases the on-board system is sufficiently good that the ground is essentially only monitoring its operation and sending it a slight modification of a pre-programmed deboost procedure.

During the hover-to-touchdown phase, however, the ground may play a more active part in controlling the LEM truck. A mitigating circumstance is that this phase can be performed using only one MSFN radar and the on-board sensors, eliminating the ground communication problem if a computer is available at the radar; this is possible since the vehicle position, velocity and attitude are known sufficiently well at hover that the radars do not contribute greatly in the remaining phase.

The LEM-Earth propagation delay effects on servo performance must still be investigated.

TV, Radio Altimeter, Beacon or Optical Drift Meter

In all of the previous discussion it has been assumed that no landing aids are available for the terminal phase of landing, and that the landing must be accomplished with on-board inertial equipment

or Earth-based radar. Three possible landing aids exist, however. These are TV, altimeter, beacon and optical drift meter. Each has advantages and disadvantages.

1. TV.

Provides a picture of the terrain to allow avoidance of hillocks, gullies and boulders. In fact, TV is useful only if there are irregularities in the terrain by which relative motion can be judged. In the absence of any reference scale for dimensions on the lunar surface, TV can not provide a clue as to height or altitude rate, except that it can indicate that the vertical velocity is positive or negative. In the presence of acceleration due to gravity or thrust, or in the presence of a large angular velocity of the TV camera, the point on the ground through which the velocity vector passes is difficult or impossible to determine. Has delay of Moon-Earth round-trip propagation time.

2. Radio Altimeter.

Provides altitude and altitude rate above lunar surface, with essentially zero delay, but gives no clue to horizontal velocity. Can be tied in with on-board control system.

3. Beacon.

Provides range and range-rate to fixed point on Moon. Without a directional antenna on the LEM, the beacon is less satisfactory than the radio altimeter. With a directional antenna on the LEM the beacon is probably too complex. There is also the problem of placing the beacon on the lunar surface.

4. Optical Drift Meter.

Provided that the lunar surface is reasonably flat, but with small scale distinguishable features. The optical drift meter can provide information about all three velocity components. There is, however, the two-second round-trip to Earth propagation time, or more on-board computing equipment must be supplied to combine optical drift meter data with attitude and attitude rate date to compute

the components of velocity.

Actually altitude rate can be determined with sufficient accuracy by a single Earth-based radar. It is only altitude and the horizontal components of velocity that must be found with these auxiliary devices.

Perhaps some combination of auxiliary devices would do the job, or some device not discussed here. This topic needs far more consideration.

Lunar Landing Orbits

Far more study of lunar landing orbits is indicated to land a maximum payload on the Moon. In the manned LEM for example, the transfer orbit brings the LEM down to 8 n.mi. from 80 n.mi. before deboost starts. In the LEM truck there appears to be no reason why the transfer orbit need not have a perilune altitude of just 4 or 5 km. with a saving in propellant since landing sight visibility and aborts are not of such great importance. Likewise, various CSM-LEM lunar orbits should be considered.

Previous Apollo Notes have indicated that visual or radar observation from the CSM will contribute little to LEM guidance and navigation unless a far better radar is installed, and there is no desire to place a radar in the LEM or CSM, so there appears to be no need for visibility between the CSM and LEM during landing.

Conclusions

A promising system for further investigation comprises three strapped-down gyros with drift rates of 0.08 mils/sec., three accelerometers accurate to 0.01 $m/sec.^2$, a rudimentary autopilot and some terminal guidance means on board the LEM truck, and three MSFN radars and a computer on the ground, plus communications equipment. From the time the LEM becomes visible on its descent path until hover, data from the three MSFN radars are combined with data from the on-board system. From hover to touchdown data from one MSFN radar and the on-board system would be used, avoiding the problem of very high-speed Earth communications.

APOLLO NOTE NO. 161

L. Lustick
30 December 1963

COMPARISON OF SCHMIDT KALMAN METHOD WITH MAXIMUM LIKELIHOOD METHOD FOR THE CASE OF A STRAIGHT LINE

Purpose

The purpose of this note is to indicate the agreement between the Schmidt-Kalman method and maximum likelihood method for determining the parameters defining a straight line.

Illustrative Problem

Consider that at time, t= 0, the estimates of the parameters defining the straight line ($z = a + bt$) are $\hat{a}_1$ & $\hat{a}_2$ and that the covariance matrix defining the uncertainty in these parameters are as defined below.

$$\begin{vmatrix} \overline{\Delta\hat{a}_1^{\,2}} & \overline{\Delta\hat{a}_1 \Delta\hat{a}_2} \\ \overline{\Delta\hat{a}_2 \Delta\hat{a}_1} & \overline{\Delta\hat{a}_2^{\,2}} \end{vmatrix} = \begin{vmatrix} \gamma_{11} & \gamma_{12} \\ \gamma_{21} & \gamma_{22} \end{vmatrix}$$

The argument will be developed in the following manner.

1. The maximum likelihood method will be used to determine the changes in the estimates $\hat{a}_1$ & $\hat{a}_2$ subsequent to the measurement of $Z(t_1)$ at time t_1.
2. Considering that the origin for the time variable is changed, that is the equation of the line is $a_1 + a_2(t-t_1)$; the changes determined in step 1 will be used to obtain the changes indicated in the parameters $a_1 + a_2$.
3. The changes in the estimators determined in (2) will be shown to be the conditional means of the joint distribution of the errors in the parameters to be estimated at time t_1, a_1 & a_2 and the measurable (measurement-predicted measurement)

Discussion

Let $\begin{bmatrix} \gamma_{11} & \gamma_{12} \\ \gamma_{21} & \gamma_{22} \end{bmatrix}$ = covariance matrix consistent with the a priori estimators $\hat{a}_1 + \hat{a}_2$.

γ_{33} = noise in the measurement.

The likelihood function is as follows:

$$\mathcal{L} = -\frac{1}{2}\left\{ \gamma^{33}\left[Z - (c_1 + c_2 t_1)\right]^2 + \left[\gamma^{11}(c_1 - \hat{a}_1)^2 + 2\gamma^{12}(c_1 - \hat{a}_1)(c_2 - \hat{a}_2) + \gamma^{22}(c_2 - \hat{a}_2)^2\right]\right\}.$$

where: $c_1 + c_2$ are the estimator of a_1 & a_2 subsequent to the measurement of Z at time t_1

$$\frac{\partial \mathcal{L}}{\partial c_1} = \gamma^{33}\left[Z - (c_1 + c_2 t_1)\right] - \gamma^{11}(c_1 - \hat{a}_1) - \gamma^{12}(c_2 - \hat{a}_2) = 0 \qquad (1)$$

$$\frac{\partial \mathcal{L}}{\partial c_2} = \gamma^{33} t_1\left[Z - (c_1 + c_2 t_1)\right] - \gamma^{12}(c_1 - \hat{a}_1) - \gamma^{22}(c_2 - \hat{a}_2) = 0 \qquad (2)$$

Equation (1) can be modified in the following manner:

$$\gamma^{33}\left[Z - (\hat{a}_1 + \hat{a}_2 t_1)\right] + \gamma^{33}(\hat{a}_1 + \hat{a}_2 t_1) - \gamma^{33}(c_1 + c_2 t_1) - \gamma^{11}(c_1 - \hat{a}_1) - \gamma^{12}(c_2 - \hat{a}_2) = 0$$

let $y = Z - (\hat{a}_1 + \hat{a}_2 t_1)$

$A_1 = c_1 - \hat{a}_1$

$A_2 = c_2 - \hat{a}_2$

then

$$A_1\left[\gamma^{33} + \gamma^{11}\right] + A_2\left[\gamma^{33} t_1 + \gamma^{12}\right] = \gamma^{33} y \qquad (3)$$

Likewise equation (2) can be modified:

$$A_1\left[\gamma^{33} t_1 + \gamma^{12}\right] + A_2\left[\gamma^{33}\Delta t^2 + \gamma^{22}\right] = \gamma^{33} t_1 y \qquad (4)$$

Solving the equations 3 and 4 for A_1 and A_2, the following is obtained:

$$A_1 = \frac{\gamma^{33}(\gamma^{22} - \gamma^{12}\Delta t)\, y}{D}$$

$$A_2 = \frac{\gamma^{33} y\left[\gamma^{11} t - \gamma^{12}\right]}{D}$$

Where:

$$D = \gamma^{33}\left[\gamma^{22} - 2\gamma^{12} t_1 + \gamma^{11} t_1^2\right] + \gamma^{11}\gamma^{22} - (\gamma^{12})^2$$

Let $A_1(t_1)$ = the indicated change at time t_1

$A_2(t_1) = A_2$

Then $$A_1(t_1) = \frac{y}{1 + \frac{\gamma_{33}\left[\gamma^{11}\gamma^{22} - (\gamma^{12})^2\right]}{\gamma^{22} - 2\gamma^{12}\Delta t + \gamma^{11}\Delta t^2}} \tag{5}$$

$$A_2(t_1) = \frac{\gamma^{33} y \left[\gamma^{11} t_1 - \gamma^{12}\right]}{\gamma^{33}\left[\gamma^{22} - 2\gamma^{12} t_1 + \gamma^{11} t_1^2\right] + \gamma^{11}\gamma^{22} - (\gamma^{12})^2} \tag{6}$$

Now $$\gamma^{11} = \frac{\gamma_{22}}{\gamma_{11}\gamma_{22} - \gamma_{12}^2} \tag{7}$$

$$\gamma^{12} = \frac{-\gamma_{21}}{\gamma_{11}\gamma_{22} - \gamma_{12}^2} \tag{8}$$

$$\gamma^{22} = \frac{\gamma_{11}}{\gamma_{11}\gamma_{22} - \gamma_{12}^2} \tag{9}$$

Substituting equations 7, 8 and 9 into 5 and 6, the following is obtained:

$$A_1(t_1) = \frac{(\gamma_{11} + 2\gamma_{12} t_1 + t_1^2 \gamma_{22})\, y}{\gamma_{11} + 2\gamma_{12} t_1 + t_1^2 \gamma_{22} + \gamma_{33}} \tag{10}$$

$$A_2(t_1) = \frac{y\left[\gamma_{22} t_1 + \gamma_{12}\right]}{\gamma_{11} + 2\gamma_{12} t_1 + \gamma_{22} t_1^2 + \gamma_{33}} \tag{11}$$

Now let us alternately define the covariance matrix consistent with the joint distribution of the errors in a_1, a_2 and y, the difference between the measured and predicted value of the measurable at time t_1.

APOLLO NOTE NO. 162

G. F. Floyd
6 January 1964

BISSETT-BERMAN PRESENTATION
at
HOUSTON

January 9, 1964

1.	Orbit Errors Program	Now
2.	Orbit Errors Program	In Debugging
	Orbit Errors Program	Future
3.	Long Range, Short Time MSFN Operation	
4.	LEM Rendezvous Picture (not included here)	
5.	MSFN Rendezvous Miss Uncertainty	
6.	Actual LEM Miss (Single Midcourse Correction)	
7.	Effect of Station Location	
8.	MSFN Stations	
9.	Ground Computations for Rendezvous	
10.	Earth Orbit Injection and Tracking Errors	
11.	Trans-Lunar Injection Tracking	
12.	Return to Earth Tracking Geometry	
13.	Return to Earth - No a priori Data	
14.	LEM Truck G & N	
15.	LEM Truck Descent Uncertainty	
16.	Best MSFN Operating Modes	

ORBIT ERRORS PROGRAM Now

1. USE

Range, Range-Rate, Angle

Fixed Biases in Range and Angle

A priori Data on Position, Velocity or Biases

Any Combination of the above with Boosts Between Measurements

2. MEASURED FROM

Fixed Points on Rotating Earth

Fixed Points on Moon in Orbit about Earth

Vehicles in Circular Orbit about Moon or Earth

Any Combination of the above

3. DETERMINE

Position and Velocity of Vehicle at anytime in Circular or Elliptic Orbit about Earth or Moon

Covariance Matrix of Errors in Position and Velocity at any time

Accuracy of Prediction of Re-entry Conditions

ORBIT ERRORS PROGRAM - IN DEBUGGING

1. Hyperbolic orbits
2. Station location errors
3. Gravitational constant errors
4. Speed of light errors

ORBIT ERRORS PROGRAM - FUTURE

1. Crossing LSOI
2. Correlated data

LONG RANGE, SHORT TIME MSFN OPERATION

1) Multiple Station Range Data Implies Large Bias

Due to time synchronization (.01 ms = 1500 m),

and uncertainty in velocity of light (10^{-6} → 400 m).

Has large σ = 15 m.

2) "$\dot{R}$" Data Really $\left(\frac{\Delta R}{t_{meas}}\right)$

Clock drift only amounts to 0.5 m in 25 min.

So get Range Change from Doppler with

σ = 1 m = Propagation Uncertainties plus

Spacecraft wobble.

3) Multiple Station 1 m Range Change

Via Doppler Cycle Counting.

MSFN RENDEZVOUS MISS UNCERTAINTY

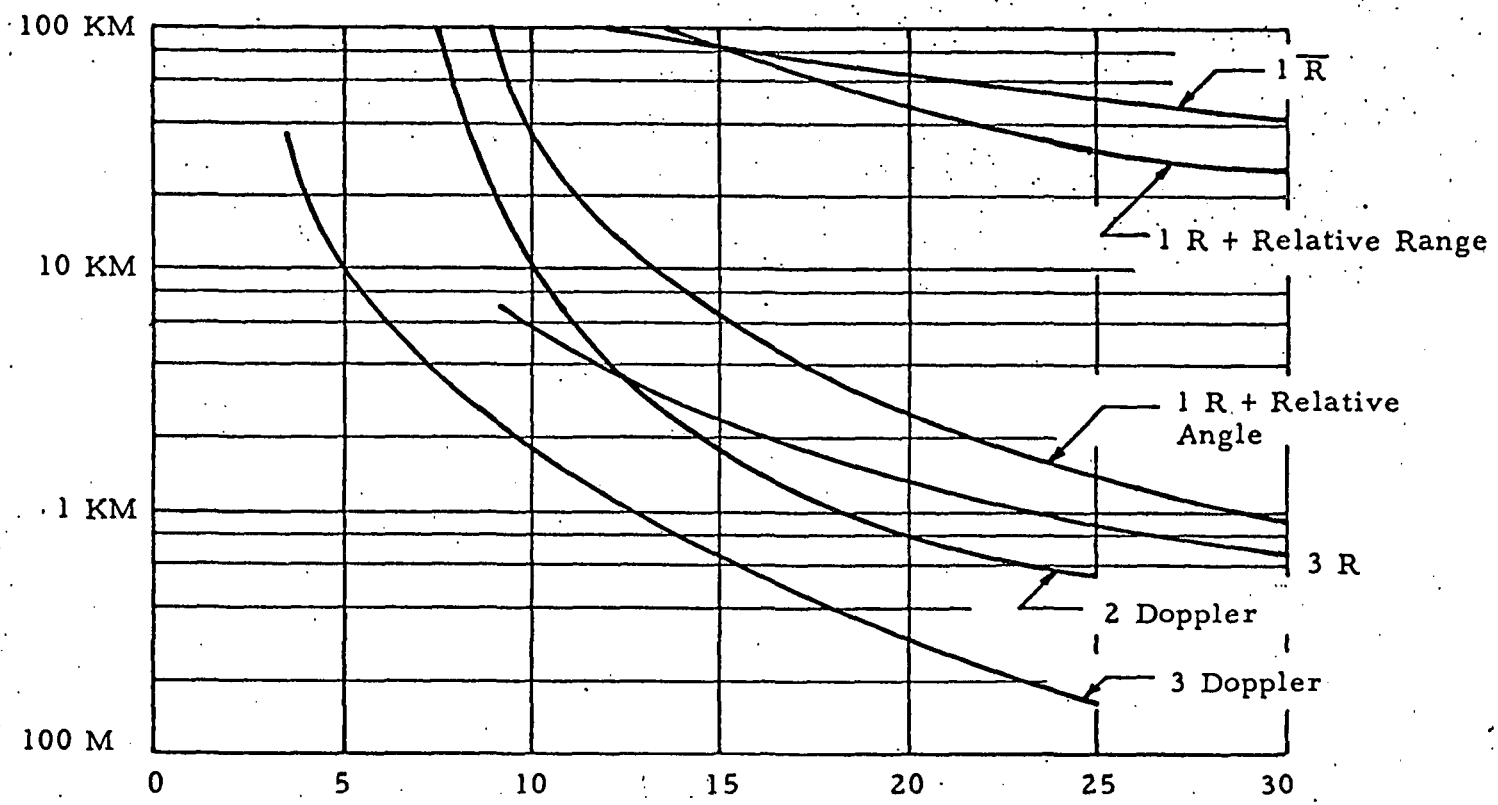

No A Priori Used

1 σ Values

Doppler:	1 m at 1 min.
Range:	15 m at 1 min. No Bias
Angles:	1 mil.(Rel); 0.8 mil
Relative Range:	750 m. (1/2%)

A Priori Data and Range Change
From Two Stations at 1 Minute Intervals $\sigma_{\Delta R}$ 0.6 m

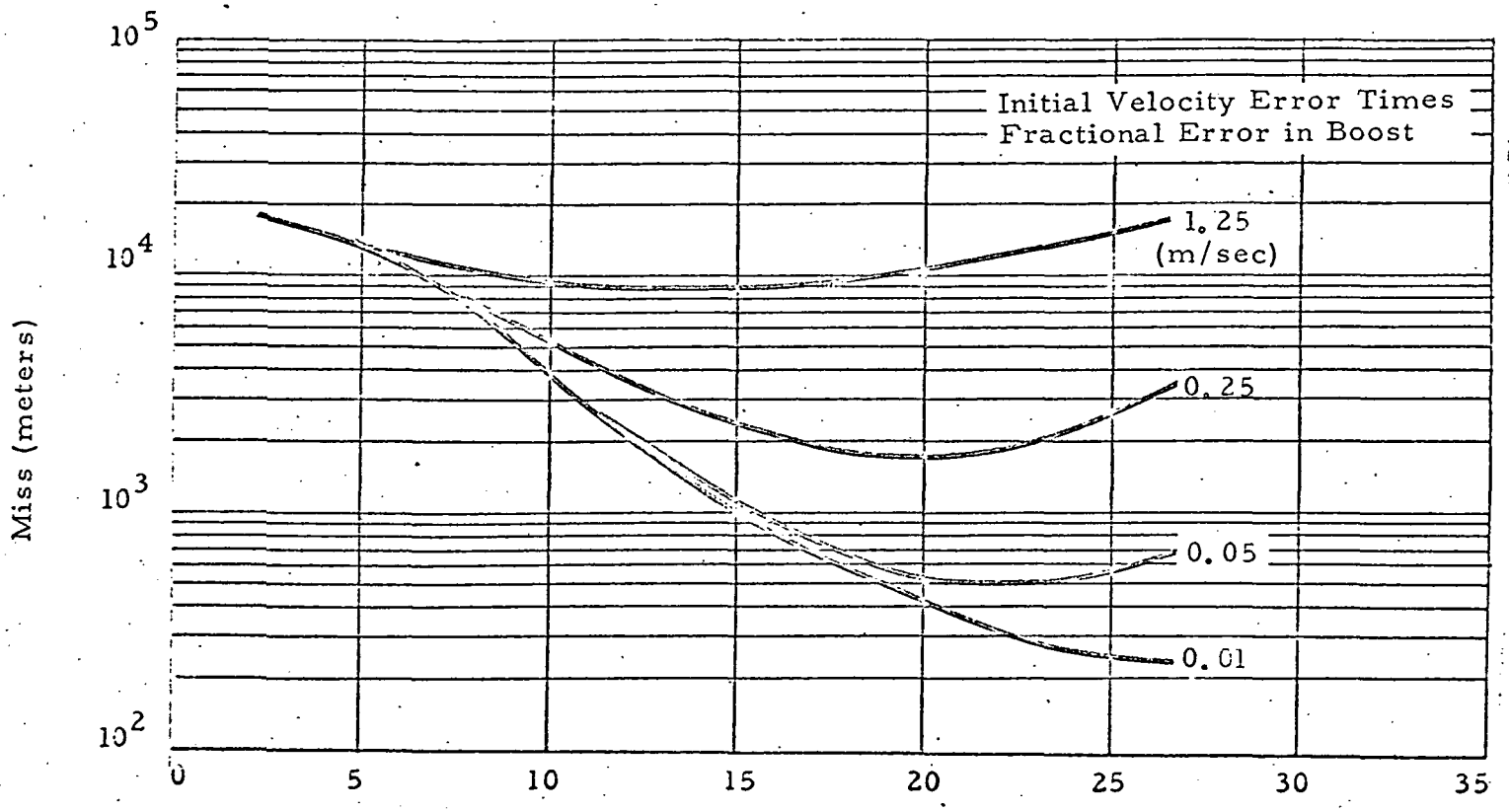

RMS Miss at Rendezvous for a
Single Corrective Boost

EFFECT OF STATION LOCATION

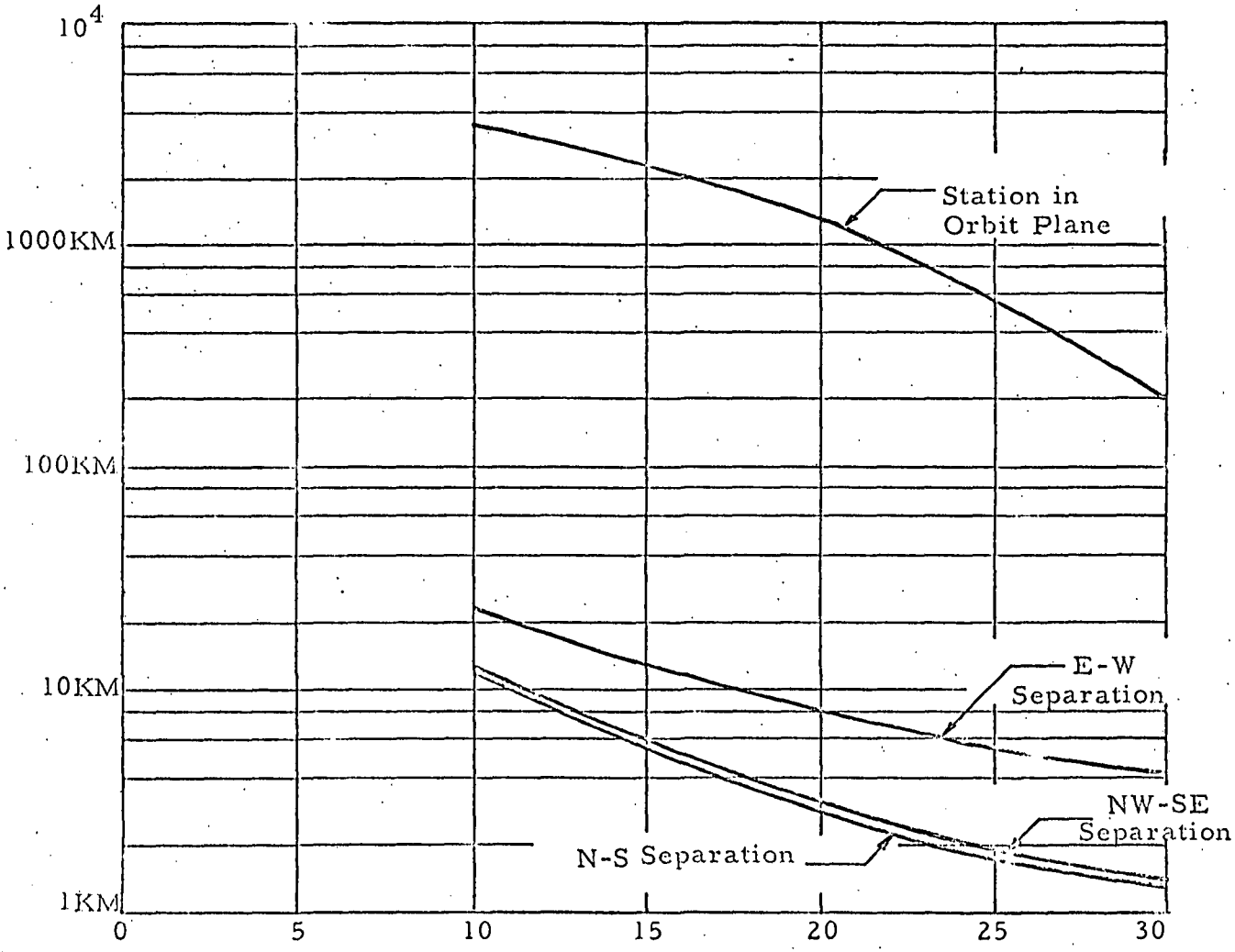

Minimum RMS Miss Near Rendezvous
Using Range-Rate from Two Stations
Separated by a Great Circle Distance
of 40°

$\sigma_{\dot{R}} = 0.03$ m/sec.

MSFN STATIONS

Must Be Out Of Orbit Plane

Want Minimum of 3 MSFN Stations That Can See Moon

Goldstone, Canaveral, Hawaii, Guam,

Carnarvon, Canberra, Ascension,

Johannesburg, Madrid

GROUND COMPUTATIONS FOR RENDEZVOUS

GIVEN:

30 Values of Range, Range-Rate and Angle from each of 3 ground stations.

Six estimated orbit parameters.

COMPUTE:

Ephemeris of vehicle using Encke method.

Expected values of measurements.

Likelihood of measurements.

Corrections to orbit parameters.

TIMING:

One complete iteration of the above using all data requires 7 seconds on 7094.

EARTH ORBIT INJECTION AND TRACKING ERRORS

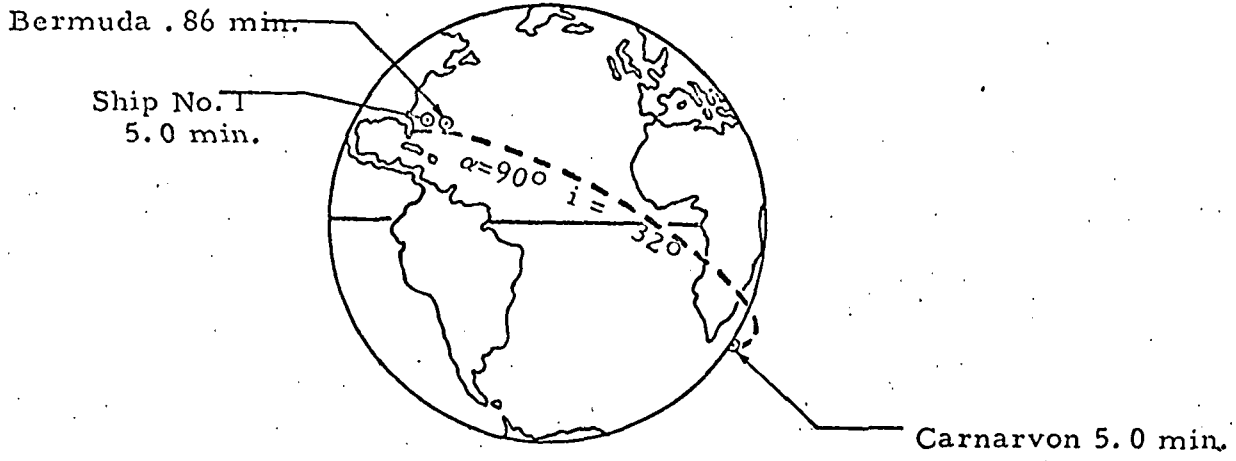

	RMS VELOCITY ERROR (M/S)		
	Bermuda Only	Bermuda + Ship No. 1	Bermuda + Ship No. 1 + Carnarvon
σ_R = 15 m $\sigma_{\dot{R}}$ = 0.1 m/s $\sigma_{\phi_1} = \sigma_{\phi_2} = 8 \times 10^{-4}$ r	3.65 (167.0)	.060 (.095)	.015
σ_R = 6 m $\sigma_{\dot{R}}$ = 6 m/s $\sigma_{\phi_1} = \sigma_{\phi_2} = 2 \times 10^{-4}$ r	1.40 (49.6)	.049 (.218)	.011
Both of above	1.16 (44.6)		

(Numbers in parenthesis indicate unknown Range and Angle Biases were included in computations)

TRANS-LUNAR INJECTION TRACKING

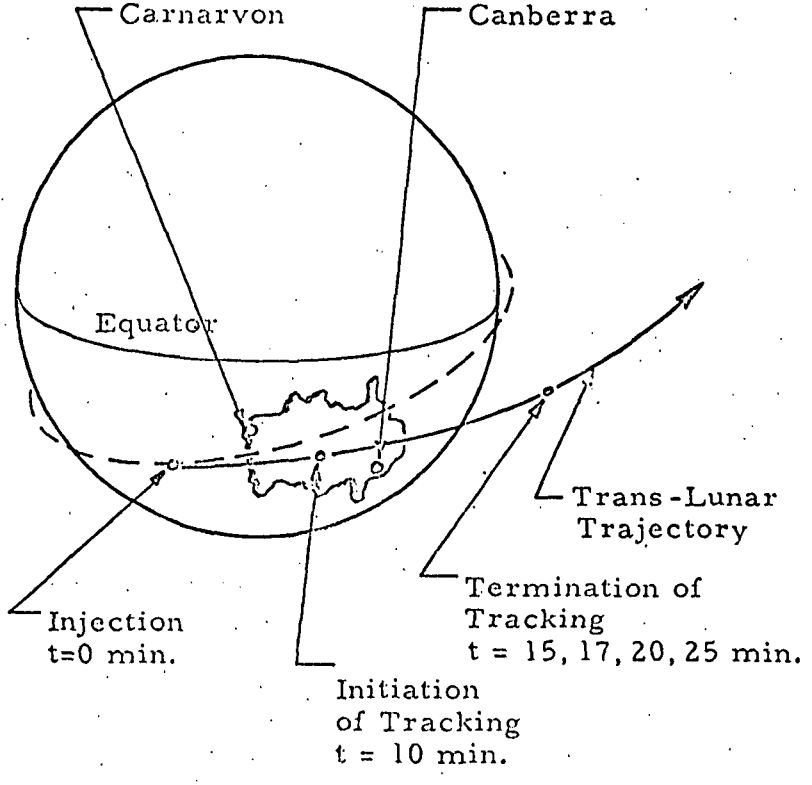

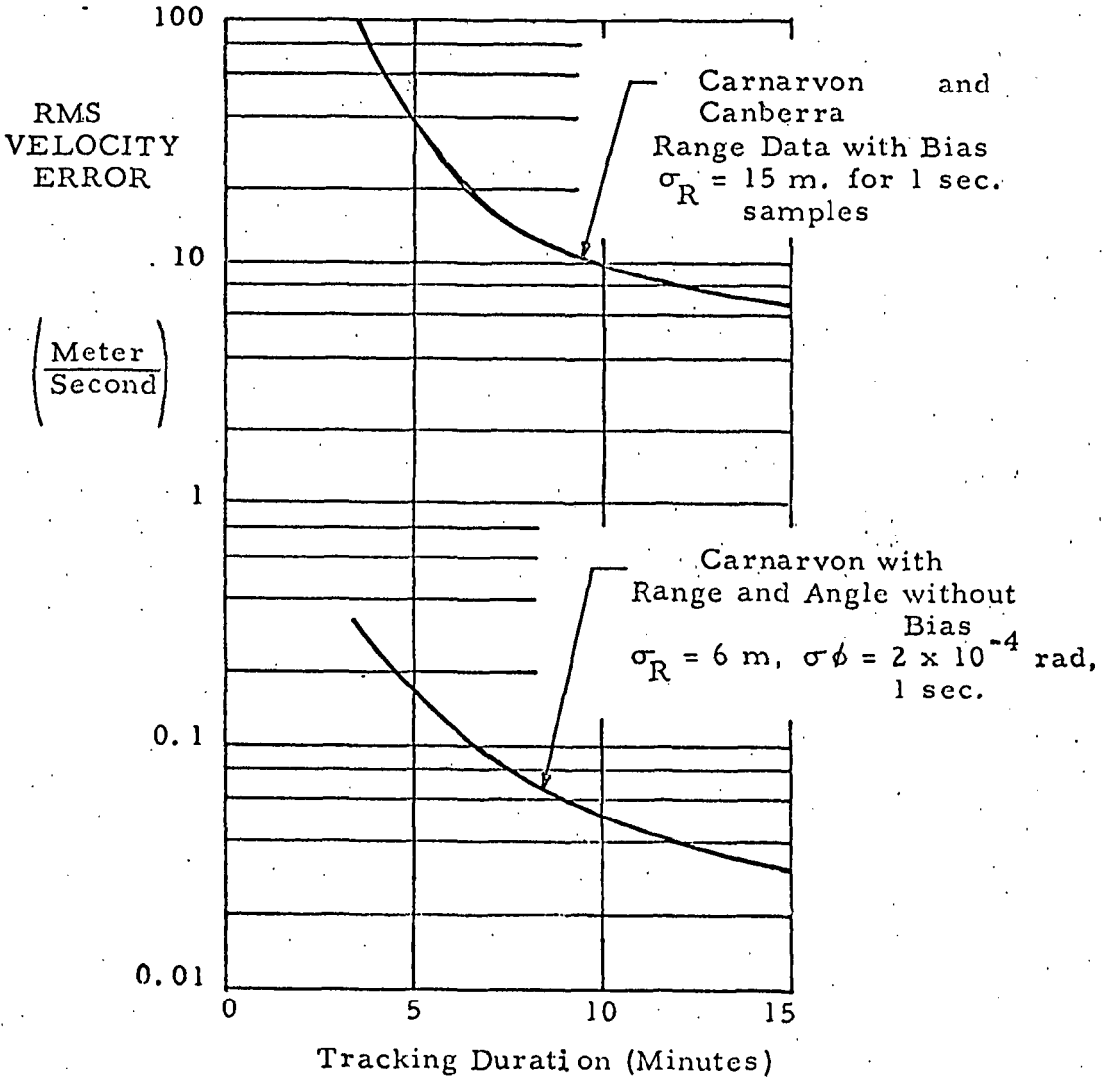

RETURN TO EARTH TRACKING GEOMETRY

Station	Lat.	Long.
1	-20°	+50°
2	+20°	-50°
3	-20°	-50°

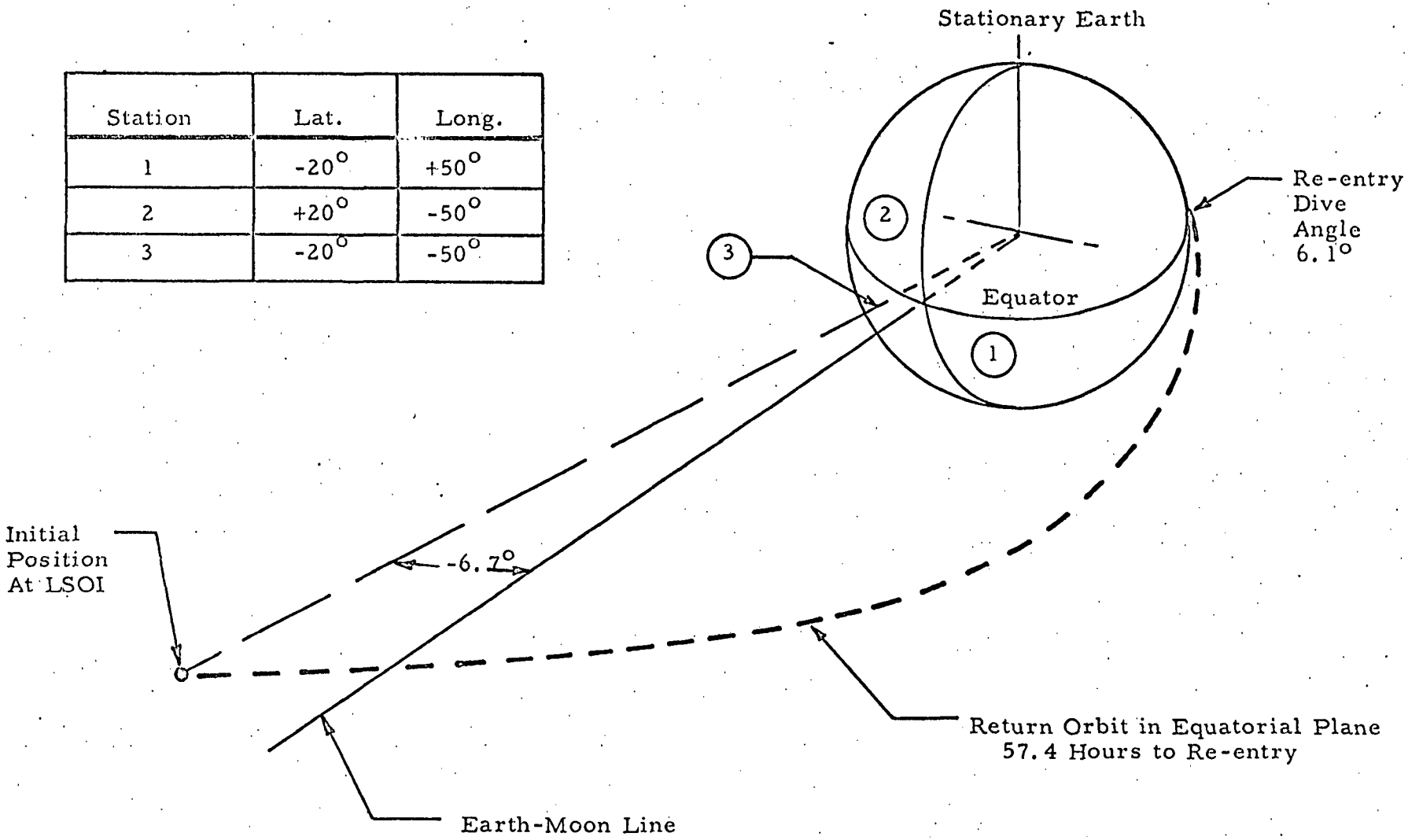

RETURN TO EARTH ——— NO A PRIORI DATA							
STATIONS	Hours To Re-Entry	Range Without Bias		Range With Bias		Range Rate	
		Dive Angle σ	RMS Miss	Dive Angle σ	RMS Miss	Dive Angle σ	RMS Miss
① ② ③	45	.0081°	1.70 KM	.455°	141 KM	5.020°	1570 KM
	33	.0017°	0.35 KM	.053°	17 KM	1.130°	374 KM
	21	.0005°	0.11 KM	.010°	4 KM	0.299°	115 KM
	9	.0002°	0.04 KM	.002°	1 KM	0.045°	27 KM
① ②	45	17.14°	8630 KM	194.0°	102000 KM	2350°	1.2×10^6 KM
	33	3.26°	1640 KM	21.8°	11000 KM	324°	1.6×10^5 KM
	21	1.14°	575 KM	3.6°	1740 KM	68°	3.3×10^4 KM
	9	0.06°	32 KM	0.36°	156 KM	6.3°	2.7×10^3 KM

Range σ = 15 meters Range Rate σ = 3 cm/sec.

LEM TRUCK G & N

1. Simple autopilot
2. 3 strapped-down rate gyros
3. 3 accelerometers, error 0.01 m/sec^2
4. Earth-based computing

1 MSFN Radar	LEM Hohmann	LEM Synchronous	LEM-CSM Hohmann
Attitude at Injection	3°	($<3^\circ$)	Does not apply
Attitude at Deboost	0.06°	0.06°	0.06°
Gyro Drift	0.04°/hr.	0.08°/hr.	0.6°/hr.
3 MSFN Radars			
Attitude at Injection	3°	($<3^\circ$)	Does not apply
Attitude at Deboost	1.7°	1.7°	1.7°
Gyro Drift	18°/hr.	18°/hr.	18°/hr.

Range Change From Two Stations
at 1 Minute Intervals $\sigma_{\Delta R} = 0.6$-m.

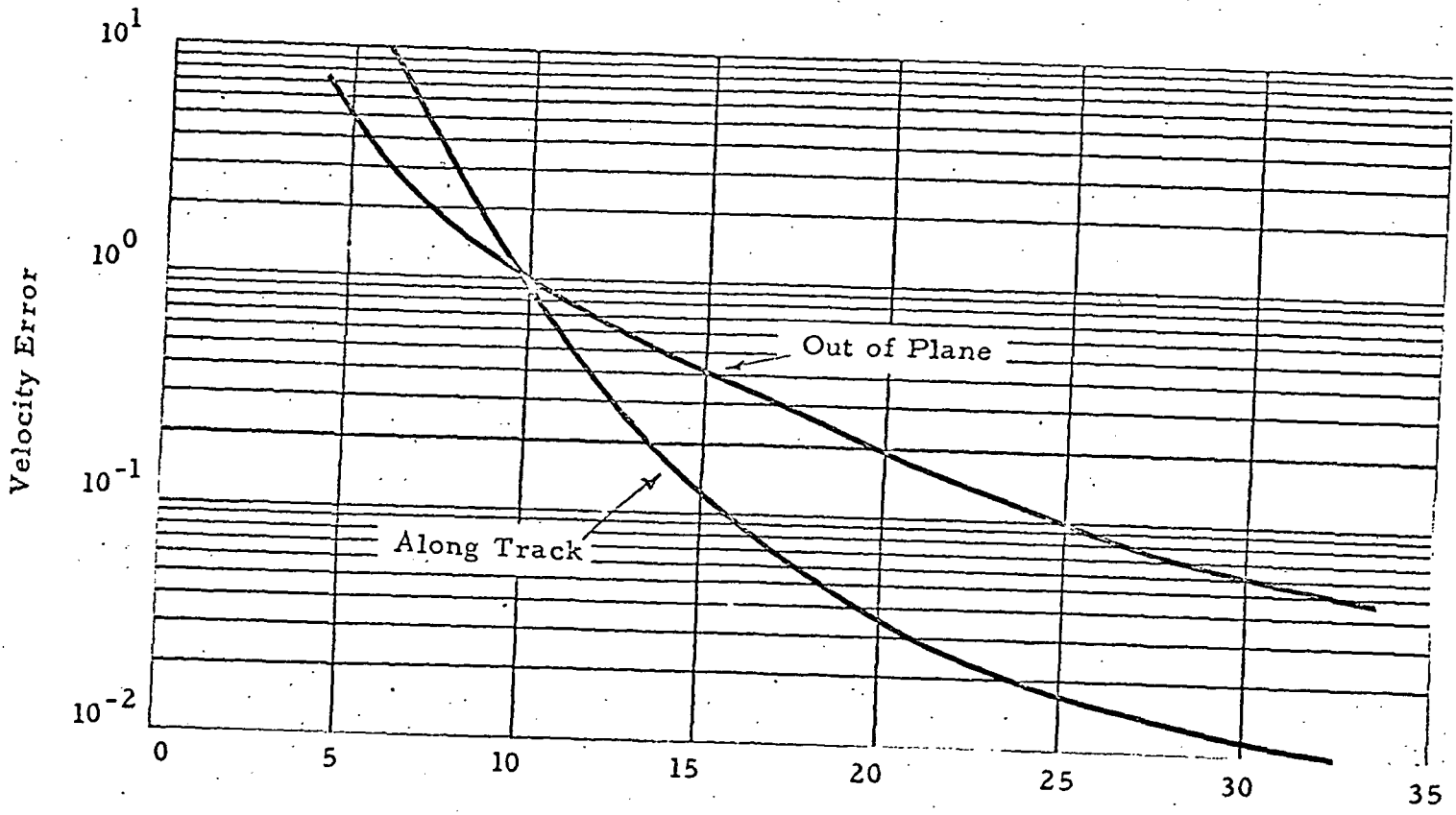

RMS Errors in Prediction
of Perilune in LEM Truck Descent

Range Change From Two Stations
at 1 Minute Intervals $\sigma_{\Delta R} = 0.6$ m

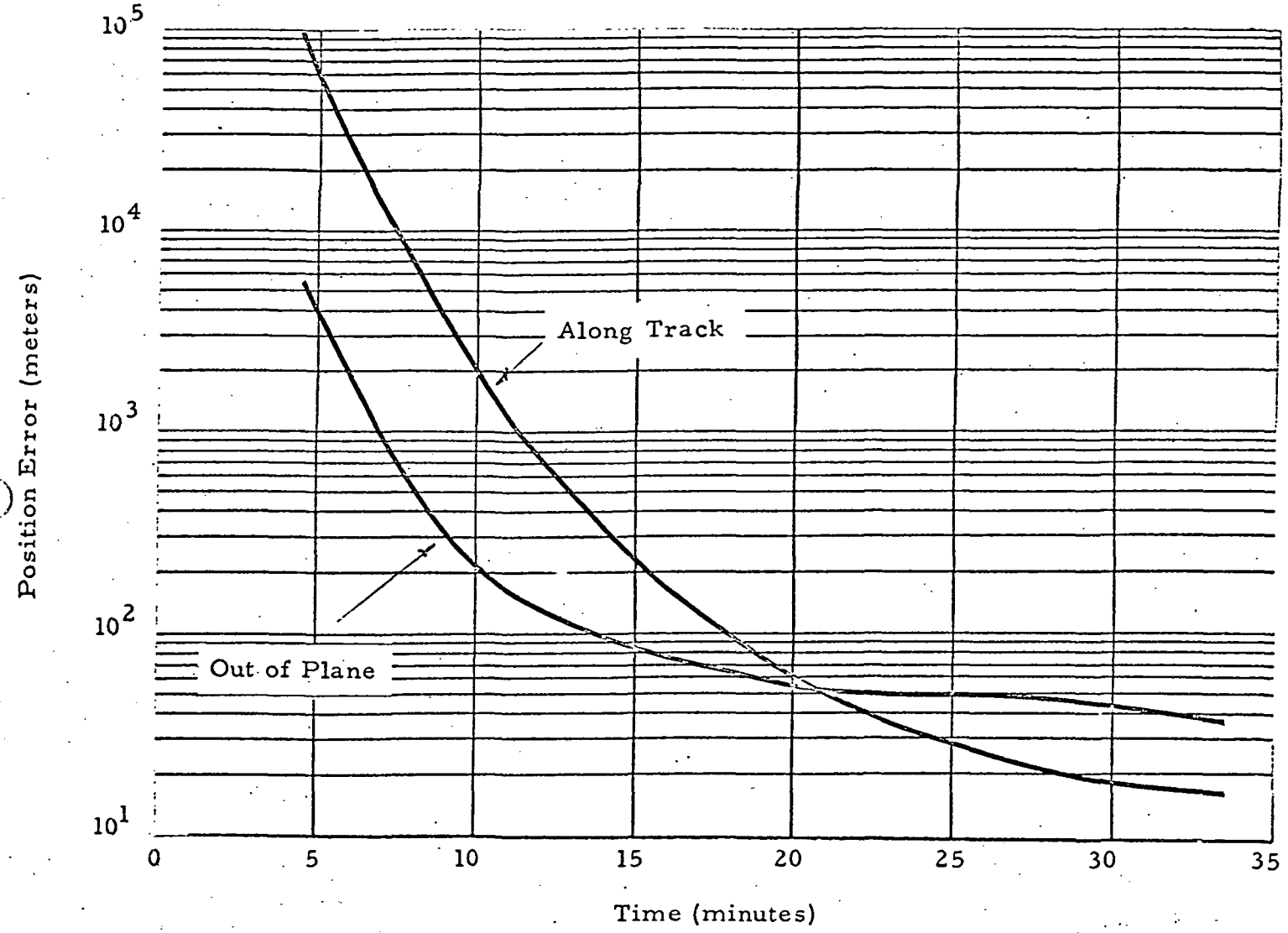

RMS Errors in Prediction
of Perilune in LEM Truck Descent

BEST MSFN OPERATING MODES

Observation Time	RANGE	
	SHORT	LONG
Short	Vector Range (R + 2 Angles)	Doppler Range Change
Long	Vector Range	Random Range Code (Time Share Stations)

The Bissett-Berman Corporation 2941 Nebraska Avenue, Santa Monica, California EXbrook 4-3270

APOLLO NOTE NO. 163

H. Engel
14 January 1964

PITFALLS OF BEST LINEAR ESTIMATES

We have previously warned that best linear estimating schemes such as the Kalman-Schmidt method do not converge to the correct answer even with an infinite amount of data. Some people have found this warning difficult to accept or to comprehend. Therefore, we give a particular example in this note.

The mathematics of orbits are too complicated to provide a clear example. Therefore we choose a much simpler instance. We wish to determine the parameter "a" in a function of the form

$$y = \sin a t$$

on the basis of measurements $y_m(t_i)$ which are corrupted by zero mean random Gaussian noise; i.e.,

$$y_m(t_i) = y(t_i) + n(t_i)$$

in which $n(t_i)$ has a zero mean Gaussian distribution independent of time and with standard deviation σ_n.

In the process of linear estimation (see Apollo Note No. 150) we assume a value a_o for "a", and have a reference "trajectory"

$$y_r = \sin a_o t$$

We then attempt to find the best linear estimate of Δa $(=a - a_o)$ in order to minimize

$$\sum_i \left(y_m - y_r - \frac{\partial y_r}{\partial a_o} \Delta a \right)^2 .$$

This is done by setting the partial derivative of the sum with respect to Δa equal to 0, leading to

$$\Delta a = \frac{\sum_i (y_m - y_r) \frac{\partial y_r}{\partial a_o}}{\sum_i \left(\frac{\partial y_r}{\partial a_o} \right)^2}$$

$$= \frac{\sum_i (y - y_r + n) \frac{\partial y_r}{\partial a_o}}{\sum_i \left(\frac{\partial y_r}{\partial a_o} \right)^2}$$

Now for a large number of uncorrelated measurements the expected value of $\sum_i n \frac{\partial y_r}{\partial a_o}$ is 0, so

$$\Delta a = \frac{\sum_i (y - y_r) \frac{\partial y_r}{\partial a_o}}{\sum_i \left(\frac{\partial y_r}{\partial a_o} \right)^2}$$

with a variance

$$\sigma^{-2} = \frac{\sigma_n^2}{N} \left\{ \sum_{i=1}^{N} \left(\frac{\partial y_r}{\partial a_o} \right)^2 \right\}^{-1}$$

Now,

$$\frac{\partial y_r}{\partial a_o} = t \cos a_o t$$

and

$$\sigma^{-2} = \frac{\sigma_n^2}{N} \left\{ \sum_{i=1}^{N} (t \cos a_o t)^2 \right\}^{-1}$$

We shall assume that the measurements are sufficiently close-spaced, i.e., ΔT small that we can replace summations by integrals. Then,

$$\sigma^2 = \frac{\sigma_n^2 (\Delta T)^2}{T} \left\{ \int_o^T t^2 \cos^2 a_o t \; dt \right\}^{-1}$$

$$= \frac{\sigma_n^2 (\Delta T)^2}{T} \left\{ \left[\frac{t^3}{6} + \left(\frac{t^2}{4a_o} - \frac{1}{8a_o^3} \right) \sin 2 a_o t + \frac{t \cos 2 a_o t}{4 a_o^2} \right]_0^T \right\}^{-1}$$

$$= \frac{\sigma_n^2 (\Delta T)^2}{T \left[\frac{T^3}{6} + \left(\frac{T^2}{4a_o} - \frac{1}{8a_o^3} \right) \sin 2 a_o T + \frac{T \cos 2 a_o T}{4 a_o^2} \right]}$$

As T increases, σ^2 decreases.

Now, let us evaluate Δa in the same fashion.

$$\Delta a = \frac{\sum (y - y_r) \frac{\partial y_r}{\partial a_o}}{\sum \left(\frac{\partial y_r}{\partial a_o} \right)^2}$$

$$= \frac{\sum (\sin a t - \sin a_o t) t \cos a_o t}{\sum t^2 \cos^2 a_o t}$$

$$= \frac{\int_o^T (\sin at - \sin a_o t) \, t \cos a_o t \; dt}{\int_o^T t^2 \cos^2 a_o t \; dt}$$

$$= \frac{\left[\frac{1}{(a-a_o)^2} \sin (a-a_o) T - \frac{T}{a-a_o} \cos (a-a_o) T + \frac{1}{(a+a_o)^2} \sin (a+a_o) T \right.}{\left. - \frac{T}{a+a_o} \cos (a+a_o) T - \frac{1}{(2a_o)^2} \sin 2 a_o T + \frac{T}{2a_o} \cos 2 a_o T \right]}$$

$$2 \left[\frac{T^3}{6} + \left(\frac{T^2}{4a_o} - \frac{1}{8a_o^3} \right) \sin 2 a_o T + \frac{T \cos 2 a_o T}{4 a_o^2} \right]$$

which for T very large becomes

$$\Delta a = \frac{3}{T^2} \left[- \frac{\cos (a-a_o) T}{a-a_o} - \frac{\cos (a+a_o) T}{a + a_o} + \frac{\cos 2 a_o T}{2a_o} \right]$$

and <u>this is not right</u>. The correct value of Δa is $a-a_o$. The difference occurs because the actual and reference "trajectories" diverge as time increases and the linear approximation is no longer valid.

Let us now consider a slightly different situation. Let us examine the situation for a fixed total time of observation, T, and decrease the interval, ΔT, between observations indefinitely. Then, according to the above equations, σ^{-2} approaches 0 but Δa does <u>not</u> approach $a-a_o$. In fact, for T small, Δa approaches

$$\Delta a = (a - a_o) - (a - a_o)^2 \frac{(a + 2 a_o T^2}{10} + \text{higher order terms.}$$

The usefulness of linear best estimates in a non-linear application such as determination of orbit parameters is limited to those cases in which good a priori knowledge of the orbit parameters (corresponding to $a-a_o$ very small in this example) is available.

The Bissett-Berman Corporation 2941 Nebraska Avenue, Santa Monica, California EXbrook 4-3270

APOLLO NOTE NO. 164

H. Engel
14 January 1964

APPLICATION OF THE MSFN TO LEM ABORTS

Introduction

The MSFN can provide useful navigation and guidance support to the Apollo vehicles. More particularly the MSFN can supply navigation and guidance information in emergencies when the on-board guidance and navigation system is malfunctioning and in abort situations.

Selected results presented here indicate that if the MSFN does not start tracking the LEM until ascent engine burnout, the MSFN can determine if the LEM orbit is safe in less than five minutes. Further, a rough analysis shows that using a combination of telemetered data from a crude on-board backup G & N system together with MSFN radar data, the LEM velocity at burnout can be determined to the order of 1 meter/sec. within seconds.

In another area, it appears that by using MSFN radar data and 1 midcourse correction, the rendezvous miss can be held to the order of 500 meters.

This note summarizes the results to date that lead to those conclusions. The results are shown and interpreted in terms of their implications regarding the Apollo mission, and in particular, regarding LEM aborts with on-board system failures. It also provides a description of the method of analyses used in evaluating the capabilities of the MSFN, and a technical Appendix detailing the analysis.

Results

Many selected problems in the determination of LEM and CSM orbits have been run on a 7090 or a 7094. These are reported in Bissett-Berman Apollo Notes having the following numbers and titles.

99. Preliminary Results of Computer Analysis.

109. Effect of Longitude of the LEM Landing Site on the Errors in Determining Rendezvous Position by the MSFN.

122. Estimate of Earth-Moon Injection Errors Using Two MSFN Stations.

128. Preliminary Results of the Effect of Range Bias Errors.

135. Computer Results for Lunar Ascent Using Range and Range-Rate Data from 1, 2 and 3 Stations.

136. MSFN Radar Angle Data in LEM Ascent.

138. Combination of MSFN and CSM Observations.

139. MSFN Station Locations and Lunar Rendezvous Determination.

142. Further Estimates of Earth-Moon Injection Errors.

144. Earth Orbit Injection and Tracking Errors.

147. MSFN Station Locations and Lunar Rendezvous Determination, II.

148. Range-Rate Prediction of Rendezvous.

151. Prediction of Re-entry Dive Angle and Miss Distance for the Return-to-Earth Phase.

152. Optimum Time for a Single Boost Correction to the Lunar Ascent Trajectory to Minimize the Rendezvous Miss.

153. MSFN Tracking of a Truck Vehicle During Lunar Descent to Perilune.

154. Further Estimates of Earth-Moon Injection Errors, II.

159. Effect of Range Bias Information on Re-entry Prediction in Return-to-Earth Phase.

All of these results, with the exception of Note No. 152 on Optimum Time for a Single Boost Correction to the Lunar Ascent Trajectory to Minimize the Rendezvous Miss, are directed toward finding out how well the actual orbit parameters can be determined, and are not concerned with whether the actual orbit is the desired orbit or not. In other words, these Apollo Notes tell how well the MSFN can determine present position and velocity, or how well it can predict what the position and velocity will be at some future time.

A picture may be of some use in clarifying this point. In Figure 1a, we show a nominal transfer orbit for LEM rendezvous with the CSM at a particular point and a particular time. By using the parameters of this nominal orbit in our computations and using the variance associated with our measurements we can compute the variances of our knowledge of the position and velocity of the nominal orbit at the nominal time of rendezvous, shown schematically as a circle in Figure 1a. This means only that there is an uncertainty associated with our knowledge of the orbit, and has nothing to do with whether the orbit is in error or not.

If the actual orbit should be in error, as shown in Figure 1b, then according to the section of this Note on the Methods of Analyses, the same computed variances calculated on the nominal trajectory still apply on the actual trajectory. For example, assume that our analysis shows that on the nominal trajectory if we observe the LEM for 25 minutes and then predict the position at the time of rendezvous (58 minutes), we have an RMS error in predicted position and velocity of 1 km and 0.1 meters/sec., respectively. Then, on the actual ascent trajectory, if we observe the LEM for 25 minutes and then predict the position and velocity at the nominal time of rendezvous

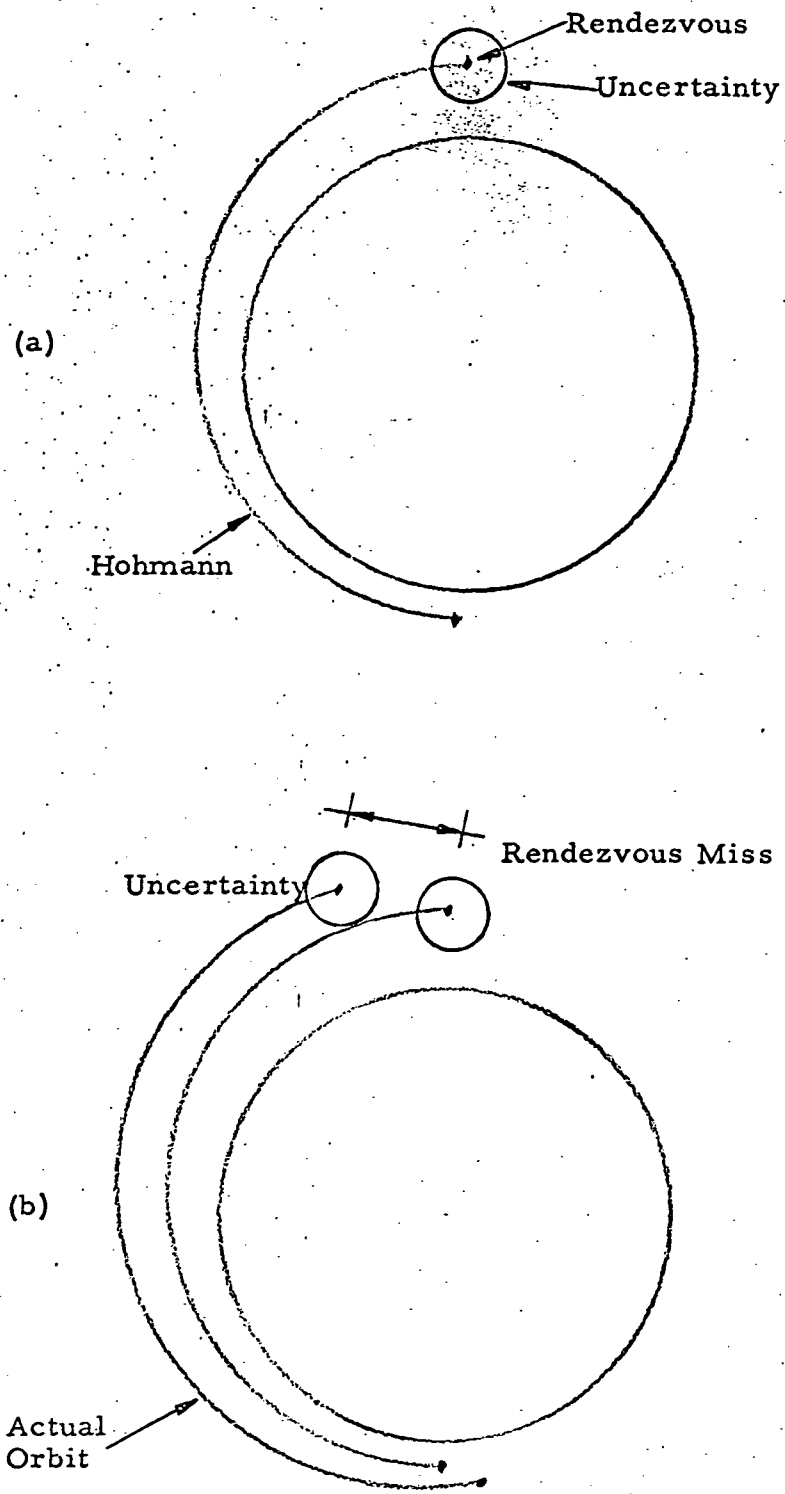
Rendezvous
Uncertainty
(a)
Hohmann
Rendezvous Miss
Uncertainty
(b)
Actual
Orbit

Figure 1.

(58 minutes), we can predict the position and velocity at that time to within 1 km and 0.1 meters/sec. even though this orbit may be such that the miss at rendezvous is 50 km. To reiterate, the analyses presented here tell how well the orbit parameters can be determined, whether or not those orbit parameters are the planned orbit parameters.

It is only a small step from these results as they stand, to results are are operationally useful. Operationally, our concern is not with how well we can predict future errors in position and velocity, but with how small we can make future errors in position and velocity. Bissett-Berman Apollo Note No. 152 on Optimum Time for Single Boost Correction to the Lunar Ascent Trajectory to Minimize the Rendezvous Miss is an illustration of the operational usefulness of the MSFN observations based on the results of these analyses. We reproduce here an outline of that note to indicate the way in which the results were determined.

After ascent engine cut-off at an altitude of 8 nautical miles, another 58 minutes is required to rendezvous back of the Moon at an altitude of 80 nautical miles using a Hohmann transfer. In this particular example the position and velocity of the LEM at cut-off are first obtained from the on-board navigation system which has an uncertainty of the order of 10 km in LEM position at the time of LEM rendezvous. The LEM is then tracked in the Doppler range change mode by two ground stations, Madrid and Johannesburg in this case, each with the ability to determine the change in range in one minute to 0.6 meters, and with measurements from each station at one minute intervals. The LEM disappears from sight behind the Moon after about 32 minutes and cannot be tracked between that time and the nominal time of rendezvous. It is necessary to predict rendezvous miss and to make course corrections on the basis of the measured data.

An error in position at ascent engine cut-off results in an error of like magnitude in position at the time of rendezvous, and this error can be eliminated by a small corrective boost at almost any time in the transfer orbit. The more important error is an error in velocity.

The longer we wait to correct this error, the larger the rendezvous position error to be eliminated and the shorter the time available to cancel it out. Hence, the longer the time after ascent engine cut-off that the corrective boost is made, the larger this boost must be. This is illustrated graphically in Figure 2, taken from Note 152. If the error in velocity at ascent engine cut-off has magnitude V_o and is equally likely to be in any direction in the plane of the orbit, then the RMS ratio of the velocity change required to correct for this error as a function of the time after cut-off at which the corrective boost is performed is shown in Figure 2. (Velocity errors out of the plane can be ignored in this example since the orbit is a Hohmann transfer and these errors result in no rendezvous miss).

Even after a corrective boost there will still be a miss at rendezvous because the orbit before boost is not perfectly known and because the boost is not executed perfectly. The RMS miss at the nominal time of rendezvous is shown in Figure 3 as a function of the velocity error at ascent engine cut-off, the accuracy with which a commanded corrective boost can be executed, and the time at which this boost is performed. Minima occur in the given curves because two conflicting factors are at work; the longer the LEM is observed the better its actual orbit and the necessary correction are known, but on the other hand, the later the correction is made the greater the correction must be and hence, the absolute error in making the correction will also be greater.

In order to see how this data may be used, let us consider a particular case. Let us assume that the magnitude of the LEM velocity error at ascent engine cut-off is 5 meters/sec., and that this error is equally likely to be in any direction in the plane of the orbit. (We have already indicated that out-of-plane errors can be neglected). If we observe the LEM for 21 minutes after ascent engine cut-off and then perform a corrective boost, the errors in this corrective boost assumed to be spherically distributed and to be equal in magnitude to 1 percent of the commanded boost, we find that the magnitude of the initial velocity error times the fractional

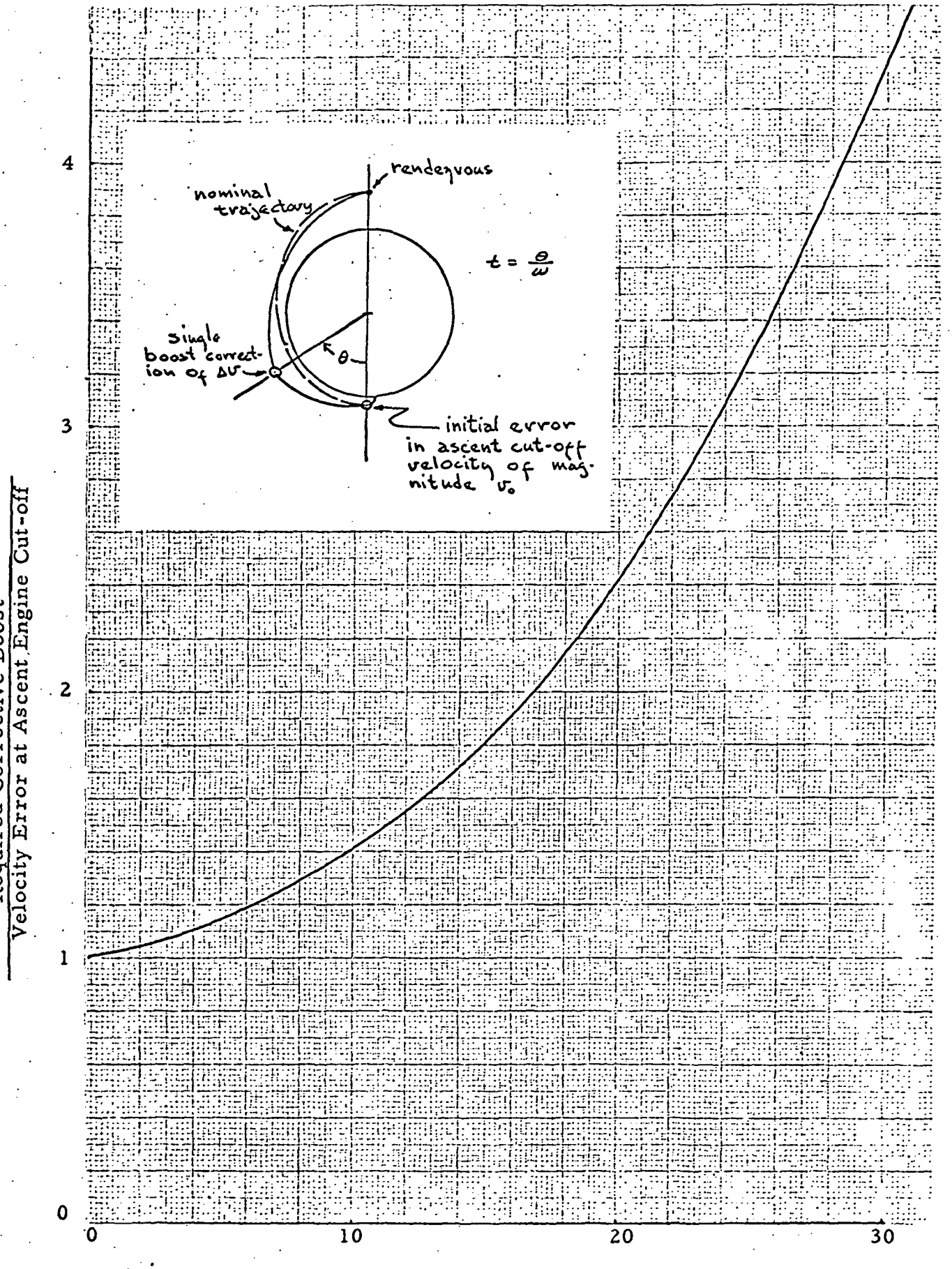
rendezvous
nominal trajectory
$t = \frac{\theta}{\omega}$
single boost correction of Δv
θ
initial error in ascent cut-off velocity of magnitude v_0
Required Corrective Boost / Velocity Error at Ascent Engine Cut-off
0
1
2
3
4
0
10
20
30
Time of Corrective Boost (Minutes) After Cut-off

error in the execution of the commanded corrective boost is 0.05 meters/sec. (= 5 meters/sec. x 0.01). Then using the curve labeled 0.05 meters/sec. in Figure 3, we read off for 21 minutes of observation that the RMS miss at the nominal time of rendezvous is just 500 meters in spite of the fact that this determination is made more than a half hour before rendezvous. This compares with the miss of about 40,000 meters that would result from the original error of 5 meters/sec. in velocity.

If the commanded boost could be performed perfectly (Velocity Error at Ascent Engine Cut-Off x Fractional Error in Commanded Boost = 0), and if this corrective boost were performed 25 minutes after cut-off, the RMS miss at the time of rendezvous would be about 230 meters, no matter what the boost error at ascent engine cut-off (within a few tens of meters per second, of course).

The results presented in other Bissett-Berman Apollo Notes listed at the beginning of this section may be applied in a similar fashion if commanded corrective boosts are performed without error. Bissett-Berman Apollo Note No. 148 and Figure 4 of the current note, for example, shows the RMS value of the uncertainty in the minimum miss near rendezvous as a function of the number of observing stations, the kinds of observations, and the duration of observations from ascent engine cut-off. The minimum miss near rendezvous is generally less than the miss at the nominal time of rendezvous when a Hohmann transfer orbit is used, as in this case. This is so since the CSM and LEM are traveling approximately horizontally and parallel at times in the vicinity of the nominal rendezvous time, and so the along-path miss goes to zero at some time near the nominal time of rendezvous. In like fashion the uncertainty in the along-path component of uncertainty in position is zero for some (unknown) time near the nominal time of rendezvous. The remaining orthogonal components of the uncertainty in position at rendezvous are called the uncertainty in the minimum miss near rendezvous. In Figure 4 this quantity is shown for range measurements and change in range measurements

A Priori Data and Range Change
From Two Stations at 1 Minute Intervals $\sigma_{\Delta R}$ 0.6 m

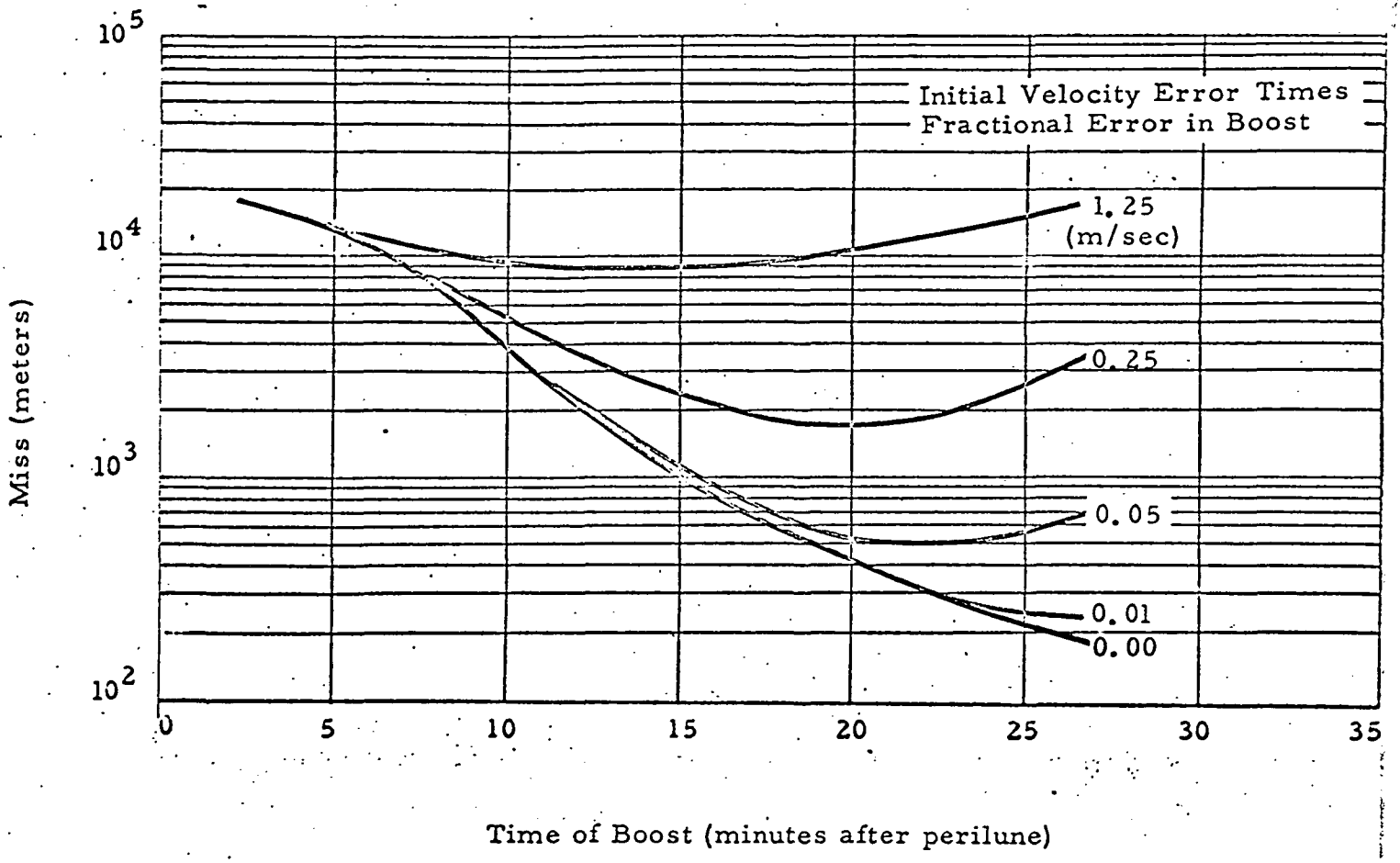

RMS Miss at Rendezvous for a
Single Corrective Boost

Figure 3.

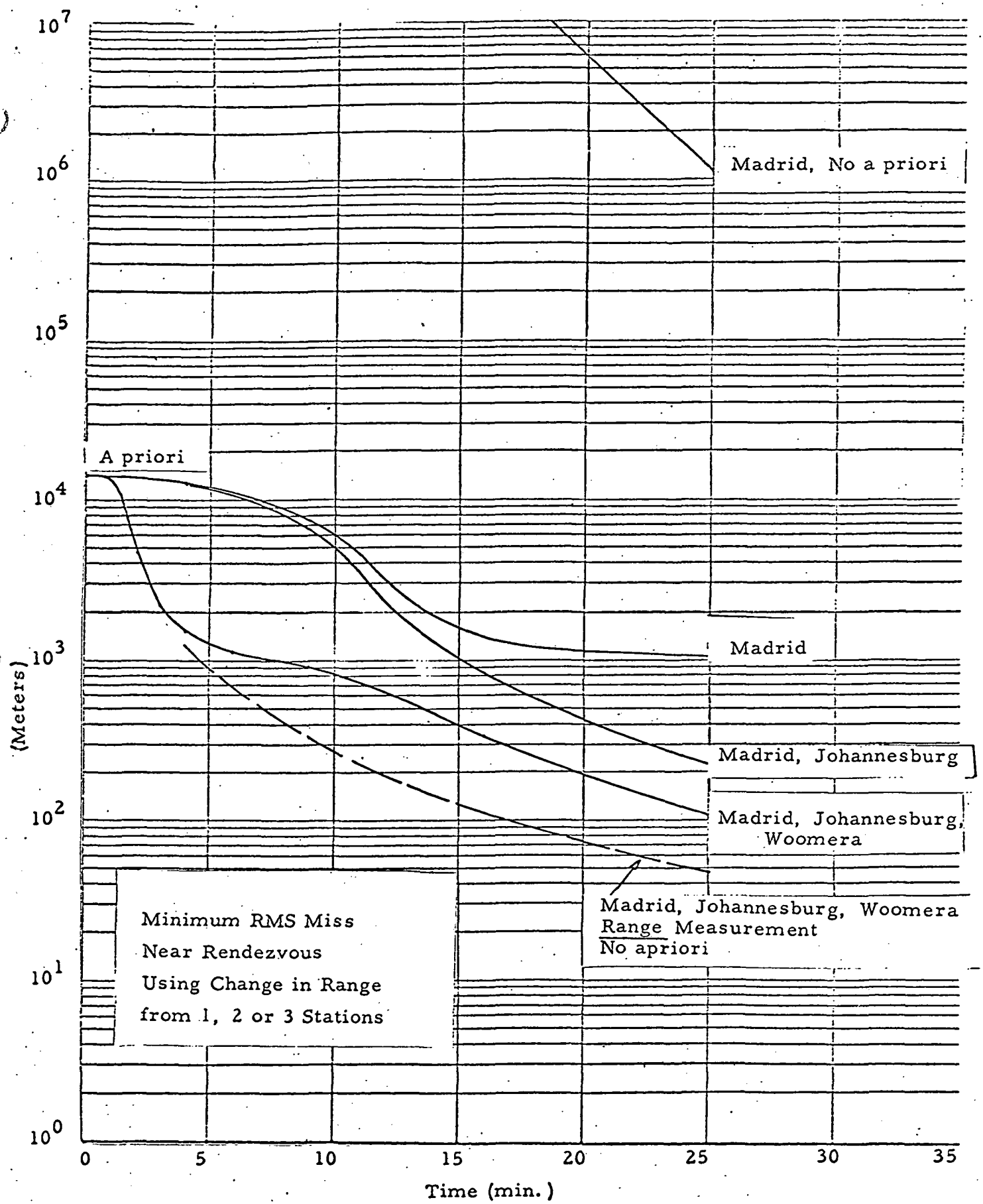
10^7
10^6
10^5
10^4
10^3
10^2
10^1
10^0
(Meters)
A priori
Madrid, No a priori
Madrid
Madrid, Johannesburg
Madrid, Johannesburg, Woomera
Madrid, Johannesburg, Woomera
Range Measurement
No apriori
Minimum RMS Miss
Near Rendezvous
Using Change in Range
from 1, 2 or 3 Stations
0
5
10
15
20
25
30
35
Time (min.)

Figure 4.

accurate to 0.6 meters with observations at one minute intervals. The separate cases shown are:

1. Range change measurements from Madrid only, with no a priori data. The uncertainties in this case are so large that it may be dismissed from further consideration.

2. Range change measurements from Madrid only, with a priori data of the accuracy obtainable from the on-board navigation system.

3. Range change measurements from Madrid and Johannesburg, with a priori data of the accuracy obtainable from the on-board navigation system.

4. Range change measurements from Madrid, Johannesburg and Woomera, with a priori data of the accuracy obtainable from the on-board navigation system.

5. Range measurements from Madrid, Johannesburg and Woomera with no a priori data, or equivalently, range change measurements from these three stations with perfect a priori data. Near perfect a priori data can be obtained by tracking the LEM from lift-off, having observed it on the Moon for a long time.

It is of interest to note in this last case that if the LEM is observed for 25 minutes after ascent engine burnout the uncertainty associated with the minimum miss distance near rendezvous is of the order of 50 meters.

Still more important operationally, the results in the last case indicate that five minutes after ascent engine burnout the uncertainty in the minimum miss distance near rendezvous is only 900 meters. This means that based on MSFN measurements only, the apolune altitude can be determined to better than 900 meters within 5 minutes of ascent engine burnout. Thus, the ground operational support

system can certainly determine if the LEM is in a safe orbit less than 5 minutes after injection in the case that a crude backup navigation and guidance system is employed!

Further data derived from Bissett-Berman Apollo Note No. 128, and adjusted for a measurement error of 0.6 meters rather than the value used in that note is shown in Figure 5. These correspond to the cases of range change measurements from Madrid and Johannesburg, and range change measurements from Madrid, Johannesburg and Woomera, with no a priori data. Even in the case of measurements from just two stations the apolune altitude is known to better than 10 km after 10 minutes, and is known to better than 10 km after 5 minutes if three stations are used. Hence, even in these cases the MSFN can determine in a very short time if the transfer orbit is safe.

Actually, as indicated in Bissett-Berman Apollo Note No. 160, entitled Introduction to LEM Truck G & N, a rough analysis shows that ground observations of the LEM during ascent boost coupled with a crude on-board backup system can determine the LEM velocity at burnout to the order of 1 meter/sec.

Methods of Analysis

There is one essential point that must be made regarding the majority of this error analysis. The point is that this error analysis finds how well the MSFN can determine the orbit of a vehicle no matter what the orbit of the vehicle, but these calculations are not performed in the manner in which the orbital data reduction would be performed in actual operations. The accuracy of orbit determination is the same in both cases, however. The analysis method used here has been selected only for ease of computation.

The method used is that of determining the error covariance matrix of the orbit parameters based on maximum likelihood. This method is presented in detail in the Appendix. It is illustrated here by means of simple examples.

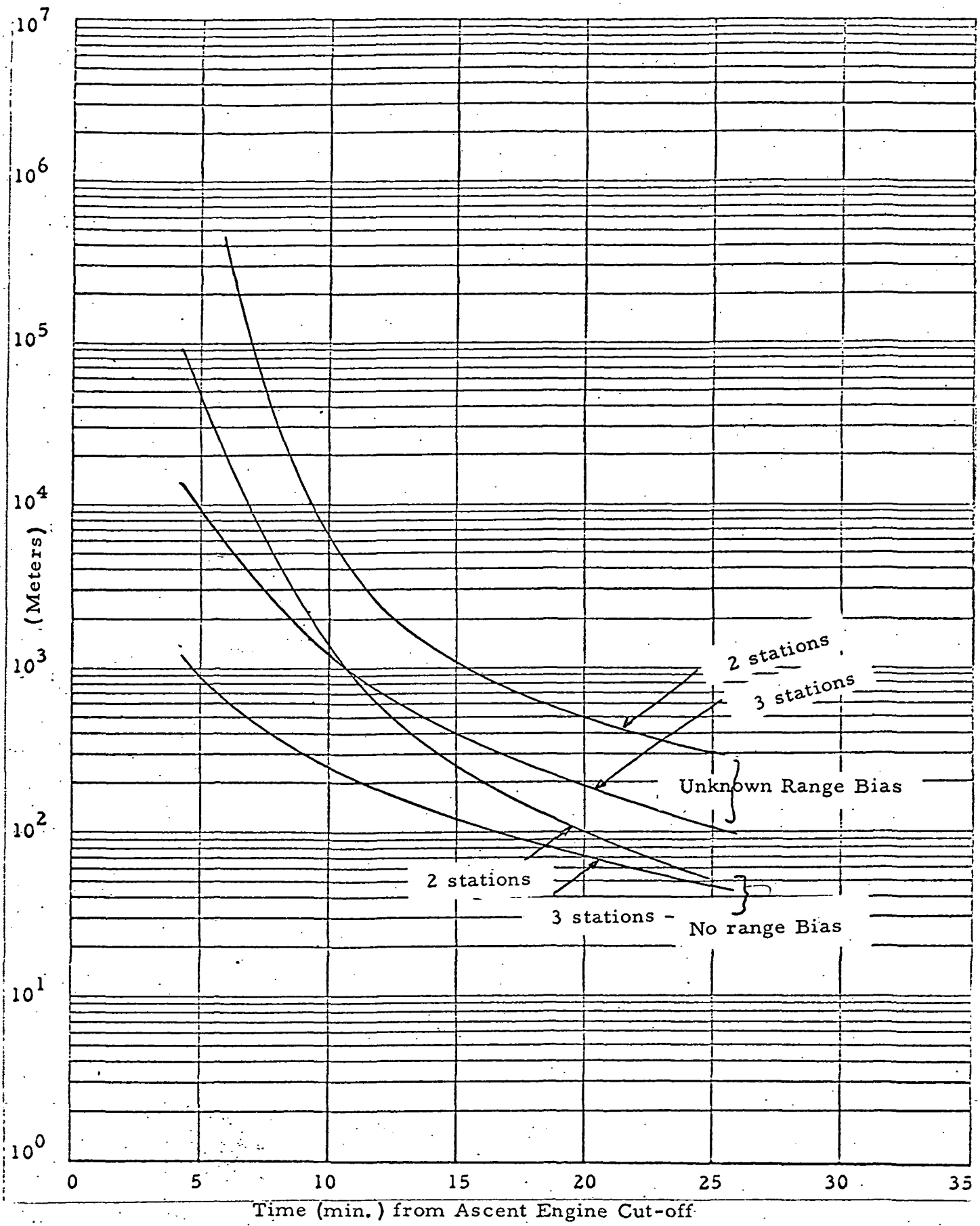

Uncertainty in Minimum RMS Miss Near Rendezvous Using Change in Range from 2 or 3 Stations. $\sigma_{\Delta R} = 0.6$ m for Measurements at 1 min. Intervals. No a priori data.

Figure 5.

As our first example, let us consider the problem of determining the equation of a straight line on the basis of a number of measurements of the ordinate y at t equal to $0, 1, 2, \ldots, n$. Let us assume that each measurement of $y(t)$ is in error by an amount $e(t)$ and that these errors are uncorrelated, have a zero mean and a Gaussian distribution with standard deviation σ. Our problem, then, is to evaluate the constants ("orbit parameters") $\underline{a}$ and $\underline{b}$ in the expression

$$y = a + bt$$

The most likely values of $\underline{a}$ and $\underline{b}$ are those which maximize the likelihood of $\underline{a}$ and $\underline{b}$, $p(a, b)$. We have

$$p(a, b) = \frac{1}{(2\pi)^{n/2}\sigma^{n}} \exp \sum_{t=0}^{n} \frac{-\left[y_m(t) - (a+bt) \right]^2}{2\sigma^2}$$

in which $y_m(t)$ is the measured value of $y(t)$ and is

$$y_m(t) = y(t) + e(t).$$

This is equivalent to minimizing the quantity $\mathcal{K}$,

$$\mathcal{K} = \sum_{t=0}^{n} \left[y_m(t) - (a + bt) \right]^2$$

and thus is equivalent to the ordinary least squares fitting of a straight line to the data. We can set the first partial derivatives of $\mathcal{K}$ with respect to $\underline{a}$ and $\underline{b}$ equal to zero and solve the resultant

pair of simultaneous linear equations for $\underline{a}$ and $\underline{b}$. We find the most likely values are

$$a = \frac{(4n+2)\sum_{t=0}^{n} y_m - 6\sum_{t=0}^{n} y_m t}{n+1}$$

$$b = 12\,\frac{\sum_{t=0}^{n} y_m t - \frac{n}{2}\sum_{t=0}^{n} y_m}{n\,(n+1)\,(n+2)}$$

and the variances of the estimates of $\underline{a}$ and $\underline{b}$ are

$$\sigma_a^2 = \frac{\sigma^2}{n}$$

$$\sigma_b^2 = \frac{6\,\sigma^2}{n(n+1)\,(2n+1)}$$

and

$$\sigma_{ab} = \frac{2\,\sigma^2}{n(n+1)}\ .$$

Let us next consider a non-linear case in which the quantity $y(t)$ is of the form

$$y(t) = \sin at$$

and in which we wish to estimate the parameter $\underline{a}$ on the basis of measurements of $y(t)$ at times t equal to $0, 1, 2, \ldots, n$. Again, it is assumed that each measurement of $y(t)$ is in error by an amount $e(t)$, and that these errors are uncorrelated, have a zero mean and a Gaussian distribution with a standard deviation σ.

The maximum likelihood value of $\underline{a}$ is that which maximizes

$$p(a) = \frac{1}{\sqrt{2\pi}\ \sigma} \exp \sum_{t=0}^{n} \frac{-\left[\ y_m(t) - \sin a\, t\ \right]^2}{2\,\sigma^2}$$

in which $y_m(t)$ is the measured value of $y(t)$ and is

$$y_m(t) = y(t) + e.(t).$$

This is equivalent to minimizing the quantity K,

$$K = \sum_{t=0}^{n} \left[\ y_m(t) - \sin a\, t\ \right]^2$$

In order to find the value of a that minimizes K we must set the first partial derivative of K with respect to a equal to zero.

$$0 = \frac{\partial K}{\partial a} = -2 \sum_{t=0}^{n} \left[\ y_m(t) - \sin a\, t\ \right] t \cos a\, t$$

Here there is an essential difference between this example and the first example: The equations for the parameters in the first example were linear, but the equation for the parameter a in this equation is non-linear.

This second example is much closer to the problem of orbit parameter determination, for in orbit parameter determination it is also necessary to solve non-linear equations. Since it is impossible to solve these non-linear equations explicitly for the orbit parameters, we use an iterative method of solution that requires only the solutions of linear equations. We can illustrate this by continuing our second example.

We start by assuming that we have an approximate value of a that we shall call a_o and we wish to obtain an improved value a_1. We let,

$$\Delta a \triangleq a - a_o$$

and then we can write both sin at and cos at in terms of a_o and Δa by expanding in a Taylor series about a_o, giving

$$\sin a\,t = \sin a_o t + t\,\Delta a \cos a_o t - \frac{t^2}{2!}(\Delta a)^2 \sin a_o t - \ldots.$$

$$\cos a\,t = \cos a_o t - t\,\Delta a \sin a_o t - \frac{t^2}{2!}(\Delta a)^2 \cos a_o t + \ldots.$$

Next we can substitute these quantities in the equation for the partial of K with respect to a and obtain after dropping higher order terms,

$$0 = \frac{\partial K}{\partial a} \doteq -2 \sum_{t=0}^{n} \left[y_m(t) - \sin a_o t - t\,\Delta a \cos a_o t \right] t \cos a_o t$$

This linearized equation can be solved for an approximate value Δa_1 of Δa,

$$\Delta a \doteq \Delta a_1 = \frac{\sum_{t=0}^{n} \left[y_m(t) - \sin a_o t \right]^2}{\sum_{t=0}^{n} t^2 \cos^2 a_o t}$$

and then a_1 is equal to a_o plus this approximate value of Δa.

This is as far as any linear best estimate kind of solution goes. The result obtained from this kind of solution is the same as that obtained through the application of the Kalman-Schmidt method, as has been demonstrated in full detail in Bissett-Berman Apollo Note No. 150.

This is not a maximum likelihood solution, and will not approach the maximum likelihood solution even with an infinite amount of data. This has been demonstrated in Bissett-Berman Apollo Note No. 163.

There it is shown that the value of Δa obtained in the linear fashion is oscillatory for large total times of observation and is

$$\Delta a_1 \cong \frac{3}{T^2}\left[- \frac{\cos (a-a_o)T}{a - a_o} - \frac{\cos (a+a_o)T}{a+a_o} + \frac{\cos 2 a_o T}{2 a_o} \right]$$

for time large. Even if the total time of observation is kept small but the number of observations is increased indefinitely the value of Δa obtained in a linearized method does not approach the correct value; in this case, as shown in Note 163, the limiting value is

$$\Delta a_1 = (a-a_o) - (a-a_o)^2 \frac{(a+2 a_o) T^2}{10} + \text{higher order terms}$$

instead of the correct value $a - a_o$.

It can be seen that the worse the initial value a_o the worse the Kalman-Schmidt or any other linear best estimate. For this reason these linear methods are applicable only when good initial values for the parameters are available.

Let us now continue with the problem of obtaining a maximum likelihood estimate for the parameter a. We have found a new estimate a_1 from the equations

$$\Delta a_1 = \frac{\sum_{t=0}^{n} \left[y_m(t) - \sin a_o t \right]^2}{\sum_{t=0}^{n} t^2 \cos^2 a_o t}$$

and

$$a_1 = a_o + \Delta a_1$$

This new value of a_1 may now be substituted for a_o and the computations repeated to obtain a better approximation a_2 to a:

$$\Delta a_2 = \frac{\sum_{t=0}^{n} \left[y_m(t) - \sin a_1 t \right]^2}{\sum_{t=0}^{n} t^2 \cos^2 a_1 t}$$

and

$$a_2 = a_1 + \Delta a_2$$

In like fashion, this may in turn be used to obtain closer and closer approximations a_3, a_4, a_5, ... to $\underline{a}$, and indeed this sequence approaches $\underline{a}$ in the limit. In actual orbit calculations it has been found by both JPL and Goddard that three iterations have been sufficient to bring the calculated values of the orbit parameters close enough to the maximum likelihood values.

We now wish to point out that very good values for the statistical uncertainties in the maximum likelihood estimates of the orbit parameters can be obtained without computing the maximum likelihood estimates of the orbit parameters. We shall demonstrate this by continuing with the second example.

Let us assume that we have obtained the maximum likelihood value of $\underline{a}$ by successive iterations and that it differs from the true value $\underline{a}$ by a small amount $\underline{\delta a}$ due to noise in the measurements. Calling this calculated value $\underline{a_M}$, we have

$$a_M = a + \delta a$$

and since this value maximizes the likelihood, we also have

$$0 = -2 \sum_{t=0}^{n} \left[y_m(t) - \sin a_M t \right] t \cos a_M t$$

Now, substituting $\underline{a + \delta a}$ for $\underline{a_M}$ and discarding higher order terms in δa, we find

$$0 = -2 \sum_{t=0}^{n} \left[y_m(t) - \sin at - \delta a t \cos at \right] t \cos at$$

or

$$\delta a = \frac{\sum_{t=0}^{n} \left[y_m(t) - \sin at \right] t \cos at}{\sum_{t=0}^{n} t^2 \cos^2 at}$$

The difference $y_m(t) - \sin at$, however, is merely the noise $e(t)$, so we may write

$$\delta a = \frac{\sum_{t=0}^{n} e(t)\, t \cos at}{\sum_{t=0}^{n} t^2 \cos^2 at}$$

The mean value of $\underline{\delta a}$ is zero. The variance is therefore,

$$\sigma_a^2 = \overline{(\delta a)^2} = \frac{\sum_{t=0}^{n} \sum_{\tau=0}^{n} \left[e(t)\, t \cos a t \right] \left[e(\tau)\, \tau \cos a\tau \right]}{\sum_{t=0}^{n} t^2 \cos^2 at \sum_{\tau=0}^{n} \tau^2 \cos a\tau}$$

Now since we have taken uncorrelated noise, we have that the expected value of $e(t)\ e(\tau)$ is σ^2 if t is equal to τ, and, is zero otherwise. Thus,

$$\sigma_a^2 = \frac{\sigma^2 \sum_{t=0}^{n} \tau^2 \cos^2 a\tau}{\sum_{t=0}^{n} t^2 \cos^2 at \sum_{\tau=0}^{n} \tau^2 \cos^2 a\tau}$$

$$= \frac{\sigma^2}{\sum_{t=0}^{n} t^2 \cos^2 at}$$

In other words, we can find the variance in the estimate of $\underline{a}$ that will result from a number of measurements $y_m(t)$, without having to calculate the estimate of $\underline{a}$ based on $y_m(t)$, if we know $\underline{a}$. In itself, this seems like a useless result, for if we knew $\underline{a}$ we would not have to calculate a value for it. The important point to be made, however, is that we can get a good value for the variance of $\underline{a}$ from an approximate value a_o. The following exercise will demonstrate this point. We have that,

$$a - a_o = \Delta a$$

and so

$$\sigma_a^2 = \frac{\sigma^2}{\sum_{t=0}^{n} t^2 \cos^2 (a_o + \Delta a)\, t}.$$

Now expanding $\cos^2 (a_o + \Delta a)\, t$ in a Taylor series about $a_o t$, we have,

$$\doteq \frac{\sigma^2}{\sum_{t=0}^{n} t^2 \cos^2 a_o t - 2\sum_{t=0}^{n} (\Delta a t)\, t^2 \sin a_o t \cos a_o t + \sum_{t=0}^{n} (\Delta a t)^2\, t^2 \sin^2 a_o t + \ldots}$$

$$\doteq \frac{\sigma^2}{\sum_{t=0}^{n} t^2 \cos^2 a_o t - \Delta a \sum_{t=0}^{n} t^3 \sin 2 a_o t + \Delta a^2 \sum_{t=0}^{n} t^4 \sin^2 a_o t + \ldots}$$

or, dividing numerator and denominator by $\sum_{t=0}^{n} t^2 \cos^2 a_o t$

and expanding in a geometric series we find

$$\sigma_a^2 = \frac{\sigma^2}{\sum_{t=0}^{n} t^2 \cos^2 a_o t} + \Delta a \frac{\sigma^2 \sum_{t=0}^{n} t^3 \sin 2 a_o t}{\left[\sum_{t=0}^{n} t^2 \cos^2 a_o t\right]^2}$$

+ higher order terms in Δa.

That is, for a_o not very different from a we can determine the variance in the estimate of a on the basis of a_o. For example, we have computed σ_a^2/σ^2 for n = 30, for a equal to 0.01 and for various values of a_o:

a_o	σ_a^2/σ^2
0.007	0.411×10^{-5}
0.008	0.384×10^{-5}
0.009	0.387×10^{-5}
0.010 (=a)	0.391×10^{-5}
0.011	0.396×10^{-5}
0.012	0.400×10^{-5}
0.013	0.406×10^{-5}

It can be seen that a thirty percent error in $\underline{a}$ results only in a 5 percent error in σ_a^2, or a $\underline{2.5}$ percent error in σ_a in this example.

This result is very important. In its more general form it provides the justification for our method of orbit determination error analysis. It implies that we do not have to know the exact orbit in order to find out how well the orbit parameters can be determined from a given set of measurements. To state this differently, we can compute a good estimate of the variance in the estimate of the orbit parameters on the actual orbit by computing the variance in the estimate of the orbit parameters on some neighboring orbit.

In our error analysis we compute the variance of the orbit parameters that would be obtained on some neighboring reference orbit and use this variance for the actual orbit. This procedure is justified more generally in the Appendix.

The method of analysis employed has some other advantages. It provides simple means for determining the effects of combining several kinds of measurements from a single location or of combining measurements from different locations. Furthermore, it allows combination of a priori data with measurements, and allows the introduction of additional errors due to faulty execution of commanded boosts or other sources. The techniques used are described in the Appendix.

APPENDIX

This Appendix is a concise summary of the mathematics involved in finding out how well the MSFN can determine the orbit of an Apollo vehicle.

If a sequence of measurements $y_m(t_i)$ are made of some quantity $y(t_i)$, and these measurements are corrupted by an additive, zero mean, random, Gaussian noise $n(t_i)$, and if $y(t_i)$ is a function of a number of fixed parameters $a_1, \ldots, a_m$ and time,

$$y(t_i) = y(a_1, a_2, \ldots, a_K, t_i)$$

then the maximum likelihood estimate of the parameters $a_1, \ldots, a_m$ is that which maximizes the probability density function.

$$p(a_1, \ldots, a_K) = \frac{1}{(2\pi)^{N/2} \sigma^N} \exp\left[-\frac{1}{2\sigma^2} \sum_{i=1}^{N} \left\{ y_m(t_i) - y(t_i) \right\}^2 \right]$$

When there is more than one kind of measurable, or when the measurement errors are correlated it is convenient to introduce matrix notation to describe the problem of determining the orbit parameters. We define

x a column vector of dimension K, the elements of which are the parameters $a_1, \ldots, a_K$

y a column vector of dimension r, the elements of which comprise <u>all</u> measurements made, whether these be at different times or of different character, or not.

n a column vector of the same dimension as y, the elements of which represent zero mean Gaussian noise. These elements may be correlated.

y_m a column vector of the measured values of y

$$y_m = y + n$$

Q the covariance matrix of the noise

$$Q = E(n\, n^T)$$

The maximum likelihood estimate of the orbit parameters is that which maximizes the probability density function.

$$p(x) = \frac{1}{(2\pi)^{r/2}\sqrt{|Q|}} \exp\left[-\frac{1}{2}(y_m - y)^T Q^{-1} (y_m - y)\right]$$

In the error analyses performed thus far the elements of the noise vector have been assumed uncorrelated, and independent of time and distance. This implies that errors in measuring range are uncorrelated with errors in measuring angle, that errors in measuring range from one station are uncorrelated with errors in measuring range from another station, and so on. Further, it implies that any two successive measurements of some quantity such as range from one station are measured at times sufficiently far apart that the measurement errors are uncorrelated (this time appears to be of the order of a second). With this assumption p(x) may be written as

$$p(x) = \frac{1}{\prod_{i=1}^{L} (2\pi)^{N_i/2} \sigma_i^{N_i}} \exp\left(-\frac{1}{2}\mathcal{L}\right)$$

in which

$$\mathcal{L} = \sum_{j=1}^{N_1} \frac{(y_{1_{j,m}} - y_{1_j})^2}{\sigma_1^2} + \ldots + \sum_{j=1}^{N_K} \frac{(y_{K_{j,m}} - y_{K_j})^2}{\sigma_L^2}$$

where

$y_{\ell j}$ is the j-th value of the measurable y_ℓ

and

$y_{\ell jm}$ is the j-th measurement of the measurable y_ℓ. It may be well to mention that in addition to assuming that the noise added to the measurements was not auto-correlated, we have also assumed that the noise processes are stationary and not cross-correlated. These assumptions are most concisely expressed by the following equation:

$$E\left[n_{\ell_1} \, n_{\ell_2 j}\right] = \delta_{ij} \, \delta_{\ell_1 \ell_2} \, \sigma_{\ell_1}^2$$

where δ_{ij} is the familiar kronecker delta function.

In order to maximize p(x) we must minimize $\mathcal{L}$. To find the parameters that minimize $\mathcal{L}$, we would set the first partial derivatives of $\mathcal{L}$ with respect to each of the parameters equal to zero and solve the resulting set of simultaneous equations. In this error analysis we are interested in obtaining the covariance matrix of the errors in the estimated orbit parameters rather than the orbit parameters themselves, but we proceed as though obtaining the orbit parameters.

We may write

$$\min \mathcal{L} = \sum_{i=1}^{K} \frac{1}{\sigma_i^2} \sum_{j=1}^{N_i} (y_{ij,m} - \hat{y}_{ij})^2$$

in which $\hat{y}_{ij}$ is the value of y_{ij} computed from the estimated orbit parameters. We may then write

$$\frac{\partial \mathcal{L}}{\partial a_p} = 0 = \sum_{i=1}^{L} \frac{1}{\sigma_i^2} \sum_{j=1}^{N_i} (y_{ij,m} - \hat{y}_{ij}) \frac{\partial \hat{y}_{ij}}{\partial a_p}$$

Now we can write the estimated value of the orbit parameter a_p as $\hat{a}_p$, and can write

$$\hat{a}_p = a_p + \delta a_p$$

in which a_p is the error in $\hat{a}_p$. Then, approximately

$$\hat{y}_{ij} = y_{ij} + \sum_{q=1}^{K} \frac{\partial y_{ij}}{\partial a_q} \delta a_q$$

and by substitution,

$$\frac{\partial \mathcal{L}}{\partial a_p} = 0 = \sum_{i=1}^{L} \frac{1}{\sigma_i^2} \sum_{j=1}^{N_i} \left(y_{ij,m} - y_{ij} - \sum_{p=1}^{m} \frac{\partial y_{ij}}{\partial a_q} \delta a_q \right) \frac{\partial y_{ij}}{\partial a_p}$$

But $y_{ij,m} - y_{ij}$ is the noise n_{ij}, so

$$0 = \sum_{i=1}^{L} \frac{1}{\sigma_i^2} \sum_{j=1}^{N_i} \left(n_{ij} - \sum_{p=1}^{m} \frac{\partial y_{ij}}{\partial a_q} \delta a_q \right) \frac{\partial y_{ij}}{\partial a_p}$$

Now let us introduce the column vectors e and δa and the square matrix C, in which the elements of these matrices are:

$$e_p = \sum_{i=1}^{L} \frac{1}{\sigma_i^2} \sum_{j=1}^{N_i} n_{ij} \frac{\partial y_{ij}}{\partial a_p}$$

$$\delta a_p = \delta a_p$$

and

$$C_{pq} = \sum_{i=1}^{L} \frac{1}{\sigma_i^2} \sum_{j=1}^{N_i} \frac{\partial y_{ij}}{\partial a_p} \frac{\partial y_{ij}}{\partial a_q}$$

Then the simultaneous equations to be solved can be written in matrix form as

$$0 = e - C\ \delta a$$

or

$$\delta a = C^{-1} e$$

The transpose of δa is

$$\delta a^T = (C^{-1} e)^T$$

$$= e^T (C^{-1})^T$$

$$= e^T C^{-1}$$

since C is a symmetric matrix.

Since the $\hat{a}_p$ are asymptotically unbiased, we may assume that the expected value of δa is 0, so the covariance matrix of δa is V,

$$V = \text{cov}(\delta a_p, \delta a_q)$$

$$= E(\delta a \, \delta a^T)$$

$$= E(C^{-1} e \, e^T C^{-1})$$

$$= C^{-1} E(e \, e^T) C^{-1}$$

Since the noise is additive, Gaussian, and uncorrelated, and has zero mean,

$$E(n_{ij} n_{k\ell}) = \delta_{ik} \delta_{j\ell} \sigma_i^2$$

where we do not intend the Einstein summation convention to hold for the repeated subscript in the above equation.

Then,

$$E(e \, e^T) = C$$

and

$$V = C^{-1} C C^{-1}$$

$$= C^{-1}$$

Thus, the covariance matrix of the errors in the estimated orbit parameters can be determined as the inverse of the matrix with the elements

$$C_{pq} = \sum_{i=1}^{L} \frac{1}{\sigma_i^2} \sum_{j=1}^{N_i} \frac{\partial y_{ij}}{\partial a_p} \frac{\partial y_{ij}}{\partial a_q}$$

We call this matrix C the total information matrix. It can be considered to be made up of a number of elementary information matrices derived from different data sources:

$$C = \sum_{i=1}^{K} C^{(i)}$$

where $C^{(i)}$ is the matrix with the elements

$$C_{pq}^{(i)} = \frac{1}{\sigma_i^2} \sum_{j=1}^{N_i} \frac{\partial y_{ij}}{\partial a_p} \frac{\partial y_{ij}}{\partial a_q}$$

This immediately indicates how covariance matrices obtained from different measurements may be combined. For example, let us say that we have a covariance matrix V_a of the orbit parameters resulting from a priori knowledge. Let us say that we also have a covariance matrix V_b associated with subsequent measurements. The inverses of V_a and V_b are information matrices C_a and C_b. These two information matrices may be added and the inverse of the sum found. This inverse is the covariance matrix V corresponding to all of the data.

$$V = (V_a^{-1} + V_b^{-1})^{-1}$$

In like manner information matrices obtained from various sources and at various times can be added, and the inverse of the sum is the covariance matrix resulting from the combination of all the data.

In all of the preceding analysis the noise has been assumed to have a zero mean. Some kinds of measurement errors do not have zero means--range bias is a good example. In order that the measurement errors may be treated as having zero means, we treat the biases as additional orbit parameters to be determined instead of as measurement errors. Thus, if we are attempting to determine the orbit of a vehicle on the basis of range measurements from three stations we have 9 parameters--6 kinematic parameters and 3 range biases--to determine. Similarly, we have a 9 x 9 covariance matrix of orbit parameter errors rather than a 6 x 6 matrix. Station location errors, errors in the speed of light, and errors in gravitational

constants are treated in the same manner.

Although all computations thus far have been performed with constant variances in the measurements it is a simple matter to alter the program to take into account variations with time or distance.

Very many of the Bissett-Berman Apollo Notes are devoted to various portions of the analysis relating to the error analysis program. Among these are

43. The Calculation of the Covariance Matrix of the Maximum Likelihood Estimators of Orbit Parameters Obtained from Range-Rate Data.

77. Calculation of Covariance Matrices for Multiple Uncorrelated Data Sources.

82. Calculation of Covariance Matrices, III.

83. Use of Range and Range-Rate Data.

85. The Equivalence of Data Processing Schemes in Linearized Error Analysis.

94. Use of Angle Data.

95. Ground Assistance to LEM, Including Midcourse Correction.

98. Multiple Data Sources with Fixed Biases.

108. Station Location Errors.

115. The Calculation of the Covariance Matrix of the Errors in the Estimators of the Orbit Parameters when the Estimates are Based upon Data which is Contaminated by Auto-correlated Noise.

149. Modifications of Orbit Determination Program for Velocity of Light and Gravitational Attraction Uncertainty.

Some elementary analysis of the effect of station location errors is also included in Section 3 of Apollo Note No. 87 on Rendezvous Aids.

It is of sufficient importance to emphasize again, that this analysis is an error analysis and is planned to yield estimates of how well the orbit parameters can be determined. It is not a program for use in orbit determination. As a consequence, we must show that the corresponding orbit determination calculations can be

performed in a small time, in order for the results of the error analysis to have any relation to what can be done operationally. Bissett-Berman Apollo Note No. 93 "Ground System Computation of LEM Orbit" has this purpose. It indicates that the necessary computations can be performed in a few seconds on a 7094. Bissett-Berman Apollo Note No. 143, "Communication and Computation Load," presents some further results along this line.

The Bissett-Berman Corporation 2941 Nebraska Avenue, Santa Monica, California EXbrook 4-3270

APOLLO NOTE NO. 165

J. Holdsworth
20 January 1964

A METHOD FOR CALCULATING THE EXPLICIT FORM OF THE ROTATION MATRIX WHICH CARRIES TWO INITIAL VECTORS INTO TWO TERMINAL VECTORS OF THE SAME LENGTH

The purpose of this note is to give a systematic method for the calculation of a proper rotation matrix given that we are told that two known three dimentional vectors $\underline{V}_1$ and $\underline{V}_2$ are transformed into two known vectors $\underline{V}_1^*$, $\underline{V}_2^*$ under the rotation, where

$$\begin{aligned} \underline{V}_1 \cdot \underline{V}_1 &= \underline{V}_1^* \cdot \underline{V}_1^* \\ \underline{V}_2 \cdot \underline{V}_2 &= \underline{V}_2^* \quad \underline{V}_2^* \end{aligned} \tag{1}$$

Equation (1) is merely a statement of the requirement that the rotation operation preserves the lengths of all vectors.

In addition to equation (1) in order to avoid degeneracies, we must assume that $\underline{V}_1$ and $\underline{V}_2$ are not collinear or equivalently that:

$$\underline{V}_1 \neq k \underline{V}_2 \quad \text{and} \quad \underline{V}_1 \neq 0 \neq \underline{V}_2 \tag{2}$$

where k is some constant.

Instead of $\underline{V}_1$, $\underline{V}_1^*$, $\underline{V}_2$, $\underline{V}_2^*$ it is convenient to work with the unit vectors; defined by:

$$\underline{u}_1 = \frac{\underline{V}_1}{\sqrt{\underline{V}_1 \cdot \underline{V}_1}} , \qquad \underline{u}_2 = \frac{\underline{V}_2}{\sqrt{\underline{V}_2 \cdot \underline{V}_2}} \tag{3}$$

Let A denote the 3 x 3 rotation matrix referred to some known fixed right-handed orthonormal system $\underline{i}$, $\underline{j}$, $\underline{k}$. Then since A is a length-preserving operation, it easily follows that:

$$\underline{u_1}^* = A\,\underline{u_1}$$

$$\underline{u_2}^* = A\,\underline{u_2} \qquad (4)$$

are also unit vectors. Furthermore, since $\underline{V_1}$, $\underline{V_2}$ are not collinear, then $\underline{u_1} \neq \underline{u_2}$ from which it follows since A is a proper rotation that $\underline{u_1}^* \neq \underline{u_2}^*$.

Thus to recapitulate, the problems may be stated as follows: Given the components of the two non-collinear unit vectors $\underline{u_1}$ and $\underline{u_2}$ with respect to some right-handed orthonormal basis $\underline{i}$, $\underline{j}$, $\underline{k}$ and given the components of $\underline{u_1}^* = A\,\underline{u_1}$ and $\underline{u_2}^* = A\,\underline{u_2}$ with respect to the same basis, we wish to calculate the explicit matrix representation of the given rotation with respect to the orthonormal $\underline{i}$, $\underline{j}$, $\underline{k}$ triad.

It is known from Euler's theorem and should be intuitively evident, that the most general displacement of a rigid body which has one point fixed, is a rotation of the given body through some angle about some axis passing through the fixed point. This is proved in some detail in reference 1 and will not be elaborated upon further.

The point of view which we shall take is the "alibi" point of view. That is to say, we shall assume that the rotation actually transforms points of the space into new points. The "alias" point of view while equivalent is to my mind more cumbersome and assumes that all vectors of the original space remain physically fixed but that we now wish to describe these vectors with respect to an orthonormal basis which has been rotated about some axis.

From what we have said, it seems physically evident that if we know the orientation of the rotation axis with respect to the fixed $\underline{i}$, $\underline{j}$, $\underline{k}$ basis, and if we know the angle of rotation, that the rotation must then be completely determined so that given this information, we should be able to explicitly compute the matrix describing the rotation. Thus we begin by showing how to compute δ, the angle of rotation and the unit vector

$$\underline{c} = c_1\underline{i} + c_2\underline{j} + c_3\underline{k} \tag{5}$$

that defines the axis of rotation from a knowledge of the given unit vectors $\underline{u}_1$, $\underline{u}_2$, $\underline{u}_1^*$, $\underline{u}_2^*$. Once we have determined these quantities, we will explicitly construct the matrix representation of the rotation A.

In the following discussion we will reason geometrically rather than analytically in order to lend physical insight into the nature of the calculations to be performed. Rigorous proofs of any of the geometric statements made are available in many sources, reference (1) in particular.

Now we assume that we know the vectors $\underline{u}_1$, $\underline{u}_2$, $\underline{u}_1^*$, $\underline{u}_2^*$ with respect to some fixed orthonormal basis $\underline{i}$, $\underline{j}$, $\underline{k}$, and that

$$\begin{aligned} \underline{u}_1^* &= A\,\underline{u}_1 \\ \underline{u}_2^* &= A\,\underline{u}_2 \end{aligned} \tag{6}$$

We have assumed that $\underline{u}_1 \neq \pm \underline{u}_2$. Furthermore, we shall also assume for the present that neither of the pairs $\underline{u}_1$, $\underline{u}_1^*$ nor $\underline{u}_2$, $\underline{u}_2^*$ are collinear. The special case where $\underline{u}_1 \neq \pm \underline{u}_2$ but where one of the pairs $\underline{u}_1$, $\underline{u}_1^*$ or $\underline{u}_2$, $\underline{u}_2^*$ may be collinear, will be considered in the section on exceptional situations.

Now since we have assumed that $\underline{u_1}$ and $\underline{u_1}^*$ are not collinear, then they determine a unique plane which passes through the origin. Moreover, the termini of $\underline{u_1}$ and $\underline{u_1}^*$ and the origin determine a unique great circle on the unit sphere which passes through the termini of the vectors $\underline{u_1}$ and $\underline{u_1}^*$. Let us denote the arc on the unit sphere which connects $\underline{u_1}$ and $\underline{u_1}^*$ by arc (1, 1*).

Similarly since $\underline{u_2}$ and $\underline{u_2}^*$ are assumed to be non-collinear, then they determine a unique plane passing through the origin as well as a unique great circle on the sphere which connects $\underline{u_2}$ and $\underline{u_2}^*$. We denote the arc of this great circle connecting $\underline{u_2}$, $\underline{u_2}^*$ by arc (2, 2*).

We now construct two additional great circles which we shall call C_1 and C_2. We construct C_1 by requiring it to bisect arc (1, 1*) so that its plane is perpendicular to the plane determined by the vectors $\underline{u_1}$ and $\underline{u_1}^*$. We construct C_2 by requiring it to bisect arc (2, 2*) and have its plane perpendicular to the plane determined by $\underline{u_2}$ and $\underline{u_2}^*$. Both C_1 and C_2 are uniquely defined and synthetically constructable from a knowledge of $\underline{u_1}$, $\underline{u_1}^*$, $\underline{u_2}$, $\underline{u_2}^*$ and the assumptions we have made.

Since C_1 and C_2 are both great circles on the unit sphere, they intersect at two antipolar points P_1 and P_2 which are collinear with the origin. The diameter determined by the points P_1 and P_2 is the axis of rotation. The proof of this statement consists in showing that the perpendicular line segments projecting the termini of $\underline{u_1}$ and $\underline{u_1}^*$ upon the P_1P_2 axis intersect on the axis and have the same length; and that a similar condition holds for the segments joining the termini of $\underline{u_2}$, $\underline{u_2}^*$ perpendicularly to the P_1P_2 axis. Furthermore, the angle between either point of these perpendicular projections, e.g., the angle between the segment perpendicular to P_1P_2 and joining $\underline{u_1}$ and that joining $\underline{u_1}^*$ to P_1P_2 is the angle of rotation δ. There are straightforward proofs both synthetic and analytic for all of these statements although they are somewhat cumbersome notationally; hence for brevity, we have omitted them. The interested and patient reader is referred

again, to reference 1.

We shall now compute the vector $\underline{c}$ and the rotation angle δ in a manner which closely parallels our geometric discussion. The use of standard vector algebra greatly facilitates the calculations and will be used extensively. The vector $\underline{u_1} + \underline{u_1}^*$ is coplanar with $\underline{u_1}$ and $\underline{u_1}^*$ and bisects the angle between them since $\underline{u_1}$, $\underline{u_1}^*$ have the same length. Now the vector

$$\underline{Z_1} = \underline{u_1} \times \underline{u_1}^* \tag{7}$$

is normal to the plane determined by $\underline{u_1}$ and $\underline{u_1}^*$. Hence the vector defined by:

$$\underline{n_1} = (\underline{u_1} + \underline{u_1}^*) \times \underline{Z_1}$$

$$= (\underline{u_1} + \underline{u_1}^*) \times (\underline{u_1} \times \underline{u_1}^*) \tag{8}$$

must be normal to the plane of the circle C_1. Since it is normal to the plane of C_1, we may write the equation of the circle in the following vector form:

$$\underline{r} \cdot \underline{r} = 1$$
$$\underline{n_1} \cdot \underline{r} = 0 \tag{9}$$

where in equations (7), (8), and (9), we have used the familiar notation for the dot and cross product of two vectors.

In a similar manner the vector $\underline{Z_2}$ defined by

$$\underline{Z_2} = \underline{u_2} \times \underline{u_2}^* \tag{10}$$

is normal to the $\underline{u_2}$, $\underline{u_2}^*$ plane. Thus since $\underline{u_2} + \underline{u_2}^*$ is coplanar with $\underline{u_2}$ and $\underline{u_2}^*$ and bisects the angle between them, the vector $\underline{u_2}$ defined by:

$$\underline{n_2} = (\underline{u_2} + \underline{u_2}^*) \times \underline{Z_2}$$

$$= (\underline{u_2} + \underline{u_2}^*) \times (\underline{u_2} \times \underline{u_2}^*) \tag{11}$$

must be normal to the plane of the circle C_2. Thus from simple analytic geometry we may write the equation of circle C_2 in the following form:

$$\underline{r} \cdot \underline{r} = 1$$
$$\underline{n_2} \cdot \underline{r} = 0 \qquad (12)$$

Now we recall that the intersections of C_1 and C_2 determine the axis of rotation; thus we wish the simultaneous solution of the vector system given by equations (9) and (12). It is reasonably easy to obtain the vector solutions, one of which must be the desired unit vector $\underline{c}$, so that solving (9) and (12) we obtain:

$$\underline{c} = \pm \frac{\underline{n_1} \times \underline{n_2}}{\sqrt{(\underline{n_1} \times \underline{n_2}) \cdot (\underline{n_1} \times \underline{n_2})}} \qquad (13)$$

so that we have obtained the axis of rotation from a knowledge of $\underline{u_1}$, $\underline{u_1}^*$, $\underline{u_2}$, $\underline{u_2}^*$.

Since δ is the angle of rotation, then the operator A carries $\underline{u_1}$ into $\underline{u_1}^*$ by rotating it through an angle δ about the rotation axis.

Now the projection of the vector $\underline{u_1}$ on the rotation axis is given by:

$$P\underline{u_1} = (\underline{u_1} \cdot \underline{c})\,\underline{c} \qquad (14)$$

Similarly, the vector projection of $\underline{u_1}^*$ on the axis of rotation is:

$$P\underline{u_1}^* = (\underline{u_1}^* \cdot \underline{c})\,\underline{c} \qquad (15)$$

Obviously, we must have

$$P\underline{u_1} = P\underline{u_1}^* \qquad (16)$$

Now the vectors connecting $P\underline{u_1}$ to $\underline{u_1}$ and $\underline{u_1}^*$ respectively are

$$\underline{d}_1 = \underline{u}_1 - P\underline{u}_1$$

$$\underline{d}_1^* = \underline{u}_1^* - P\underline{u}_1 . \tag{17}$$

Moreover, they also have the same length.

Thus, the fact that A carries $\underline{u}_1$ into $\underline{u}_1^*$ by rotating it through angle δ in the $\underline{d}_1$, $\underline{d}_1^*$ plane, allows us to write the following expression for δ:

$$\cos\delta = \frac{\underline{d}_1 \cdot \underline{d}_1^*}{\underline{d}_1 \cdot \underline{d}_1} \tag{18}$$

$$= \frac{(\underline{u}_1 - P\underline{u}_1) \cdot (\underline{u}_1^* - P\underline{u}_1)}{(\underline{u}_1 - P\underline{u}_1) \cdot (\underline{u}_1 - P\underline{u}_1)}$$

Thus to partially summarize, given two vectors $\underline{V}_1$ and $\underline{V}_2$ and their images $\underline{V}_1^*$ and $\underline{V}_2^*$ under a rotation we have shown how to explicitly calculate the unit vector $\underline{c}$ defining the axis of rotation and the angle of rotation δ. We conclude by showing how the rotation matrix A may be explicitly constructed given a knowledge of $\underline{c}$ and δ.

It is a well-known fact that every linear operator and its matrix representation may be uniquely expressed as the sum of two other operators, one of which is symmetric and one of which is skew symmetric. Furthermore, in the case of rotation matrices, the symmetric component may be decomposed into two symmetric subcomponents, (ref. 2), so that the rotation matrix A may be expressed in terms of δ and $\underline{c}$ in the following fashion.

$$A = \begin{pmatrix} a_{11} & a_{12} & a_{13} \\ a_{21} & a_{22} & a_{23} \\ a_{31} & a_{32} & a_{33} \end{pmatrix} = \begin{pmatrix} 1 & 0 & 0 \\ 0 & 1 & 0 \\ 0 & 0 & 1 \end{pmatrix} \cos\delta$$

$$+ (1 - \cos\delta) \begin{pmatrix} c_1^2 & c_1c_2 & c_1c_3 \\ c_1c_2 & c_2^2 & c_2c_3 \\ c_1c_3 & c_2c_3 & c_3^2 \end{pmatrix} + \sin\delta \begin{pmatrix} 0 & -c_3 & c_2 \\ c_3 & 0 & -c_1 \\ -c_2 & c_1 & 0 \end{pmatrix} \quad (19)$$

Exceptional Situations:

In the preceding analysis, we have explicitly assumed that $\underline{u}_1$ and $\underline{u}_2$ are not collinear. However, the validity of the computations required in addition that neither the pair $\underline{u}_1$, $\underline{u}_1^*$ nor $\underline{u}_2$, $\underline{u}_2^*$ were collinear for if either pair were, say $\underline{u}_1$, $\underline{u}_1^*$, then $\underline{u}_1$, $\underline{u}_1^*$ would not determine a plane so that the great circle $\underline{C}_1$ which bisects arc (1, 1*) perpendicularly would not be well defined. However, if $\underline{u}_1$ and $\underline{u}_2$ are not collinear but one of the pairs $\underline{u}_1$, $\underline{u}_1^*$ or $\underline{u}_2$, $\underline{u}_2^*$ are, then the rotation matrix A may still be determined from the following considerations.

Let us assume that $\underline{u}_1$ and $\underline{u}_2$ are not collinear but that $\underline{u}_1$ and $\underline{u}_1^*$ are. Since $\underline{u}_1^*$ is the image of the unit vector $\underline{u}_1$ under a rotation, then the only way that $\underline{u}_1$ and $\underline{u}_1^*$ can be collinear is if $\underline{u}_1 = \underline{u}_1^*$ or $\underline{u}_1 = -\underline{u}_1^*$. We first consider the case where $\underline{u}_1 = \underline{u}_1^*$.

Now if $\underline{u}_1 = \underline{u}_1^*$, then all vectors collinear with $\underline{u}_1$ are left invariant under the rotation so that we immediately obtain the result that the axis of the rotation is collinear with $\underline{u}_1$. To obtain the angle δ, we note that in the present special case that the vector given by:

$$Pu_2 = (\underline{u}_2 \cdot \underline{u}_1)\ \underline{u}_1 \quad (20)$$

is the vector projection of both the vectors $\underline{u}_2$ and $\underline{u}_2^*$ upon the axis of rotation. This implies that δ must be the angle between the vectors $\underline{d}_2$ and $\underline{d}_2^*$ where:

$$\underline{d_2} = \underline{u_2} - P\underline{u_2}$$

$$\underline{d_2}^* = \underline{u_2}^* - P\underline{u_2} \qquad (21)$$

Hence, since the vectors $\underline{d_2}$ and $\underline{d_2}^*$ have the same length, we obtain the angle δ from the following equation:

$$\cos\delta = \frac{\underline{d_2} \cdot \underline{d_2}^*}{\underline{d_2} \cdot \underline{d_2}} \qquad (22)$$

On the other hand, if $\underline{u_1}^* = -\underline{u_1}$, then the rotation is a reflection about some axis which lies in the equatorial plane that perpendicularly bisects the diameter defined by $\underline{u_1}$ and $\underline{u_1}^*$. The orientation of the axis is determined by the intersection of the great circle which perpendicularly bisects arc (2, 2*) with the above-mentioned equatorial plane.

An entirely similar argument holds if $\underline{u_2}$, $\underline{u_2}^*$ are collinear. Thus even in these atypical situations we are able to explicitly determine our rotation matrices.

Summary:

Given the knowledge of two non-collinear vectors $\underline{V_1}$, $\underline{V_2}$ together with their images $\underline{V_1}^*$, $\underline{V_2}^*$ under a rotation operation, we have shown how to explicitly calculate the matrix which effects this rotation. The derivation was intentionally placed in a geometric framework in an attempt to impart some geometric significance to the necessary calculations. Undoubtedly alternative means of computing A given $\underline{V_1}$, $\underline{V_2}$, $\underline{V_1}^*$ and $\underline{V_2}^*$ exist which are strictly algebraic and which can be obtained by invoking the special conditions that a rotation matrix must satisfy. From a strictly algebraic point of view, it is interesting to note that any proper rotation in three dimensional space has one real and two complex conjugate eigen values. The real eigen value for a proper rotation is 1. The complex eigen values are given by

$$\lambda = e^{\pm i\delta}$$

where δ is the angle of rotation. Furthermore, the vector $\underline{c}$ which we have considered is the normalized eigen vector of the rotation corresponding to the real eigen value $\lambda = 1$.

The angle δ and the components of the vector $\underline{c}$ may also be related to the Euler angles, which are often used to characterize a rotation. The interested reader will find these relationships discussed in reference (3).

REFERENCES

1. W. D. MacMillan, "Theoretical Mechanics, Statics And The Dynamics of a Particle," chapter 8.

2. Korn and Korn, "Mathematical Handbook For Scientists and Engineers," chapter 14.

3. Goldstein, "Classical Mechanics," chapter 4.

The Bissett-Berman Corporation 2941 Nebraska Avenue, Santa Monica, California EXbrook 4-327(

APOLLO NOTE NO. 166

L. Lustick
20 January 1964

DETERMINATION OF ATTITUDE OF SPACECRAFT VIA APPLICATION OF TWO NON-COLLINEAR BOOSTS

Purpose:

The purpose of this note is to indicate the feasibility of determining the orientation of the body axes of the LEM by applying two non-collinear boosts.

Method:

1. A small boost is made along a particular LEM body axis.
2. The LEM is tracked in order to determine the boost velocity directions in space.
3. Another boost is made along another axis and this boost velocity is determined in space.
4. Thus two of the body axes of the LEM have been located in space and the third is, of course, perpendicular to its plane of the other two.

Discussion:

The accuracy of this method is dependent on how well the tracking stations from the earth can measure the change made in the velocity.

The following assumptions will be made:

1. Prior to the boost, no uncertainty in velocity and 1 km error in position components were assumed.
2. The boost magnitude is approximately 3 meters/sec.
3. An a priori knowledge subsequent to the boost for each component of velocity of 3 meters/ sec. was assumed.

4. Measurements of range change from three stations was assumed. The accuracy of each measurement was assumed as (. 6 meter 1 σ).

Results:

The following results are consistent with measuring range change from three stations (Madrid, Johannesburg, Woomera).

Observation Time	Uncertainty in Direction of Axes		
	1 sample/min.	10 samples/min.	60 samples/min.
2 min.	24. 5°	7. 75	3. 16
3 min.	13	4. 12	1. 68
6 min.	5. 7	1. 8	. 737
12 min.	4. 1	1. 3	. 53

The errors will be approximately inversely proportional to the boost velocity. For example, for other boost velocities than 3 meters/sec., the above errors should be multiplied by the factor $\left(\frac{3}{V \text{ boost}}\right)$.

If it is assumed that the required boost perturbation must be corrected for the required boost velocity is doubled.

Conclusion:

For a total boost velocity of 6-12 meters/sec., the orientation of the body axes can optimistically be determined to about 3° in a total time of about 5 minutes. It would seem, therefore, that this technique is, at best, marginally useful.

The Bissett-Berman Corporation 2941 Nebraska Avenue, Santa Monica, California EXbrook 4-3270

APOLLO NOTE NO. 167

B. Saltzberg
21 January 1964

ACCURACY OF ATTITUDE DETERMINATION BASED ON MSFN MEASUREMENT OF THE MOTION OF THE TRANSPONDER WITH RESPECT TO THE C. G.

In order to simplify the error analysis, assume that the transponder is rotating about the c. g. of the vehicle at a rate ω in a plane which makes an angle α with the line-of-sight from one of the ground tracking stations. Then the instantaneous doppler velocity due to this attitude change measured at the tracking station is given by

$$v(t) = \omega L \cos \alpha \cos (\omega t + \phi) \qquad (1)$$

where

L	=	length of the line from the c. g. to the transponder
α	=	angle between line-of-sight and the plane defined by the motion of L (the line from the center of rotation to the transponder). From one station this can be any tangent plane to a cone with α as its generating angle and the line-of-sight as its axis of symmetry.
ω	=	attitude rate
ϕ	=	initial orientation of L in the plane of rotation.

Assuming ω and L known, we wish to determine a best estimate of α and ϕ based on measurements of v.

Denoting

$$\omega L \cos \alpha = V \qquad (2)$$

gives

$$v = V \cos (\omega t + \phi) \qquad (3)$$

The error in the maximum likelihood estimators of V and ϕ are: (see Appendix)

$$\sigma_V = \sqrt{\frac{2}{N}}\ \sigma$$

$$\sigma_\phi = \sqrt{\frac{2}{N}}\ \frac{\sigma}{V} \tag{5}$$

where σ = standard deviation in the doppler velocity measurement
N = number of independent samples of v(t).

From (2) and (4) we can write the standard deviation in α, as

$$\sigma_\alpha = \frac{\sigma_V}{\omega L \sin \alpha} = \sqrt{\frac{2}{N}}\ \frac{\sigma}{\omega L \sin \alpha} \tag{6}$$

It is of interest to compute the number of samples required

$$N = \left(\frac{\text{Total Smoothing Time Required}}{\text{Time Between Independent Measurements of v}} \right)$$

to achieve a 1 sigma error in α of 0.5 degrees under the nominal conditions

ω = 0.6 rad/sec.
L = 2 meters
α = 30°
σ = 0.03 meters/sec

From (6)

$$N = \frac{2}{(\omega L \sin \alpha)^2} \left(\frac{\sigma}{\sigma_\alpha} \right)^2 \tag{7}$$

then for $\sigma_\alpha = \frac{1}{120}$ rad $\approx$ 0.5 degrees

$$N \simeq 75$$

The number of samples required to determine the initial orientation of L in the plane to an accuracy of 0.5 degrees is

$$N = \frac{2}{(\omega L \cos \alpha)^2} \left(\frac{\sigma}{\sigma_\phi} \right)^2 \qquad (8)$$

Using the same nominal values and $\sigma_\phi = \frac{1}{120}$ rad. gives

$$N = 24$$

Thus, it requires about three times as many samples to determine α to the same degree of accuracy as ϕ

If the time between independent samples is ΔT, then it is necessary to smooth for 75 ΔT seconds to determine both angles to 0.5 degrees or better in the nominal case calculated.

If σ = 0.03 meters/sec. is predicated on one minute samples then this would rule out the approach on a time basis alone, since this implies that 75 minutes are required to achieve marginal accuracy in the determination of α. However if a σ = 0.03 meters/sec. can be obtained for independent 1 second samples then further analysis would be warranted to determine the accuracy with which the other orientation parameters can be determined using three tracking stations.

APPENDIX

Error in the maximum likelihood estimators of V and ϕ where

$$v(t_i) = V \cos(\omega t_i + \phi) \tag{9}$$

The estimators are the values of V and ϕ which minimize

$$\sum_{i=1}^{N} \left[v_m(t_i) - v(t_i) \right]^2 = \sum_{i=1}^{N} \left[v_m(t_i) - V \cos(\omega t_i + \phi) \right]^2 \tag{10}$$

Setting the p.d. of (10) w.r.t. V and ϕ equal to zero, gives

$$0 = \sum_{i=1}^{N} \left[v_m(t_i) - V \cos(\omega t_i + \phi) \right] \left[-\cos(\omega t_i + \phi) \right] \tag{11}$$

$$0 = \sum_{i=1}^{N} \left[v_m(t_i) - V \cos(\omega t_i + \phi) \right] \left[V \sin(\omega t_i + \phi) \right] \tag{12}$$

Writing

$$V \cos(\omega t_i + \phi) = V_o \cos(\omega t_i + \phi_o) + \Delta V \cos(\omega t_i + \phi_o) - \Delta\phi \; V_o \sin(\omega t_i + \phi_o) + \text{h.o.t.} \tag{13}$$

Denoting

$$v_m(t_i) - V_o \cos(\omega t_i + \phi_o) \equiv n(t_i) \tag{14}$$

Using (13) and (14) in (11) and (12) gives

$$0 = \sum_{i=1}^{N} \left[n(t_i) - \Delta V \cos(\omega t_i + \phi_o) + \Delta\phi\, V_o \sin(\omega t_i + \phi_o) \right] \left[-\cos(\omega t_i + \phi_o) \right] \tag{15}$$

$$0 = \sum_{i=1}^{N} \left[n(t_i) - \Delta V \cos(\omega t_i + \phi_o) + \Delta\phi\, V_o \sin(\omega t_i + \phi_o) \right] \left[V_o \sin(\omega t_i + \phi_o) \right] \tag{16}$$

Simplifying, (15) and (16) become

$$\Delta V \sum_{i=1}^{N} \cos^2(\omega t_i + \phi_o) - \Delta\phi \sum_{i=1}^{N} V_o \sin(\omega t_i + \phi_o) \cos(\omega t_i + \phi_o) \tag{17}$$

$$= \sum_{i=1}^{N} n(t_i \cos(\omega t_i + \phi_o)$$

$$-\Delta V \sum_{i=1}^{N} V_o \sin(\omega t_i + \phi_o) \cos(\omega t_i + \phi_o) + \Delta\phi \sum_{i=1}^{N} V_o^2 \sin^2(\omega t_i + \phi_o) \tag{18}$$

$$= - \sum_{i=1}^{N} n(t_i)\, V_o \sin(\omega t_i + \phi_o)$$

The information matrix, C, corresponding to (17) and (18) is

$$C = \begin{pmatrix} C_{11} & C_{12} \\ C_{21} & C_{22} \end{pmatrix} \tag{19}$$

where

$$C_{11} = \sum_{i=1}^{N} \cos^2 (\omega t_i + \phi_o) \tag{20}$$

$$C_{21} = C_{12} = - V_o \sum_{i=1}^{N} \sin (\omega t_i + \phi_o) \cos (\omega t_i + \phi_o) \tag{21}$$

$$C_{22} = V_o^2 \sum_{i=1}^{N} \sin^2 (\omega t_i + \phi_o) \tag{22}$$

Approximating the sums (20), (21) and (22) by integrals over the total smoothing time, T, gives

$$C_{11} = \frac{N}{T} \int_o^T \cos^2 (\omega t + \phi_o) \, dt \tag{20}'$$

$$C_{21} = C_{12} = \frac{N}{T} V_o \int_o^T \sin (\omega t + \phi_o) \cos (\omega t + \phi_o) \, dt \tag{21}'$$

$$C_{22} = \frac{N}{T} V_o^2 \int_o^T \sin^2 (\omega t + \phi_o) \, dt \tag{22}'$$

To simplify the calculations, let $T = \frac{2\pi}{\omega}$, and (20)', (21)' and (22)' become:

$$C_{11} = \frac{N}{2} \tag{23}$$

$$C_{21} = C_{12} = 0 \tag{24}$$

$$C_{22} = \frac{N}{2} V_o^2 \tag{25}$$

Thus,

$$C = \begin{pmatrix} N/2 & 0 \\ 0 & N/2\, B_o^2 \end{pmatrix} \tag{26}$$

and

$$C^{-1} = \begin{pmatrix} \frac{2}{N} & 0 \\ 0 & \frac{2}{NB_o^2} \end{pmatrix} \tag{27}$$

giving

$$\sigma_V^2 = \frac{2}{N}\,\sigma^2 \tag{28}$$

$$\sigma_\phi^2 = \frac{2}{NV_o^2}\,\sigma^2 \tag{29}$$

where σ^2 is the doppler noise variance.

The standard deviations are

$$\sigma_V = \sqrt{\frac{2}{N}}\,\sigma \tag{30}$$

$$\sigma_\phi = \sqrt{\frac{2}{N}}\,\frac{\sigma}{V_o} \tag{31}$$

The Bissett-Berman Corporation 2941 Nebraska Avenue, Santa Monica, California EXbrook 4-3270

APOLLO NOTE NO. 168

L. Horowitz
21 January 1964

GROUND STATION DETERMINATION OF LEM ATTITUDE

Introduction:

It has been suggested that DSIF determination of LEM attitude be accomplished by exploiting ground station range-rate differentials introduced through transponder offset from the LEM c. g. For this formulation, multiple DSIF's are used to locate the transponder with respect to the LEM c. g. where c. g. motion is itself taken to be accurately known from continued ground tracking. Accurate telemetered data from strapped-down attitude rate gyros aboard the LEM are also assumed to be available for the computation. Hence, multiple DSIF determination of LEM attitude from observed range-rate data reduces to effecting maximum likelihood estimates on the LEM-DSIF coordinate transformation parameters.

This paper attempts to estimate the accuracy to which such a determination may be effected by analyzing a simplified model of the actual situation. We note in particular that precise location of the transponder and the c. g. fails to fully define LEM attitude, since rotations about the line so defined cannot be observed. Elimination of this ambiguity can be accomplished by commanding changes in angular velocity components through use of LEM attitude control jets, then solving the simultaneous system so defined for the attitude parameters.

Results of this analysis are presented in the concluding section.

Geometrical Formulation:

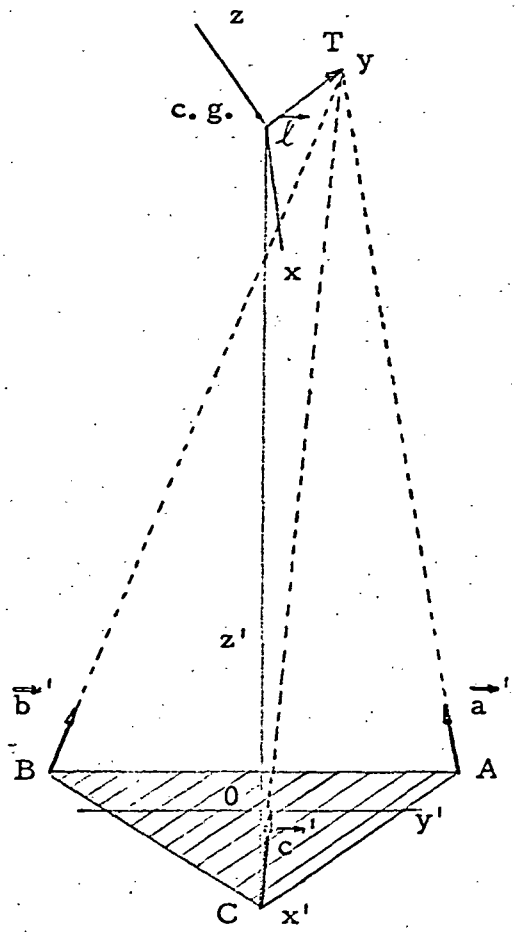

Figure 1

Here, A, B, C represent DSIF stations; c. g. and T, the LEM center of gravity and transponder respectively, with $\vec{\ell}$ the vector connecting them; xyz the LEM inertial axes about which angular velocities are accuartely known, and x' y' z' the Earth inertial reference. ABC is taken to be an equilateral triangle and $\overline{O\text{-c. g.}}$ the Earth-Moon distance. $\vec{a}'$, $\vec{b}'$, $\vec{c}'$ are unit vectors from the three DSIF stations to the transponder. In what follows, attitude determination will be inferred from the Euler angles ϕ, ψ, θ of xyz with respect to x' y' z' (Goldstein's notation used) and $\vec{\omega}^{\,i} = \left[\omega_x^i,\ \omega_y^i,\ \omega_z^i\right]$ the LEM angular velocity after

the i'th angular thrust; i = 1, 2, 3. In every case, unprimed quantities refer to the xyz system and primed quantities to the x' y' z' system, with E the orthogonal matrix rotating vectors in x' y' z' to xyz. The observed measurables are $\dot{r}_1$, $\dot{r}_2$ and $\dot{r}_3$ (range -rate along $\vec{a}'$, $\vec{b}'$, $\vec{c}'$ respectively) together with $\vec{\omega}^i$. The parameters to be estimated are ϕ, ψ, and θ.

Likelihood Equations:

For this simplified analysis, we take the LEM c. g. to be fixed in space. The velocity of T is then $\vec{\omega} \times \vec{\ell}$ in xyz and $(\vec{\omega} \times \vec{\ell})' = E\vec{\omega} \times E\vec{\ell}$ $= E(\vec{\omega} \times \vec{\ell})$ in x'y'z'. The measured quantities $\dot{r}_k$ are then just

$$(1) \qquad \dot{r}_k = E(\vec{\omega} \times \vec{\ell}) \cdot \vec{a}_k'; \quad k = 1, 2, 3,$$

so that

$$(2) \qquad \frac{\partial \dot{r}_k}{\partial a_i} = \frac{\partial E}{\partial a_i} (\vec{\omega} \times \vec{\ell}) \cdot \vec{a}_k'; \quad i = 1, 2, 3, \text{ when } a_1, a_2, a_3$$

represent ϕ, ψ, and θ, respectively. The rotation matrix is

$$E = \begin{pmatrix} \cos\psi\cos\phi - \cos\theta\sin\phi\sin\psi & \cos\psi\sin\phi + \cos\theta\cos\phi\sin\psi & \sin\phi\sin\theta \\ -\sin\psi\cos\phi - \cos\theta\sin\phi\cos\psi & -\sin\psi\sin\phi + \cos\theta\cos\phi\cos\psi & \cos\phi\sin\theta \\ \sin\theta\sin\phi & -\sin\theta\cos\phi & \cos\theta \end{pmatrix} \quad (3)$$

also denoted by E_{ij}. The inverse of E is its transpose:

$$E^{-1} = E_{ji}. \qquad (4)$$

Terms C_{ij} of the information matrix C are then

$$C_{ij} = \sum_{k=1}^{3} \frac{\partial \dot{r}_k}{\partial a_i} \frac{\partial \dot{r}_k}{\partial a_j}$$

$$= \sum_{k=1}^{3} \frac{\partial E}{\partial a_i} (\vec{\omega} \times \vec{\ell}) \cdot \vec{a}_k' \frac{\partial E}{\partial a_j} (\vec{\omega} \times \vec{\ell}) \cdot \vec{a}_k' \qquad (5)$$

by (2), where

$$\vec{a}' = \left[\frac{1}{2}\cos\lambda\,,\ -\frac{\sqrt{3}}{2}\cos\lambda,\ \sin\lambda\right]$$

$$\vec{b}' = \left[\frac{1}{2}\cos\lambda,\ \ \frac{\sqrt{3}}{2}\cos\lambda,\ \sin\lambda\right]$$

$$\vec{c}' = \left[-\cos\lambda,\ \ 0\,,\ \ \sin\lambda\right]\ ; \qquad (6)$$

λ the angle between $\vec{a}'$, $\vec{b}'$, $\vec{c}'$ and the plane ABC. $\sigma^2 C^{-1}$ is then the desired covariance matrix for the maximum likelihood estimators $\hat{a}_i$.

One might suppose that the system (1), being three simultaneous equations in three unknowns (ϕ, ψ, θ), could at least in theory be solved. As noted above, however, coordinate rotations about $\vec{\omega} \times \vec{\ell}$ constitute an additional degree of freedom independent of point T. Hence, the best that three simultaneous measurements $\dot{r}_k$ (k = 1, 2, 3) can accomplish is to establish the location of T, with ambiguity over rotations about $\vec{\omega} \times \vec{\ell}$ unresolved until more data is acquired. An interesting by-product of this analysis was the discovery that the covariance matrix $\sigma^2 C^{-1}$ of the maximum likelihood estimators $\hat{a}_i$ for the coordinate transformation parameters a_i does <u>not</u> reveal this ambiguity, since finite covariance terms for all nine elements of the matrix were obtained. L. Lustick points out that tacit linearization performed in defining covariance matrices in the first place was responsible for obscuring this intrinsic ambiguity. Thus, independent physical appraisal is required to establish the determinism of simultaneous systems such as (1).

<u>Nominal Case:</u>

For a nominal case, we take $|\vec{\omega}| = 45^\circ/\text{sec}$; $(\phi, \theta, \psi) = (0, 45^\circ, 0)$; $\vec{\ell} = \left[0,\ 2,\ 0\right]$ meters; and $\overline{0T}$ the Earth-Moon distance. Then by (5), terms in the information matrix are

$$C_{ij} = \sum_{k=1}^{3} \frac{\partial E}{\partial a_i}\ (\vec{\omega} \times \vec{\ell}) \cdot \vec{a}_k' \frac{\partial E}{\partial a_j}\ (\vec{\omega} \times \vec{\ell}) \cdot \vec{a}_k'$$

where for a typical case, we orient the angular velocity so that $\vec{\omega} = \left[45^\circ/\text{sec.},\ 0,\ 0\right]$ (by the previous argument, only components of $\vec{\omega}$ perpendicular to $\vec{\ell}$ can be estimated here, anyway; so we need consider only those case $\vec{\omega} \perp \vec{\ell}$.)

Then with E given by (3), we have

$$\frac{\partial E}{\partial \phi} = \begin{pmatrix} 0 & 1 & 0 \\ -\frac{1}{\sqrt{2}} & 0 & 0 \\ \frac{1}{\sqrt{2}} & 0 & 0 \end{pmatrix}$$

$$\frac{\partial E}{\partial \theta} = \begin{pmatrix} 0 & 0 & 0 \\ 0 & -\frac{1}{\sqrt{2}} & \frac{1}{\sqrt{2}} \\ 0 & -\frac{1}{\sqrt{2}} & -\frac{1}{\sqrt{2}} \end{pmatrix}$$

$$\frac{\partial E}{\partial \psi} = \begin{pmatrix} 0 & \frac{1}{\sqrt{2}} & \frac{1}{\sqrt{2}} \\ -1 & 0 & 0 \\ 0 & 0 & 0 \end{pmatrix} \qquad (7)$$

and

$$\vec{\omega} \times \vec{\ell} = \begin{vmatrix} \vec{i} & \vec{j} & \vec{k} \\ \frac{\pi}{4} & 0 & 0 \\ 0 & 2 & 0 \end{vmatrix} = \frac{\pi}{2}\,\vec{k}, \qquad (8)$$

where $\vec{i}$, $\vec{j}$, $\vec{k}$ are unit vectors along x, y, z. Carrying out these computations we obtain

$$C = \frac{\pi^2}{8} \begin{pmatrix} 0 & 0 & 0 \\ 0 & \frac{3}{2}\cos^2\lambda + 2\sin^2\lambda & 0 \\ 0 & 0 & \frac{3}{2}\cos^2\lambda \end{pmatrix} \quad (9)$$

where we have eclectically chosen a particularly simple situation in which all but two terms of C vanish. It is emphasized that $C_{ij} \neq 0$ in the general case, as can be seen by inspection of (3). Since the information terms $C_{1j} = C_{j1}$ happen to be zero for this special case, we consider only the lower 2 x 2 submatrix C':

$$C' = \frac{\pi^2}{8} \begin{pmatrix} \frac{3}{2}\cos^2\lambda + 2\sin^2\lambda & 0 \\ 0 & \frac{3}{2}\cos^2\lambda \end{pmatrix}, \quad (10)$$

so that the desired covariance matrix is

$$\mathrm{Cov}(\hat{a}_i, \hat{a}_j) = \frac{8\sigma^2}{\pi^2} \begin{pmatrix} \frac{2}{3\cos^2\lambda + 4\sin^2\lambda} & 0 \\ 0 & \frac{2}{3\cos^2\lambda} \end{pmatrix} \quad (11)$$

where σ^2 is the variance of the associated noise process and

$$a_1 = \theta, \quad a_2 = \psi.$$

Conclusions:

For the assumed situation, λ is roughly 89.5°; $\cos\lambda \approx .009$, so that (11) is roughly

$$\text{Cov}\,(\hat{a}_i, \hat{a}_j) = \sigma^2 \begin{pmatrix} .5\ \frac{\text{sec}^2}{\text{m}^2} & 0 \\ 0 & 10^5\ \frac{\text{sec}^2}{\text{m}^2} \end{pmatrix}, \qquad (12)$$

with all covariance terms measured in $(\text{radian})^2$. Thus, for $\sigma_{\dot{r}} = .03\text{m/sec.}$, the standard deriation in θ is approximately one degree for three simultaneous $\dot{r}$ measurements. Thus, θ can be estimated surprisingly accurately for this geometrical configuration. Unfortunately ψ and ϕ can barely be estimated at all in this case.

The next note on this subject will attempt to determine ψ and ϕ to better accuracy by commanding angular thrusts to alter the problem.

The Bissett-Berman Corporation 2941 Nebraska Avenue, Santa Monica, California EXbrook 4-3270

APOLLO NOTE NO. 169

H. Engel
31 January 1964

CHECKOUT OF REVISED ERROR PROGRAM

The error analysis program has been revised to include hyperbolic orbits, station location errors, errors in the speed of light, errors in gravitational constants, and clock-rate errors. All of these have been discussed in previous Bissett-Berman Apollo Notes.

This revised program has been checked by comparing slide rule computations with computer printouts. In all of those cases where there is apparently substantial disagreement the difference is actually small enough not to affect the usefulness of the program, and can be attributed to the use of trigonometric, inverse trigonometric, hyperbolic or inverse hyperbolic series approximations.

Five test cases were employed. In the first three the parameters were

a_1 0.17525 + 7 meters

a_4 0

a_5 0.170172 + 4 meters/sec.

GAM ID 1

β 0°

ξ 0°

η 180°

ζ 180°

λ	0^o
α	0^o
ω_e	0
ω_M	0
ρ_e	.63781 + 7 meters
ρ_M	.385 + 9 meters
μ	.4896 + 13 meters^3/sec^2

in which a + b means a x 10^b. The first test case determined certain partial derivatives at time T = 0 for measurements of range, range-rate and two angles. In the second test case these quantities were determined at T = 1 minute, checking a number of quantities known to be 0 at T = 0. In the third test case the sums of the computed quantities based on computations at T = 0.1, 0.2, 0.3, ..., 1.0 minutes were computed to verify that results were being properly combined. The quantities in parentheses below are analytical or slide rule results, while those without parentheses are computer results.

	Case 1	Case 2	Case 3	
$\frac{\partial s}{\partial b}$	1.00 (1)	1.00 (1)	1.00 + 1 (✓)	Range bias
$\frac{\partial s}{\partial x}$	-1.00 (-1)	-1.00 (-1)	1.00 + 1 (✓)	Station location
$\frac{\partial s}{\partial y}$	.45 - 14 (0)	.272-3 (.266-3)	.136-2 (✓)	Station location

$\frac{\partial s}{\partial z}$	.83 - 25 (0)	.500-14 (0)	.250-13 (✓)	Station location
$\frac{\partial s}{\partial k}$	1 (1)			Fractional speed of light
$\frac{\partial \dot{s}}{\partial b}$	1.00 (1)	1.00 (1)		Doppler bias
$\frac{\partial \dot{s}}{\partial x}$	.204-19 (0)	.122-8 (.118-8)		Station location
$\frac{\partial \dot{s}}{\partial y}$	.452-5 (.444-5)	.451-5 (.44-5)		Station location
$\frac{\partial \dot{s}}{\partial z}$	.832 -16 (0)	.830-16 (0)		Station location
$\frac{\partial \dot{s}}{\partial k}$		.961 + 2 (1.00 + 2)		Fractional speed of light

The partials of the angles with respect to biases, station location and speed of light were essentially 1 or 0 as they should be. The partial of range with respect to clock-rate error was 60 at T = 1 minute as expected, and partials of other measurables with respect to clock-rate error were essentially 0.

In order to determine the correctness of the program for errors in the gravitational constant, the computed partials of each quantity with respect to μ at T = 1 minute were compared with the analytic values.

j	$\frac{\partial x_j}{\partial \mu}$ (computed)	$\frac{\partial x_j}{\partial \mu}$ (analytic)
1	-.586 - 9	-.587-9
2	-.114 - 10	-.118 - 10
3	0	0
4	-.195 - 10	-.196 - 10
5	-.570 - 12	-.59 - 12
6 - 11	0	0
12	1.00 + 0	1

Test cases four and five were used to check the new hyperbolic program. Test case four is a highly elliptic orbit with e = 0.997, and test case five is a slightly hyperbolic orbit with e = 1.003. The two orbits are very nearly identical for small times, and hence should result in nearly identical information matrices. The parameters used were the same as in test cases one through three except that a_5 = .1668936 + 4 meters/sec. in case four, and a_5 = .1673950 + 4 meters/sec. in case five. It was deemed sufficient to check only the range measurable.

The information matrix is symmetric, so only half is shown here. The results of case four are in parentheses, those of case five are not.

T = 0

1.00 + 0 (1.00 + 0)						
.974-12 (1.02-12)	.948-24 (1.04-24)					
0 (0)	0 (0)	0 (0)				
.455-24 (-.107-7)	0 (-.109-19)	0 (0)	0 (.144-23)			
1.14-12 (.682-12)	1.11-24 (.696-24)	0 (0)	0 (.729-20)	1.29-24 (.465-24)		
0 (0)	0 (0)	0 (0)	0 (0)	0 (0)	0 (0)	
-1.00 +0 (-1.00 +0	-.974-12 (-1.02-12)	0 (0)	-.455-24 (.107-7)	-1.14-12 (-.682-12)	0 (0)	1.00 + 0 (1.00 + 0)

T = 10 minutes

.137 + 2 (.137 + 2)						
.314 + 0 (.314 + 0)	.141-1 (.141-1)					
0 (0)	0 (0)	0 (0)				
.410 + 4 (.410 + 4)	.138 + 3 (.138 + 3)	0 (0)	.157 + 7 (.157 + 7)			
760 + 2 (759 + 2)	.370 + 1 (.369 + 1)	0 (0)	.345 + 5 (.345 + 5)	.987 + 3 (.985 + 3)		
0 (0)	0 (0)	0 (0)	0 (0)	0 (0)	0 (0)	
-.122 + 2 (-.122 + 2)	-.254 + 0 (-.254 + 0	0 (0)	-.348 + 4 (-.348 + 4)	-.607 + 2 (-.607 + 2)	0 (0)	.110 + 2 (.110 + 2)

The elements of the Q matrix are essentially the identity matrix at T = 0, as they should be. The Q matrices at time T = 10 minutes for the elliptic and hyperbolic cases are compared below. (The Q matrix is not symmetric).

Q Matrix. T = 10 minutes

.132 + 1 (.131 + 1	.863-1 (.862-1)	0 (0)	.658 + 3 (.658 + 3)	.257 + 2 (.257 + 2)	0 (0)
.951-1 (.950-1)	.866 + 0 (.866 + 0)	0 (0)	.266 + 2 (.266 + 2)	.577 + 3 (.577 + 3)	0 (0)
0 (0)	0 (0)	.841 +0 (.841 + 0)	0 (0)	0 (0)	.568 + 3 (.568 + 3)
.102-2 (.103-2)	.407-3 (.407-3)	0 (0)	.127 + 1 (.127 + 1)	.164 + 0 (.164 + 0)	0 (0)
.479 - 3 (.479 - 3)	-.351-3 (-.352 -3	0 (0)	.173 + 0 (.173 + 0)	.916 + 0 (.916 + 0)	0 (0)
0 (0)	0 (0)	-.516-3 (-.516-3)	0 (0)	0 (0)	.841 + 0 (.841 + 0)

The Bissett-Berman Corporation 2941 Nebraska Avenue, Santa Monica, California EXbrook 4-3270

APOLLO NOTE NO. 170

H. Epstein
7 February 1964

AN APPROXIMATE TECHNIQUE TO ESTIMATE THE RANGE ERRORS DUE TO THE TROPOSPHERE

This note is being written to indicate the approximate magnitude of range bias and RMS range errors associated with the troposphere. The bias errors are associated with changes in the troposphere of a predominantly diurnal and seasonal nature. Correlation times of the refractive index (η) may be considered as hours or longer. The so-called RMS range errors are treated as associated with deviations in the troposphere from the ideal spherical nature of the refractive index. Significant deviations may occur in the refractive index with correlation times as low as a few seconds. The shorter correlation times are associated with smaller refractive index changes. For example, a correlation time of about 4 seconds might correspond to a refractive index anomaly of about 10^{-4}.

The bias error is defined in terms of the difference between the actual path length delay and the path length delay for a vacuum between the transmitter and the receiver. The geometry for the tropospheric bias analysis is indicated in Figure 1. The troposphere may be considered as a region with normal dispersion in the microwave frequency region of interest. That is, the index of refraction is essentially independent of frequency in the frequency region of interest. Where the ray theory is applicable, the path taken by the wave will correspond to a minimum time trajectory. Situations can arise where an appropriate analysis would require that several rays be required to accommodate peculiar tropospheric effects. In this situation, the wave is considered as occurring in several "modes." This effect rarely occurs to an appreciable extent for the troposphere aside from very low elevation depression angles. Moding is not treated in this analysis. The use of Fermat's principle or the calculus of variations leads to the following equations for a spherical stratisfied troposphere.

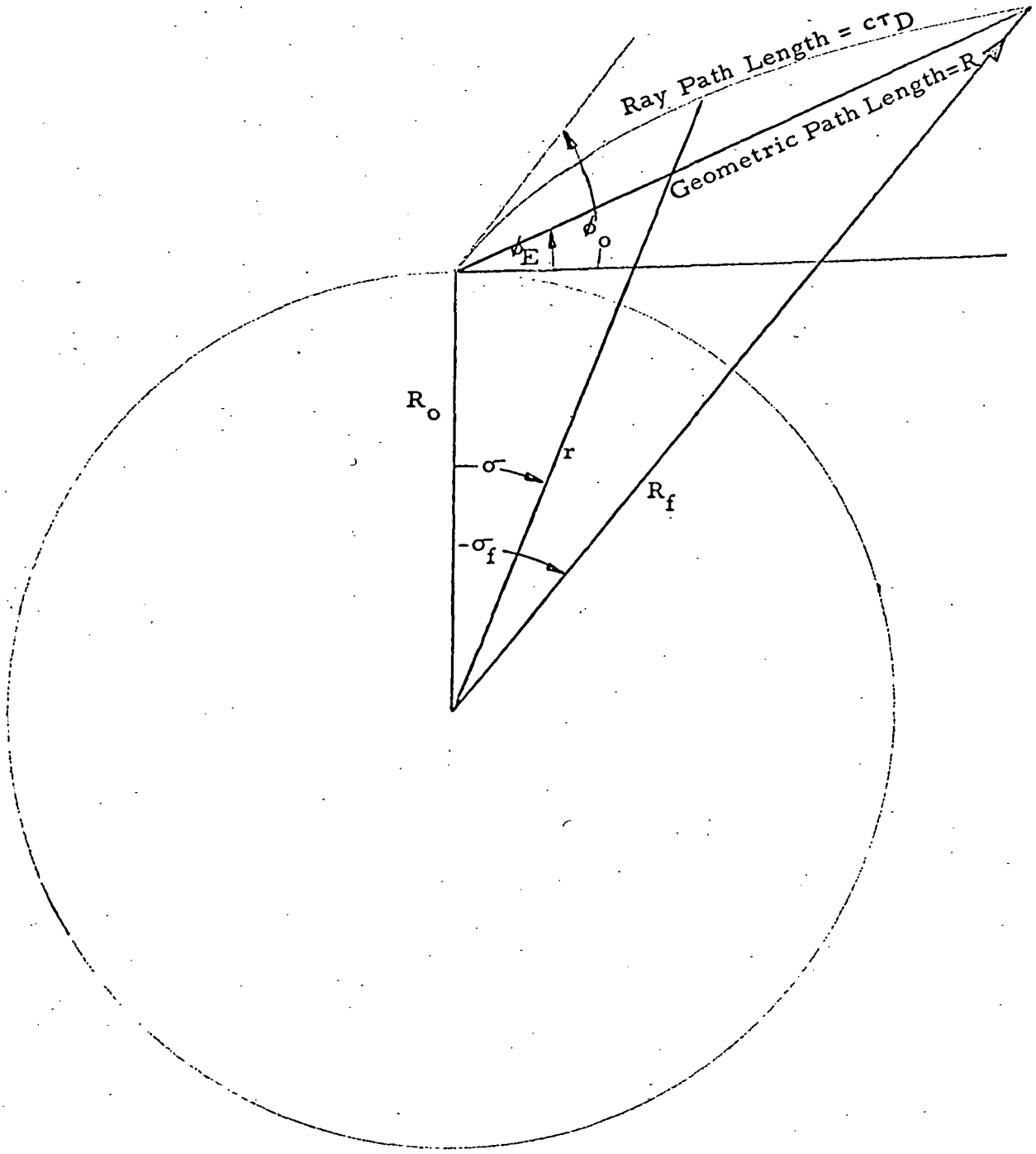

Figure 1.

Geometry for Tropospheric Bias Analysis

$$c\tau_D = \int_{R_o}^{R_f} \frac{\eta^2 \, r \, dr}{\sqrt{\eta^2 r^2 - \eta_o^2 R_o^2 \cos^2 \phi_o}} \qquad (1)$$

$$\sigma_f = \int_{R_o}^{R_f} \frac{\eta_o R_o \cos \phi_o \, dr}{r\sqrt{\eta^2 r^2 - \eta_o^2 R_o^2 \cos^2 \phi_o}} \qquad (2)$$

where

$\eta = 1 + N$ = refractive index at a given altitude

$\eta_o = 1 + N_o$ = refractive index at the minimum altitude (taken as the Earth's surface).

From the Law of cosines,

$$R^2 = R_f^2 - 2R_f R_o \cos \sigma_f + R_o^2 \qquad (3)$$

and defining the range bias error (ΔR) by:

$$\Delta R = c\tau_D - R \qquad (4)$$

One can now obtain the range bias error as a function of the assumed variation of refractive index with altitude. The best approximation to the refractive index variation from unity is given by an exponential or bi-exponential model. However, for the purposes of estimation of the error rather than calibration of the error, it is adequate to assume a much simpler model. The model selected is believed to be quite adequate quantitatively and yet indicate in a much simplified fashion the primary factor affecting range bias errors--namely, the elevation depression angle.

The simplified model is taken as:

$\eta = \eta_o \qquad R_o \leq R < R_1$

$= 1 \qquad R > R_1$

Performing the required integration of Equations (1) and (2) for this model, one can obtain

$$c\tau_D = \eta_o \left[\sqrt{R_1^2 - R_o^2 \cos^2 \phi_o} - R_o \sin \phi_o\right] + \sqrt{R_f^2 - \eta_o^2 R_o^2 \cos^2 \phi_o} - \sqrt{R_1^2 - \eta_o^2 R_o^2 \cos^2 \phi_o} \tag{5}$$

$$\sigma_f = \cos^{-1}\left(\frac{R_o \cos \phi_o}{R_1}\right) - \phi_o + \cos^{-1}\left(\frac{\eta_o R_o \cos \phi_o}{R_f}\right) - \cos^{-1}\left(\frac{\eta_o R_o \cos \phi_o}{R_1}\right) \tag{6}$$

Recognization that the final altitude is well beyond the region where the troposphere will have an appreciable effect, one can take the limiting expressions as R_f goes to infinity to arrive at the following results for ΔR and σ_f.

$$\lim_{R_f \to \infty} \Delta R = \Delta R_\infty = \eta_o \left[\sqrt{R_1^2 - R_o^2 \cos^2 \phi_o} - R_o \sin \phi_o\right] + R_o \cos \sigma - \sqrt{R_1^2 - \eta_o^2 R_o^2 \cos^2 \phi_o} \tag{7}$$

$$\lim_{R_f \to \infty} \sigma_f = \sigma_f = \frac{\pi}{2} - \phi_o + \cos^{-1}\left(\frac{R_o \cos \phi_o}{R_1}\right) - \cos^{-1}\left(\frac{\eta_o R_o \cos \phi_o}{R_1}\right) \tag{8}$$

After some mathematical manipulations of Equations (7) and (8) the following result can be obtained:

$$\Delta R_\infty = \frac{(\eta_o^2 - 1)(R_1^2 - R_o^2)}{\left[\eta_o + \sqrt{\frac{R_1^2 - \eta_o^2 R_o^2 \cos^2 \phi_o}{R_1^2 - R_o^2 \cos^2 \phi_o}}\right]\left[\sqrt{R_1^2 - R_o^2 \cos^2 \phi_o} + R_o \sin \phi_o\right]} \tag{9}$$

A suitable accurate approximation of Equation (9) then yields the desired result.

$$\Delta R_\infty \approx \frac{4 N_o H}{\left[\sin \phi_o + \sqrt{\sin^2 \phi_o + 2\frac{H}{R_o}}\right]\left[1 + \sqrt{\frac{\sin^2 \phi_o + 2\left(\frac{H}{R_o} - N_o\right)}{\sin^2 \phi_o + 2\frac{H}{R_o}}}\right]} \tag{10}$$

where $H = R_1 - R_o$ = scale height of the troposphere $\approx$ 7.15 km.

$\eta_o = 1 + N_o$ = surface refractive index ($N_o \approx 3.4 \times 10^{-4}$)

R_o = earth's radius = 6378 km.

for $\sin \phi_o \gg \sqrt{\frac{2H}{R_o}} \approx .0473$,

$$\Delta R_\infty \approx \frac{N_o H}{\sin \phi_o} \approx \frac{2.43}{\sin \phi_o} \text{ meters} \tag{11}$$

This indicates that for depression angles greater than a few degrees the planar Earth model is adequate for computation purposes. Lower depression angles should be avoided since for extremely low grazing angles other effects are encountered in the troposphere of an essentially pathological nature in addition to the high range bias errors that can occur.

Figure 2 indicates the tropospheric bias error for the assumed values of the parameter involved in the refractive index. The bias error is shown to vary from a few meters for high elevation depression angles to about 112 meters for very low elevation depression angles. Above an elevation depression angle of a few degrees, the spherical nature of the refractive index (spherical Earth model) can be adequately approximated by a vertically stratisfied troposphere (planar Earth model). As an interesting sidelight, it can be shown that a good approximation to the more laborious calculations involved can be obtained by considering a ray which proceeds on a straight line path between the transmitter and receiver for calculation of the range bias error. The results obtained in this fashion will be slightly greater than the results for the minimum time path for typically refractive index profiles.

Analytical expressions for the RMS range error associated with the troposphere (σ_{rt}) has been developed by Muchmore and Wheelon[1/] A convenient form is as follows:

$$\sigma_{rt} = \Delta N \sqrt{2LL_o} \qquad (12)$$

where

ΔN = RMS refractive index variation

L = path length

L_o = scale length of the anomalies

Typical values for the troposphere are indicated in Figure 3 .

1/ Muchmore and Wheelon, Line of Sight Propagation Phenomena, Proc. IRE, Vol. 43, No. 10, October 1955.

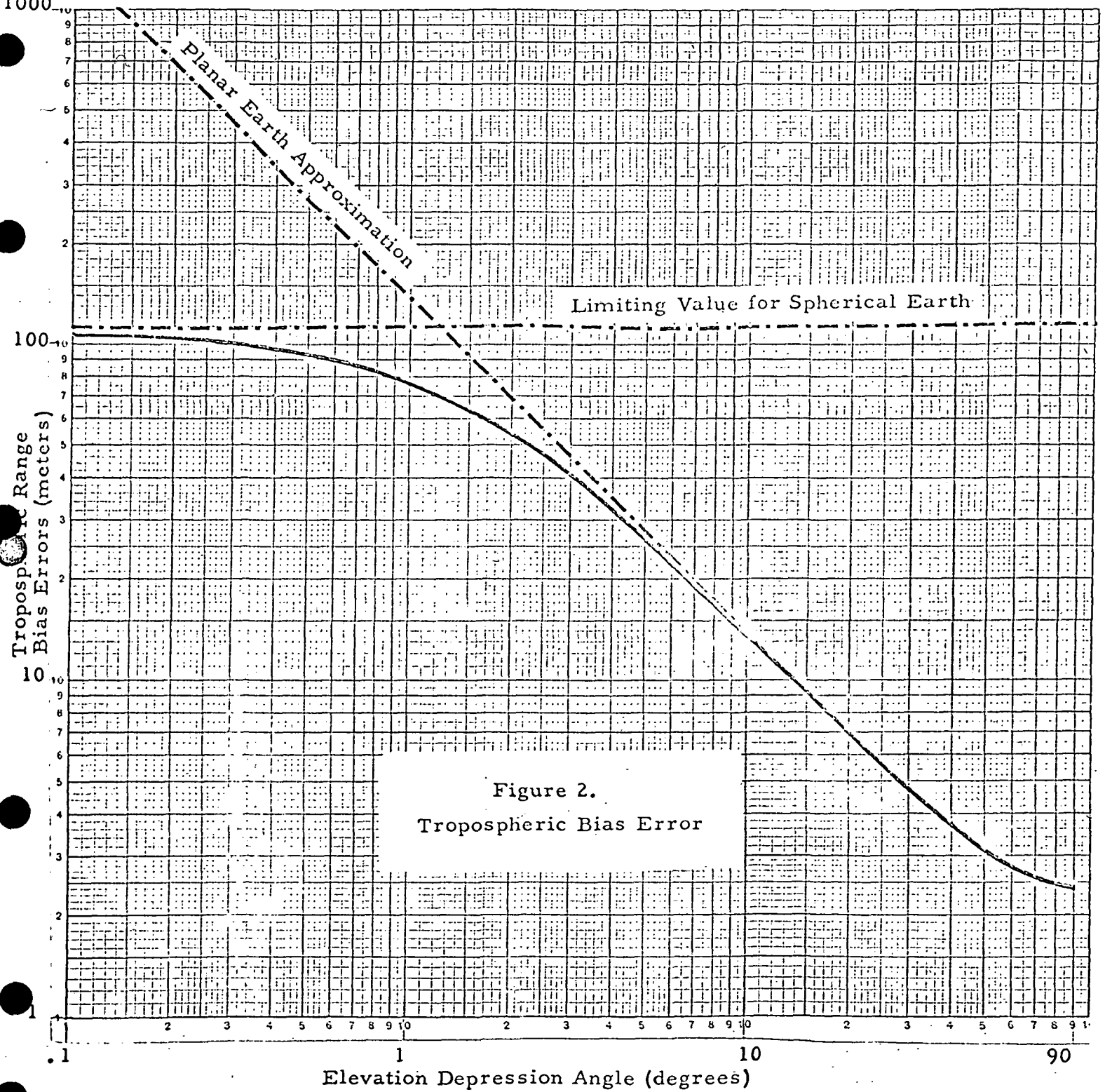

Figure 2.
Tropospheric Bias Error

Weather Condition	ΔN	L_o (meters)
Heavy Cumulus	30×10^{-4}	300
Average Air	$.5 \times 10^{-4}$	60

Figure 3.
Typical Parameters for RMS Tropospheric Error Calculations

As mentioned earlier, a good approximation is to take the straight line path between the transmitter and receiver. Referring to Figure 1, one can obtain the following approximate model for the effective path length L_o.

$$L_o = \frac{R_1^2 - R_o^2}{R_o \sin \phi_E + \sqrt{R_o^2 \sin^2 \phi_E + R_1^2 - R_o^2}} \tag{13}$$

$$\approx \frac{2H}{\sin \phi_E + \sqrt{\sin^2 \phi_E + \frac{2H}{R_o}}} \tag{14}$$

For elevation angles above a few degrees,

$$L \approx \frac{H}{\sin \phi_E} \approx \frac{H}{\sin \phi_o} \tag{15}$$

This later form (Equation 15) indicates that the depression angle regime in which the Earth's curvature may be neglected.

The two weather conditions indicated in Figure 3 are shown in Figure 4. It is assumed that the entire path length is composed of either the heavy cumulus type condition or the average air condition. The numerical results of this figure indicate that the RMS tropospheric error can be expected to be quite small. The worst situation (heavy cumulus) indicates RMS range errors of only about 6 - 40 cm over the regime of depression angles.

The correlation time of the larger range errors will typically be tens of seconds or greater. An estimate of the correlation time of these error sources can be made from the characteristic length of the anomaly (L_o) and the effective speed of the disturbance.

The analysis presented in this note has been directed specifically towards the range bias and RMS range errors. The errors in differential range and/or range-rate can also be computed for various trajectories of interest.

One other comment should be made pertaining to the minimum depression angle. The depression angle should be maintained above several degrees to prevent possible severe signal fading and distortion. This effect will be particularly serious for broad bandwidth transmissions such as television. This factor is substantially negligible for depression angles greater than about 3 antenna elevation beamwidth. This corresponds to about 1-1/2 degrees for the 80 feet MSFN antenna at its S-band frequency of operation.

The tropospheric bias error can be calibrated to some extent a priori. Typical calibrations are accurate to about 10-20%. Substantial improvement in this predicated calibration would require extensive measurements of refractive index.

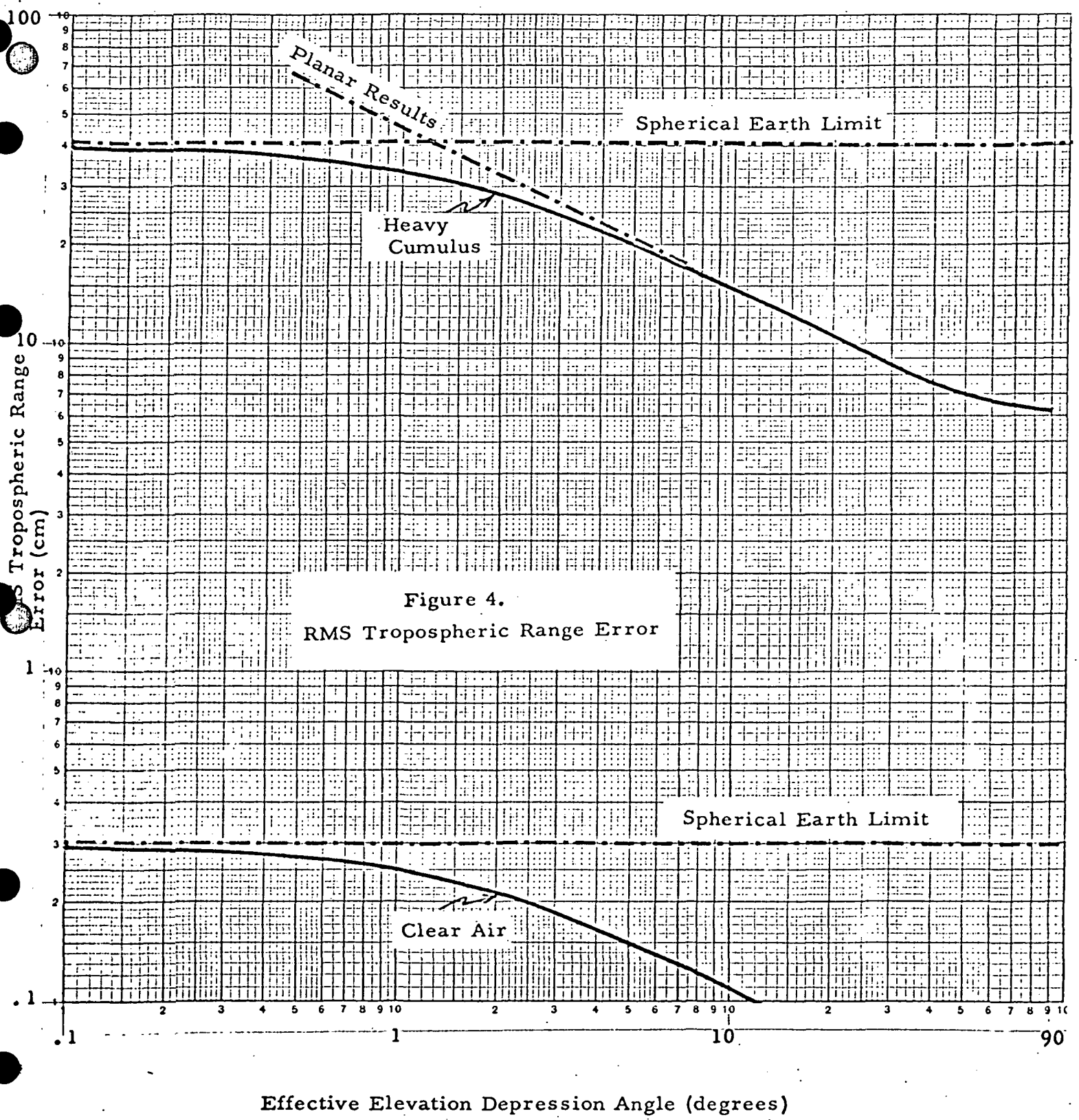

Figure 4.
RMS Tropospheric Range Error

The Bissett-Berman Corporation 2941 Nebraska Avenue, Santa Monica, California EXbrook 4-3270

APOLLO NOTE NO. 171

G. F. Floyd
6 February 1964

BISSETT-BERMAN PRESENTATION
at
HOUSTON
11 February 1964

1. Bissett-Berman Study
2. Orbit Errors Computer Program
3. Best MSFN Operating Modes
4. Long Range-Short Time MSFN Operation
5. LEM Rendezvous
6. MSFN Rendezvous Miss Uncertainty - Monitoring Mode
7. MSFN Rendezvous Miss Control Capability
8. Effect of Nuisance Parameters on MSFN Rendezvous Uncertainty
9. Ground Computations for Rendezvous
10. Earth Orbit Injection and Tracking Errors
11. Trans-Lunar Injection Tracking
12. MSFN Uncertainty on CSM--Return to Earth
13. RMS Errors in Prediction of Perilune in LEM Truck Descent
14. Preliminary Estimate of the Utility of MSFN During Powered Lunar Ascent
15. MSFN Stations

BISSETT-BERMAN STUDY

Objective:

Determine Capabilities of MSFN for Apollo G & N Monitoring and Back-up

Status:

1. Computer Program to calculate MSFN Errors during Free Flight in Operation.

2. Computer Program being expanded to include Powered Flight.

3. Results indicate multiple station MSFN highly useful in all phases of mission.

ORBIT ERRORS COMPUTER PROGRAM

Input Data:

1. Range, Range-Rate, Angle with Biases.
2. A priori Data on Position, Velocity, or Biases.
3. Errors in Station Location, Gravitational Constant, Speed of Light, Clock Drift.

Measured From:

1. Earth Stations, Moon Stations, Satellites of either.

Program Outputs:

1. Position and Velocity of Vehicle at any Time with Covariance Matrix of MSFN Errors.

BEST MSFN OPERATING MODES

Observation Time	RANGE	
	SHORT	LONG
Short	Vector Range (R + 2 Angles)	Doppler Range Change ($R-R_o$)
Long	Vector Range	Random Range Code (Time Share Stations)

LONG RANGE, SHORT TIME MSFN OPERATION

1. $\dot{R}_{meas} = \dfrac{\text{Change in Doppler Cycle Counter}}{\text{Sampling Time}} = \dfrac{\Delta R}{\text{Sampling Time}}$

2. 2×10^{-12} Unknown clock drift and propagation uncertainties only cause 0.5 m range change error over 25 minutes, and can be calibrated out from CSM data.

3. With Spacecraft attitude information, range change ($R - R_o$) accuracy possible = .6 m

LEM RENDEZVOUS

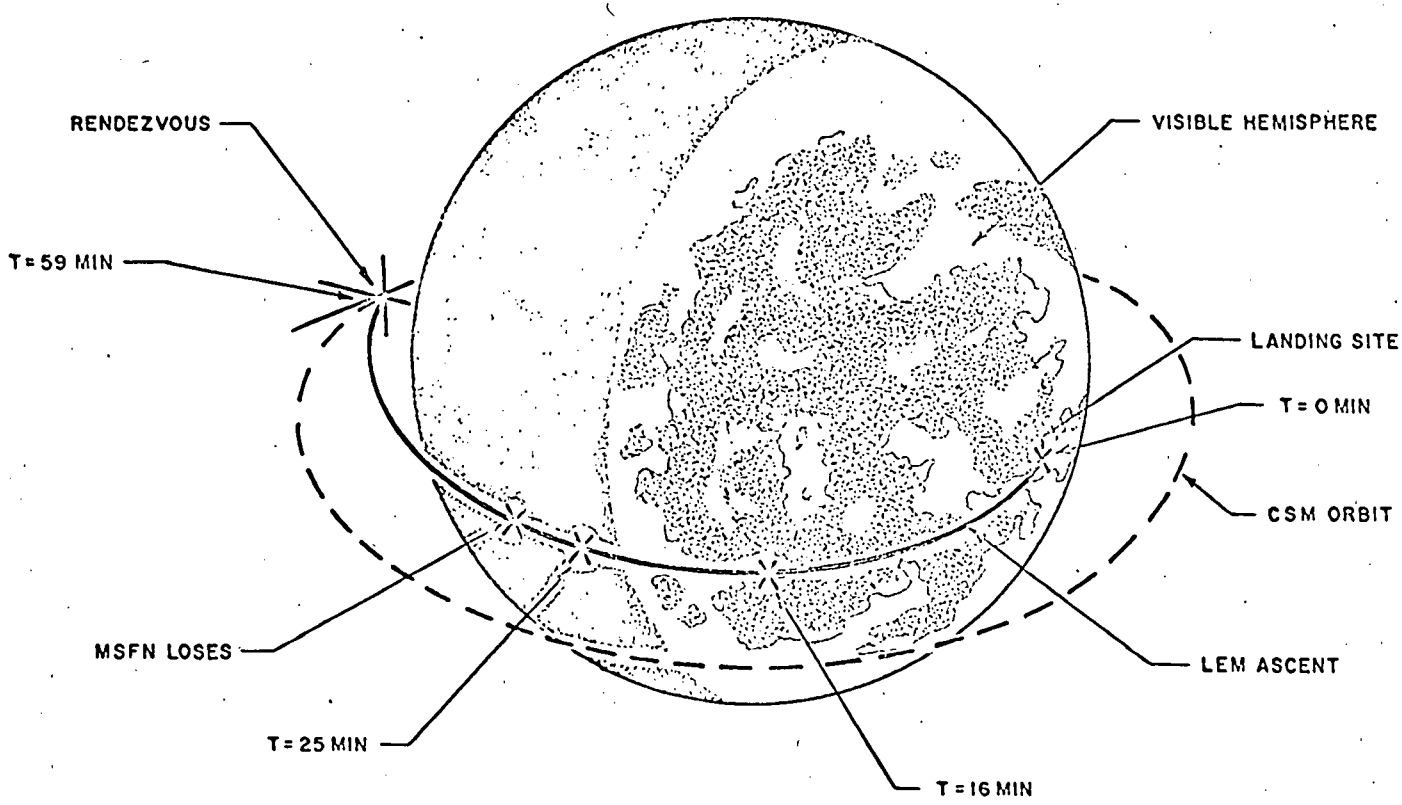

MONITORING MODE

MSFN RENDEZVOUS MISS UNCERTAINTY

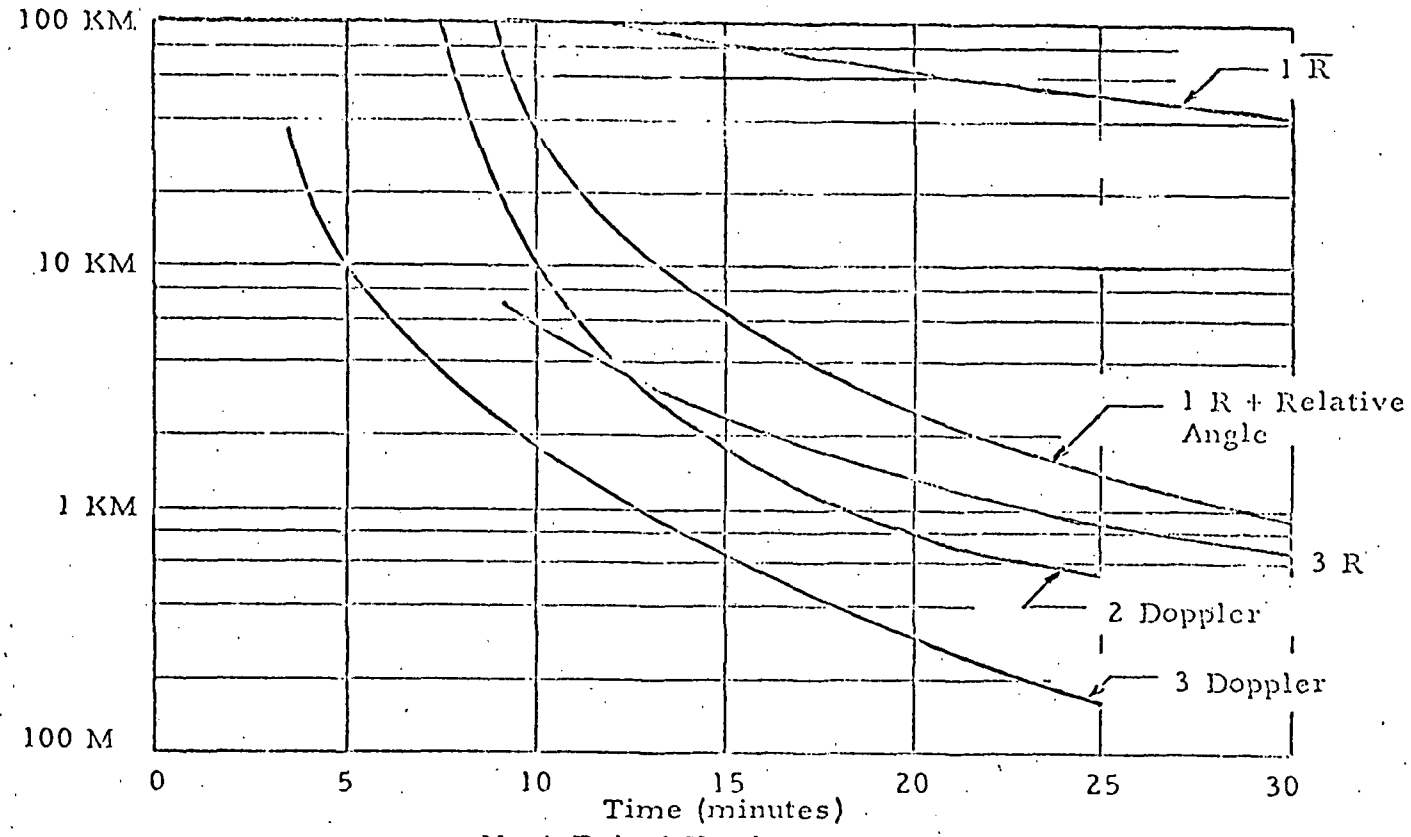

No A Priori Used

1 σ Values

Doppler:	1 m at 1 min.
Range:	15 m at 1 min. No Bias
Angles:	1 mil. (Rel); 0.8 mil

MSFN RENDEZVOUS MISS CONTROL CAPABILITY

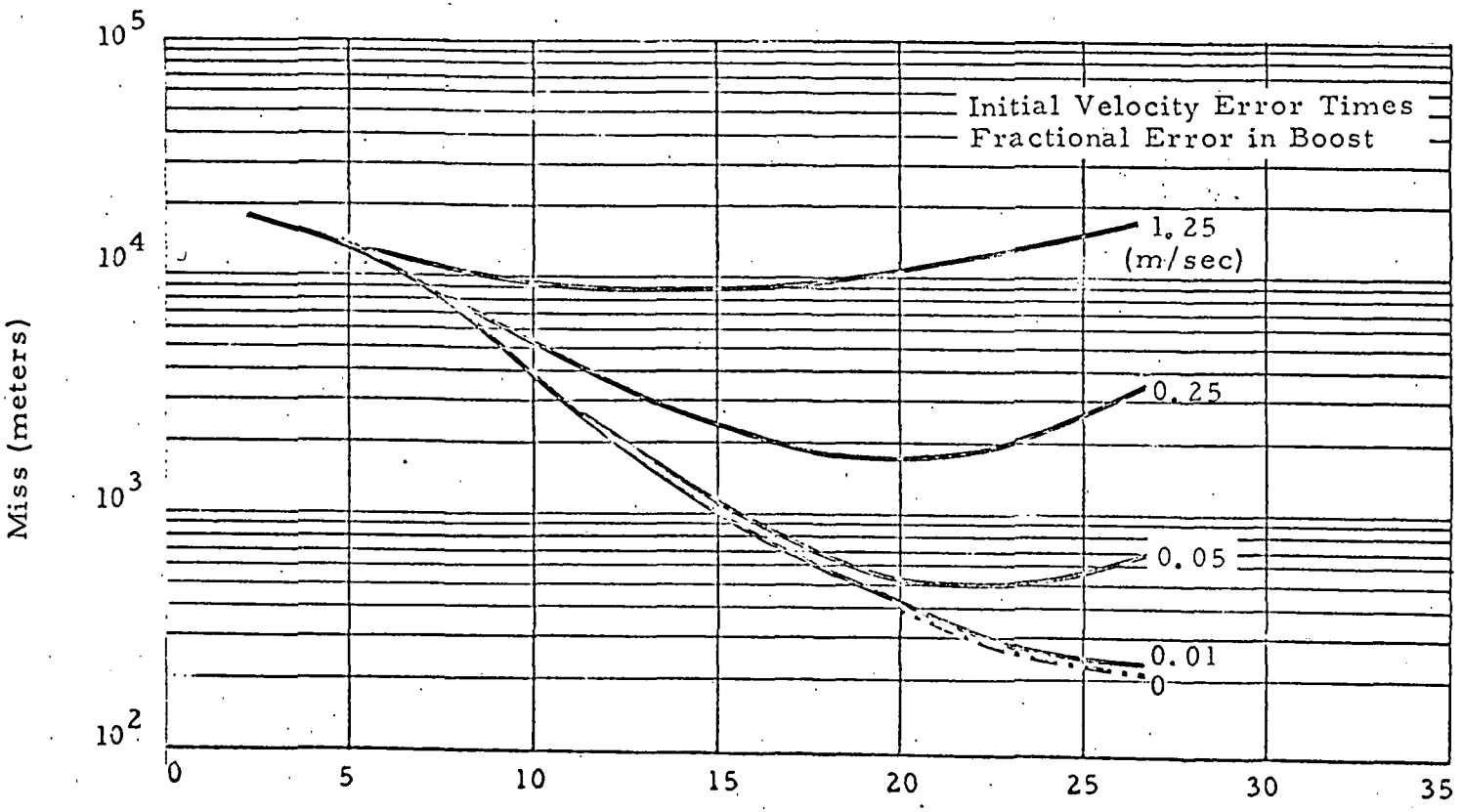

A Priori Data and Range Change

From Two Stations at 1 Minute Intervals $\sigma_{\Delta R}$ 0.6 m

Single Mid-Course Correction

EFFECT OF NUISANCE PARAMETERS ON MSFN RENDEZVOUS UNCERTAINTY

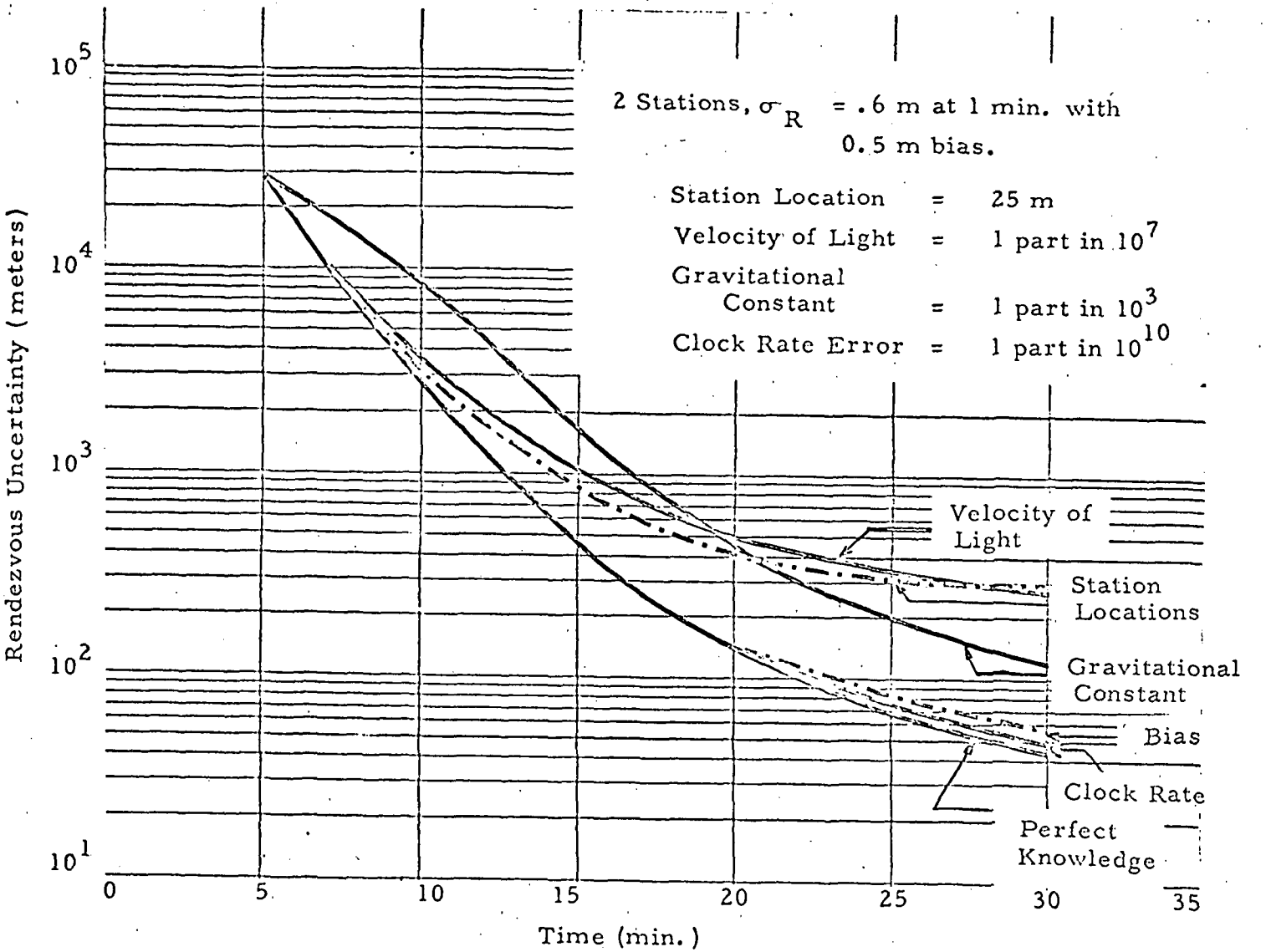

GROUND COMPUTATIONS FOR RENDEZVOUS

GIVEN:

30 Values of Range, Range-Rate and Angle from each of 3 ground stations.

Six Estimated Orbit Parameters.

COMPUTE:

Ephemeris of Vehicle Using Encke Method.

Expected Values of Measurements.

Likelihood of Measurements.

Corrections to Orbit Parameters.

TIMING:

One Complete Iteration of the Above Using All Data Requires 7 Seconds on 7094.

EARTH ORBIT INJECTION AND TRACKING ERRORS

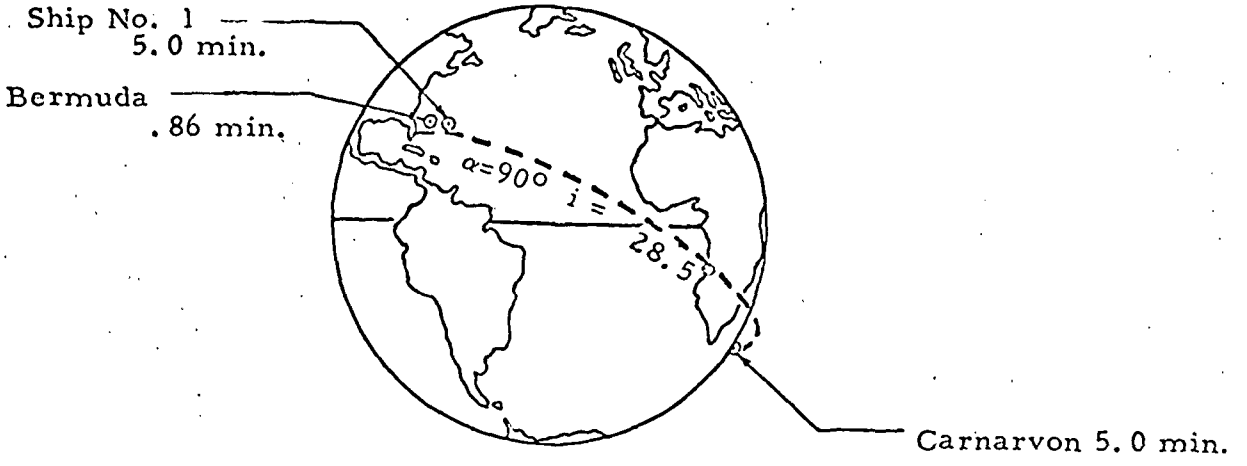

	RMS VELOCITY ERROR (m/sec.)		
	Bermuda Only	Bermuda + Ship No. 1	Bermuda + Carnarvon
$\sigma_R = 15$ m $\sigma_{\phi_1} = \sigma_{\phi_2} = 8 \times 10^{-4}$ r	3.3	.16	.07
$\sigma_R = 6$ m $\sigma_{\phi_1} = \sigma_{\phi_2} = 2 \times 10^{-4}$ r	.94	.05	.02

1 σ Station Location Errors

Land Stations: 10, 64, 64 m
Ship Stations: 20, 200, 200 m

} smallest is distance from Earth's axis.

TRANS-LUNAR INJECTION TRACKING

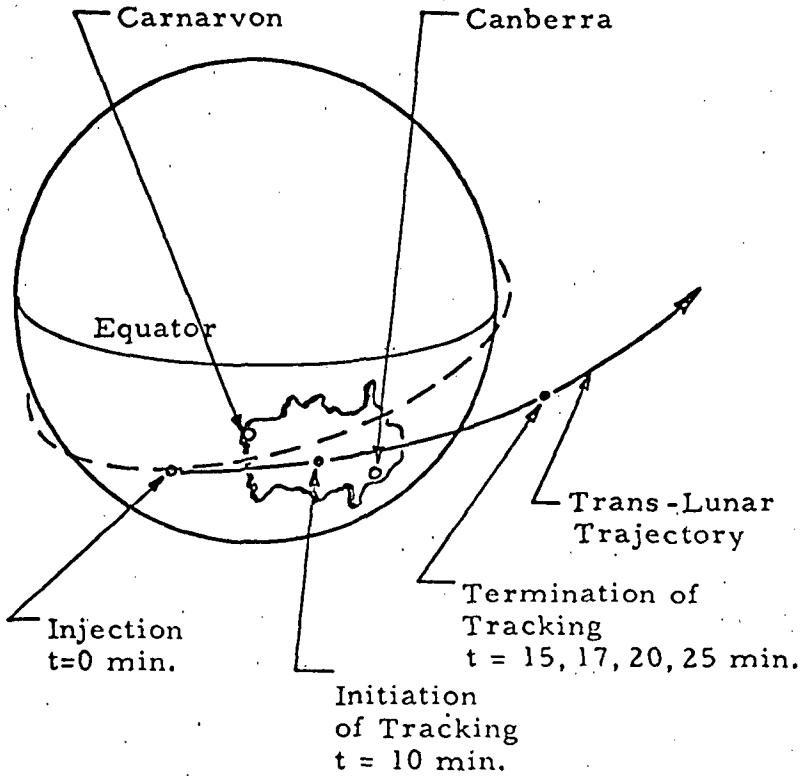

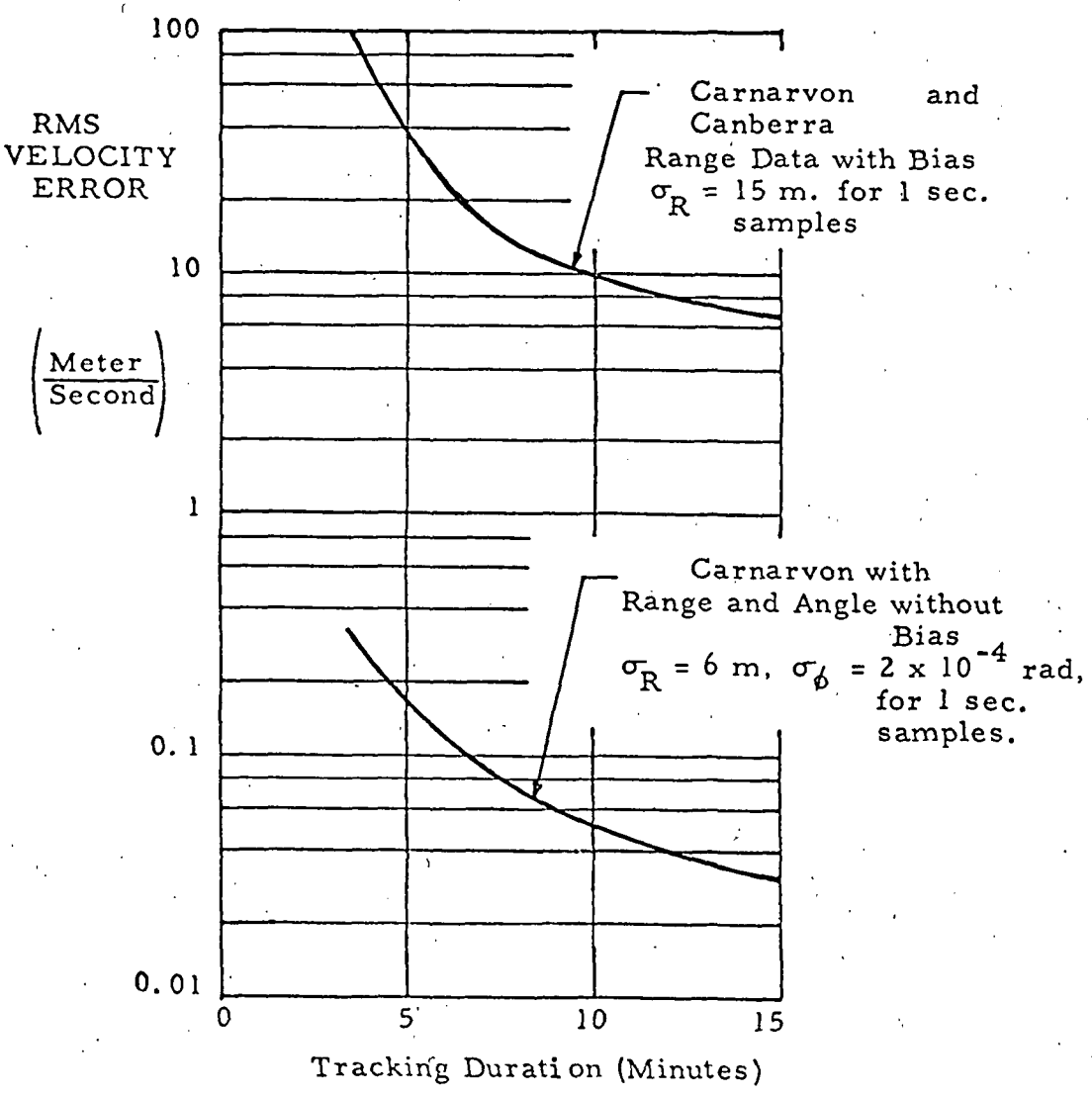

MSFN UNCERTAINTY ON CSM

RETURN TO EARTH-- NO A PRIORI DATA

Hours Until Re-entry	3 Stations			
	15 m Range With Bias		.3 m/sec. Range Rate	
	Dive Angle (degrees)	Miss (km)	Dive Angle (degrees)	Miss (km)
45	.45	140	5.0	1500
33	.05	17	1.1	374
21	.01	4	.30	115
9	.002	1	.05	27

RMS ERRORS IN PREDICTION OF PERILUNE IN LEM TRUCK DESCENT

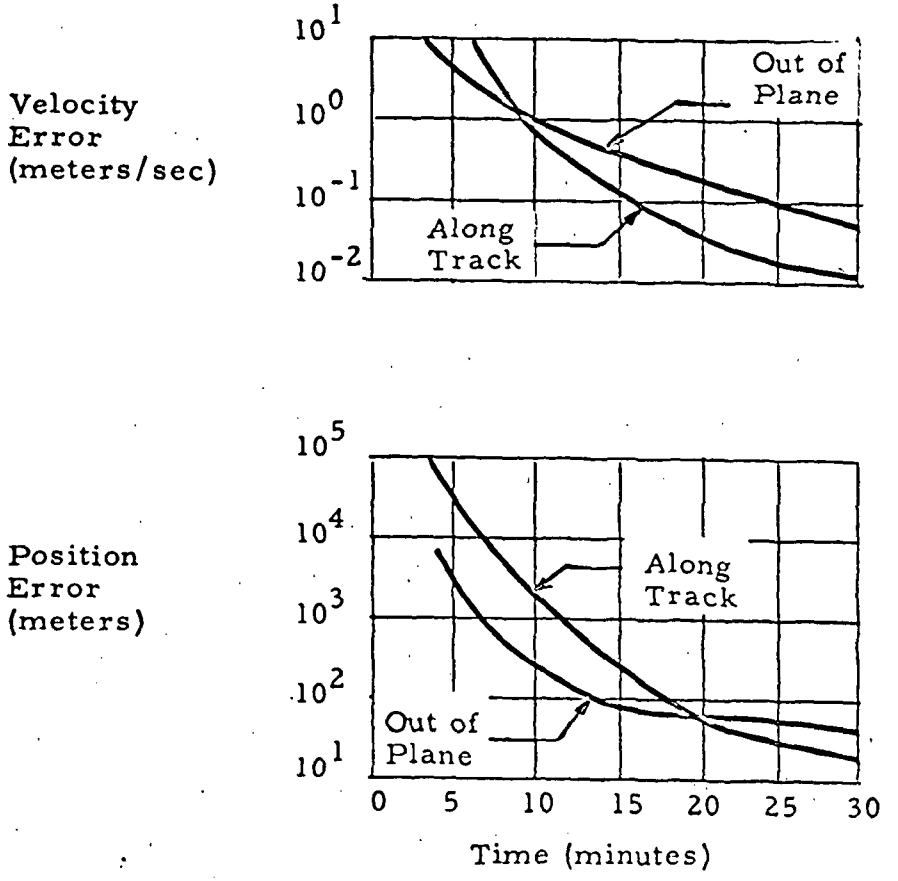

Range Change from Two Stations at 1 Minute Intervals $\sigma_{\Delta R} = 0.6$ m

PRELIMINARY ESTIMATE OF THE UTILITY OF MSFN DURING POWERED LUNAR ASCENT

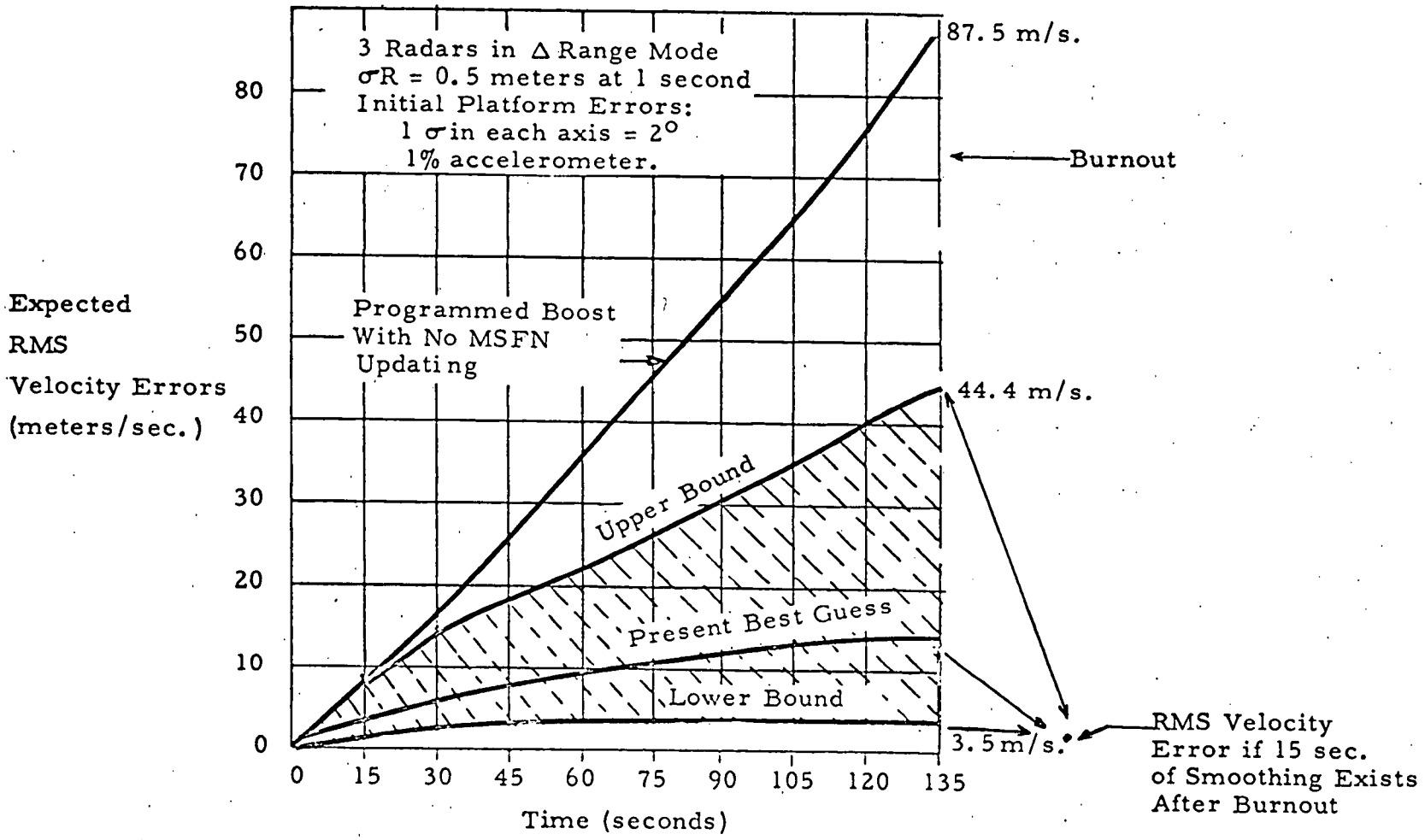

MSFN STATIONS

Must Be Out Of Orbit Plane

Want 3 MSFN Stations That Can See Moon

Goldstone, Kennedy, Hawaii, Guam,

Carnarvon, Canberra, Ascension,

Johannesburg, Madrid